AD A042981

AFAPL-TR-76-90

COMPUTER PROGRAM OPERATION MANUAL ON "SHABERTH" A COMPUTER PROGRAM FOR THE ANALYSIS OF THE STEADY STATE AND TRANSIENT THERMAL PERFORMANCE OF SHAFT-BEARING SYSTEMS

RESEARCH LABORATORY
SKF INDUSTRIES, INC.
ENGINEERING & RESEARCH CENTER
KING OF PRUSSIA, PA.

DDC
RECEIVED
AUG 15 1977
C

OCTOBER 1976

TECHNICAL REPORT AFAPL-TR-76-90

AD No.
DDC FILE COPY

Approved for public release; distribution unlimited.

AIR FORCE AERO PROPULSION LABORATORY
AIR FORCE WRIGHT AERONAUTICAL LABORATORIES
AIR FORCE SYSTEMS COMMAND
WRIGHT-PATTERSON AIR FORCE BASE, OHIO 45433

AND

NAVAL AIR PROPULSION TEST CENTER
TRENTON, NEW JERSEY 08628

NOTICE

When Government drawings, specifications, or other data are used for any purpose other than in connection with a definitely related Government procurement operation, the United States Government thereby incurs no responsibility nor any obligation whatsoever; and the fact that the government may have formulated, furnished, or in any way supplied the said drawings, specifications, or other data, is not to be regarded by implication or otherwise as in any manner licensing the holder or any other person or corporation, or conveying any rights or permission to manufacture, use, or sell any patented invention that may in any way be related thereto.

Publication of this report does not constitute Air Force approval of the reports findings or conclusions. It is published only for the exchange and stimulation of ideas.

This manual describes the work performed by SKF Industries, Inc. at its Technology Center in King of Prussia, Pa. for the United States Government, including the United States Air Force Systems Command, Air Force Aero Propulsion Laboratory, Wright-Patterson Air Force Base, Ohio and for the Naval Air Propulsion Test Center, Trenton, N. J. Work was performed over a seven month period starting in February 1976 under U. S. Air Force Contract No. F33615-76-C-2061 and Navy MIPR No. N62376-76-MP-00005. Mr. John Schrand administered the project for the Air Force and Mr. Raymond Valori administered the project for the Navy.

The project was conducted at SKF under the direction of Messrs. P. S. Given and T. E. Tallian. The SKF report designation is No. AL76P030.

The manual contains the results of analytical modelling and computer program development.

This report has been reviewed by the Information Office, (ASD/OIP) and is releasable to the National Technical Information Service (NTIS). At NTIS, it will be available to the general public, including foreign nations.

This technical report has been reviewed and is approved for publication.

John B. Schrand
John B. Schrand
Project Engineer

Raymond Valori
Raymond Valori
Project Engineer

FOR THE COMMANDER

Howard F. Jones
Howard F. Jones
Chief, Lubrication Branch
Fuels and Lubrication Division
Air Force Aero Propulsion Lab.

FOR THE COMMANDING OFFICER

Al Lockwood
Al Lockwood, Supervisor
Lubricants and Power Drive
Systems Division, Naval Air
Propulsion Test Center

AIR FORCE/56780/10 August 1977 — 210

UNCLASSIFIED

SECURITY CLASSIFICATION OF THIS PAGE (When Data Entered)

REPORT DOCUMENTATION PAGE

READ INSTRUCTIONS BEFORE COMPLETING FORM

1. REPORT NUMBER: AFAPL-TR-76-90

2. GOVT ACCESSION NO.

3. RECIPIENT'S CATALOG NUMBER

4. TITLE (and Subtitle): Computer Program Operation Manual on "SHABERTH": A Computer Program for the Analysis of the Steady State and Transient Thermal Performance of Shaft-Bearing Systems

5. TYPE OF REPORT & PERIOD COVERED: A Computer Program Operation Manual

6. PERFORMING ORG. REPORT NUMBER: AL76P030

7. AUTHOR(s): W. J. Crecelius, J. Pirvics

8. CONTRACT OR GRANT NUMBER(s): AF Contract No. F33615-76-C-2061; 76-C-2061; Navy MIPR No. M62376-76-MP-00005

9. PERFORMING ORGANIZATION NAME AND ADDRESS: SKF Industries, Inc., Technology Center, 1100 First Ave., King of Prussia, PA 19406

10. PROGRAM ELEMENT, PROJECT, TASK AREA & WORK UNIT NUMBERS

11. CONTROLLING OFFICE NAME AND ADDRESS: Air Force Aero Propulsion Laboratory, Air Force Systems Command, Wright-Patterson Air Force Base, Ohio

12. REPORT DATE: July 1976

13. NUMBER OF PAGES: 246 p.

14. MONITORING AGENCY NAME & ADDRESS (if different from Controlling Office): Air Force Aero Propulsion Laboratory and Naval Air Propulsion Test Center, Trenton, New Jersey 08628

15. SECURITY CLASS. (of this report): Unclassified

15a. DECLASSIFICATION/DOWNGRADING SCHEDULE

16. DISTRIBUTION STATEMENT (of this Report): Approved for public release; distribution unlimited

17. DISTRIBUTION STATEMENT (of the abstract entered in Block 20, if different from Report)

DDC RECEIVED AUG 15 1977 C

18. SUPPLEMENTARY NOTES

19. KEY WORDS (Continue on reverse side if necessary and identify by block number): Ball and Cylindrical Roller Bearings, Shaft Bearing System Performance, Deflections, Steady State and Transient Temperature Maps, Rolling Element Bearing Lubrication; Elastohydrodynamics (EHD) and Starvation, Hydrodynamics, Boundary, Friction, Hydrodynamic, EHD, Asperity-Partial EHD, Cage and Rolling Element Dynamics, Shaft

20. ABSTRACT (Continue on reverse side if necessary and identify by block number)

This report is a self contained manual describing an advanced state-of-the-art analytical computer program (SHABERTH) for the study of steady state and transient thermal performance of rolling element bearing and shaft systems. This program embodies mathematical models describing the role of the lubricant in bearing behavior. Descriptions of these models are set forth along with a detailed description of the program organization method of solution and convergence criteria. Input data preparation forms and

DD FORM 1 JAN 73 1473 EDITION OF 1 NOV 65 IS OBSOLETE

UNCLASSIFIED

SECURITY CLASSIFICATION OF THIS PAGE (When Data Entered)

400941

19. Key Words

and Housing Fits and Bearing Clearance Change

20. Abstract

program output are discussed and examples are included.

ACCESSION for
NTIS
DDC
UNANNOUNCED
JUSTIFICATION
BY
DISTRIBUTION/AVAILABILITY CODES
SPECIAL
A

TABLE OF CONTENTS

	Page
1. Introduction	1
2. Problem Formulation and Solution	4
2.1 Temperature Calculations	5
2.2 Bearing Dimensional Change Analysis	17
2.3 Bearing Inner Ring Equilibrium	18
2.4 Bearing Quasi-dynamic Solution	20
3. Program Input	29
3.1 Types of Input Data	29
3.2 Data Set I - Title Cards	30
3.3 Data Set II - Bearing Data	32
3.4 Data Set III - Thermal Data	45
3.5 Data Set IV - Shaft Data	51
4. Computer Program Output	54
4.1 Introduction	55
4.2 Bearing Output	55
4.3 Rolling Element Output	59
4.4 Thermal Data	61
4.5 Shaft Data	61
4.6 Program Error Messages	61
5. Guides to Program Use	66
6. References	69

APPENDICES I MATHEMATICAL MODELS

Appendix I 1	Heat Transfer Information
Appendix I 2	Bearing Diametral Clearance Change Analysis from Cold Unmounted to Mounted Operating Conditions
Appendix I 3	Elastic Shaft Analysis
Appendix I 4	Concentrated Contact Calculations
Appendix I 5	Lubricant Property and EHD Film Thickness Models
Appendix I 6	Traction and Inlet Friction Calculations
Appendix I 7	Rolling Element Inertia Forces and Moments
Appendix I 8	Rolling Element Bearing Cage Model
Appendix I 9	Bearing Fatigue Life Calculations

APPENDICES II PROGRAM INFORMATION

Appendix II 1 SKF Computer Program Shaberth/SKF Flow Chart
Appendix II 2 SKF Computer Program Shaberth/SKF Input Format Forms
Appendix II 3 SKF Computer Program Shaberth/SKF Sample Output

LIST OF FIGURES

Fig. No.		
2.1	Convective Heat Transfer	12
2.2	Divided Flow From Node i	13
2.3	Contact Geometry and Temperatures	16
2.4	Bearing Inertial (XYZ) and Rolling Element (xyz) Coordinate Systems	22
2.5	Inner Ring-Cage Land Contact Geometry	24
2.6	Outer Ring-Cage Land Contact Geometry	25
2.7	Cage Pocket Normal and Friction Forces Affecting Equilibrium	27
3.1	Angular Contact Ball Bearing Geometry	36
3.2	Split Inner Ring Ball Bearing Geometry	38
3.3	Roller-Raceway Contact Geometry	40

LIST OF TABLES

Table No.	Title	Page
1	Properties of Four Lubricants	44

LIST OF TABLES APPEARING IN THE APPENDICIES

		Page
I 5.1	Lubricant Properties of Four Oils Used in Program SHABERTH	I 5-3
I 6.1	Tabulation of Constants for Four Oils	I 6-9
I 6.2	Dimensionless Coefficients for the Calculation of Line Contact Inlet Friction	I 6-20

LIST OF FIGURES APPEARING IN THE APPENDICIES

Fig. No.	Title	Page
I 1.1	Parallel Conduction	I 1-3
I 1.2	Series Conduction	I 1-3
I 1.3	Heat Transfer Area	I 1-8
I 2.1	Bearing Assembly Equivalent Sections	I 2-3
I 2.2	Ring Radial Expansion Vs. Rotational Speed Squared	I 2-13
I 3.1	Shaft Coordinate System and Shaft Loading	I 3-2
I 3.2	Shaft Schematic Showing Stepwise and Linear Diameter Variation	I 3-2
I 3.3	Schematic Shaft Supports	I 3-3
I 4.1	Ball Bearing Geometry	I 4-4
I 4.2	Ball Coordinate System Showing Ball Center Position Vectors	I 4-5
I 4.3	Roller Bearing Geometry and Roller Coordinate Systems	I 4-8
I 4.4	Ball Coordinate System Showing Ball-Race Contact Position Vectors	I 4-13
I 4.5	Ball Race Deformed Contact and Deformed Surface Radius	I 4-14
I 4.6	Calculation of Traction Force Components	I 4-16
I 5.1	Film Geometry	I 5-10
I 6.1	Auxiliary Function y* vs. x*	I 6-2
I 6.2	Typical Traction Curves	I 6-6
I 6.3	Notation for Rolling Sliding Point Contact	I 6-11
I 6.4	Friction Forces on Sliding and/or Rolling Disks	I 6-12

Fig. No.	Title	Page
I 6.5	Variation of Fs with ρ_1	I 6-16
I 6.6	Variation of F_R with the Dimensionless Meniscus Distance ρ_1	I 6-17
I 6.7	Configuration of Contacts	I 6-19
I 8.1	Cage and Rolling Element Speeds and Displacements	I 8-6
I 8.2	Cage Pocket Geometry	I 8-8
I 8.3	Load Capacity Vs. Film Thickness for Hydrodynamic and Elastohydrodynamic Operating Regimes	I 8-12

NOMENCLATURE

Symbol	Definition	Units*
A	a constant in Walther's equation	(-)
A	surface of contact between media	(mm^2)
A_c	cage-land surface area	(mm^2 or $in.^2$)
A_e	area of outer cylindrical surface	(mm^2)
A_i	area of inner cylindrical surface	(mm^2)
A_v	ball frontal area	(mm^2)
B	auxiliary variable	(-)
B	$B = \Delta\chi/\alpha$, a constant in Walther's equation	(-)
C	a constant tabulation by Fresco	(mm^2/N or $in.^2/lb$)
C_o	a non dimensional fluid-geometry parameter	(-)
C_p	specific heat at constant pressure	(W/kg-DegC)
C_r	cage pocket clearance	(mm)
C_v	drag coefficient	(-)
D	ball or roller diameter	(mm)
D	a constant tabulated by Fresco	(mm^2/N or $in.^2/lb$)
E	a constant tabulated by Fresco	(mm^2/N or $in.^2/lb$)
E_1, E_2	Young's modulus for the contacting bodies	(N/mm^2 or psi)
F_A	axial force	(N or lb)
F_{n1}, F_{n2}	normal components of resultant force of the inlet pressure distribution	(N or lb)

*Where multiple units are indicated, the first units given are those associated with the computer program input and output.

NOMENCLATURE (CONTD)

Symbol	Definition	Units*
F_R	sliding force acting on the ball	(N or lb)
F_{R1}, F_{R2}	pumping forces acting on the ball	(N or lb)
F_{R3}, F_{S3}	tangential forces due to inlet rolling and shearing between ball and cage	(N or lb)
F_S	shearing force acting on the ball	(N or lb)
F_{S1}, F_{S2}	inlet friction forces	(N or lb)
F_x, F_y, F_z	force components in the x,y,z coordinate system	(N or lb)
F_w	windage force or drag force	(N or lb)
$\vec{F}$	the vector of inertia and drag forces	(N or lb)
$\vec{F}_m$	the vector sum of the hydrodynamic forces acting on the ball at the m-th contact	(N or lb)
$\vec{F}_b$	a vector of bearing loads and moments	(N or lb & mm-N or in.-lb)
$\vec{F}_{si}$	a vector of shaft loads and moments	(N or lb. & mm-N or in.-lb)
G	lubricant coefficient of thermal expansion	(1/DegC or 1/DegF)
H	non dimensional film thickness parameter	(-)
J	moment of inertia of the ball	kg-mm^2
K_f	conductivity of the film	(lb/degF-sec)
K_{ij}	the proportion of the heat flow from node i going to node j.	(-)
K_9, K_{10}	constants in expression for heat transfer coefficient	(-)
L	characteristic length	(mm or in.)
$L_{10\infty}$	full film fatigue life	(hrs)
M_c	moment due to fluid friction between the cage and the ring land	(mm-N or in.-lb

*Where multiple units are indicated, the first units given are those associated with the computer program input and output.

NOMENCLATURE (CONTD)

Symbol	Definition	Units*
M_x, M_y, M_z	ball moment components in the x,y,z coordinate system	(mm-N or in.-lb)
$\vec{M}$	ball moment vector	(mm-N or in.-lb)
N_u	Nusselt's number	(-)
P_r	Prandtl's number	(-)
P_d	diametral clearance	(mm or in.)
PE	bearing end play	(mm or in.)
P_1, P_2	forces acting normal to the ball surface within the outer and inner raceway contact ellipse	(N or lb)
P_3	ball-cage normal force	(N or lb)
Q	load	(N or lb)
Q_a	average asperity borne load	(N or lb)
Q_r	the radial component of the minimum rolling element-race normal force	(N or lb)
$\bar{Q}$	non dimensional load parameter	(-)
$\vec{Q}_m$	the vector normal load per unit length of the contact ellipse	(N/mm or lb/in.)
R	radius of outer ring groove centers	(mm)
R_e	Reynold's number	(-)
R_x, R_y	effective radii of curvature parallel and transverse to the rolling direction respectively	(mm or in.)
S	coordinate along the contact in the direction perpendicular to rolling friction	(mm or in.)

*Where multiple units are indicated, the first units given are those associated with the computer program input and output.

NOMENCLATURE (CONTD)

Symbol	Definition	Units*
Sd	diametral play	(mm or in.)
T	time	(sec)
T_o	long time duration	(sec)
T_s	starting time	(sec)
T_1, T_2	traction forces	(N or lb)
$\vec{T}$	traction force vector at a general location within the contact	(N or lb)
U	characteristic speed	(m/sec or in./sec)
V	fluid entrainment velocity at the contact center	(m/sec or in./sec)
V	volume of the nodal element	(m^3 or $in.^3$)
V	voltage	(volt)
V_i	volume flow rate through node i	(m^3/sec)
V_o	voltage over long time duration	(volt)
V_x	rolling velocity in x direction	(m/sec or in./sec)
V_y	rolling velocity in y direction	(m/sec or in./sec)
X,Y,Z	inertial coordinate system	(-)
DCL	diametral clearance	(mm or in.)
EPSFIT	user specified convergence criterion	(-)
EP1, EP2	a user supplied convergence criterion	(-)
EQ	temperature equilibrium convergence criteria for Eq. (3-41)	(-)
NEQ	number of equations in bearing solution	(-)
XCAV	volume fraction of lubricant in bearing cavity oil/air mixture	(-)

*Where multiple units are indicated, the first units given are those associated with the computer program input and output.

NOMENCLATURE (CONTD)

Symbol	Definition	Units*
a	a constant coefficient in Nusselt's number	(-)
a	contact ellipse semi-major axis	(mm or in.)
a	free convection temperature-exponent	(-)
b	an exponent in Nusselt's number	(-)
b	half the contact width	(mm or in.)
c	an exponent in Nusselt's number	(-)
c	coefficient of specific heat	(W/kg-Deg C)
d	exponent in free convection heat transfer equations	(-)
d_ℓ	cage-land diameter	(mm)
d_m	bearing pitch diameter	(mm or in.)
$\vec{f}_m$	the vector of friction force per unit length of the contact ellipse	(N/mm)
g	gravitational constant	(m/sec^2/ or $in./sec^2$)
h	elastohydrodynamic film thickness	(mm or μ -in.)
h_c	critical value of film thickeness	(mm or μ -in.)
h_f	the film thickeness under fully flooded conditions	(mm or μ -in.)
h_s	starved plateau thickness	(mm or μ -in.)
$h_{A.C.}$	film thickness calculated by Archard-Cowking formula	(mm or μ -in.)
$h_{D.H.}$	film thickness calculated by Dowson-Higginson formula	(mm or μ -in.)
i j	indices of heat flow nodes	(-)

*Where multiple units are indicated, the first units given are this associated with the computer program input and output.

NOMENCLATURE (CONTD)

Symbol	Definition	Units*
ℓ	separation distance between temperature nodes	(mm)
ℓ_{re}	contact length, or in the case of an elliptical contact area, 0.8 times the contact length	(mm)
n	number of rolling elements, total number of heat flow nodes	(-)
P_o	maximum contact pressure	(N/mm^2 or psi)
q	heat generation rate, net heat transfer	(W)
q_c	heat generated by fluid shearing between the cage and land	(W)
q_f	fluid drag heat	(W)
q_I	heat generated by shearing force in the ball-raceway and ball-cage inlet region	(W)
q_i	heat energy in the i-th nodal element	(W)
q_T	heat generated by traction in the contact zone	(W)
q_{ti}	heat carried by mass flow from node i	(W)
q_{gi}	heat generated at node i	(W)
q_{oi}	heat flow from all neighboring nodes to node i	(W)
$q_{Ri,j}$	the heat energy transferred by radiation between nodes i and j	(W)
$q_{ci,j}$	heat flow transferred by conduction from node i to node j	(W)
$q_{ui,j}$	the heat flow between nodes i and j	(W)
$q_{vi,j}$	heat flow transferred by free convection from node i to node j	(W)

*Where multiple units are indicated, the first units given are those associated with the computer program input and output.

NOMENCLATURE (CONTD)

Symbol	Definition	Units*
$q_{wi,j}$	heat flow by forced convection from node i to node j	(W)
r	groove radius	(mm or in.)
$\vec{r}_m$	a vector from the rolling element center to the point of contact	(mm or in.)
r*	meniscus distance from center of contact along direction of rolling	(mm or μ-in.)
t	temperature	(Deg C or Deg K)
u	sliding velocity at the contact center	(m/sec or in./sec)
$\vec{u}$	sliding velocity vector	(m/sec or in./sec)
u_1, u_2	surface velocity of bodies 1 and 2 relative to the contact	(m/sec or in./sec)
u_s	sliding speed	(m/sec or in./sec)
u_s*	sliding speed at which traction coefficient is a maximum	(m/sec or in./sec)
x,y,z	a local coordinate system established at each ball location	(-)
x	sliding velocity scaled by u_s*	(m/sec or in./sec)
x_1	ball axial position relative to the outer race	(mm or in.)
x_m	maximum variation of x	(mm)
y_1	ball radial position relative to the outer race	(mm or in.)
y_m	maximum variation of y	(mm)

*Where multiple units are indicated, the first units given are those associated with the computer program input and output.

Symbol	Definition	Units*
z_c	ball center-cage pocket offset	(mm or in.)
Δ	diametral clearance between cage and land	(mm or in.)
$\vec{\Delta}$	shaft displacement at a bearing location	(mm or in.)
Δ_{DCL}	change in bearing diametral clearance	(mm or in.)
Δ_T	a small increment of time	(sec)
$\Delta\phi$	angular distance between rolling elements	(deg)
$\vec{\Delta}_b$	bearing deflection vector	(mm or rad)
$\Delta\zeta$	lubricant replenishment layer thickness	(mm)
$\Phi(\cdot)$	cumulative distribution function of standard normal distribution	(-)
Ω	resistance of heat flow	(degC/W)
Ω	angular velocity	(rad/sec)
Ω_c	cage angular velocity	(rad/sec)
Ω_{res}	resultant resistance to heat flow	(degC/W)
α	contact angle	(deg)
α	scaling factor in modified Newton-Raphson technique	(-)
α	pressure-viscosity index	(in.^{2}/lb)
α_i	inner race contact angle	(deg)
α_o	outer race contact angle	(deg)
α_o	auxiliary contact angle	(deg)
α_v	film coefficient of heat transfer by free convection	(W/m^2-degC)

*Where multiple units are indicated, the first units given are those associated with the computer program input and output.

NOMENCLATURE (CONTD)

Symbol	Definition	Units*
α_W	film coefficient of heat transfer by forced convection	(W/m^2-degC)
β	temperature-viscosity coefficient	(1/degC)
β	ball speed vector pitch angle	(deg)
δ	the first variation	(-)
δ_e	elastic deformation	(mm)
$\delta_x, \delta_y, \delta_z$	the linear deflection components of $\vec{\Delta}_b$	(mm)
ε	surface emissivity	(-)
ε	a small arbitrary constant	(-)
η	dynamic viscosity	(centipoise or lb_f sec/in.^{2})
θ_y, θ_z	the angular deflection components of $\vec{\Delta}_b$	(rad)
λ	thermal conductivity	(W/M-degC)
λ	a viscoelastic constant (oil parameter)	(-)
μ	traction coefficient	(-)
μ_a	coulomb friction coefficient	(-)
μ_r	μ scaled by μ^*	(-)
μ_{EHD}	fluid traction coefficient	(-)
μ^*	maximum EHD traction coefficient	(-)
ν	kinematic viscosity	(centistokes)
ν_1, ν_2	Poisson's ratio for contacting bodies	(-)

*Where multiple units are indicated, the first units given are those associated with the computer program input and outputs.

NOMENCLATURE (CONTD)

Symbol	Definition	Units*
ρ	density	(kg/m^3)
ρ_o	density of the oil	(kg/m^3)
ρ_1	dimensionless meniscus distance	(-)
σ	Stefan-Boltzmann radiation constant	W/m^2-degK*)
σ_θ	RMS value of the distribution of asperity slope angles	(deg)
σ_ϕ	RMS value of surface roughness aximuth angle	(micrometers) (deg)
$\Phi(\cdot)$	density function of standard normal distribution	(-)
ϕ_s	starvation reduction factor	(-)
ϕ_t	the film thickness reduction factor, due to heating	(-)
ψ	thermal diffusivity	(mm^2/sec)
ω_c	cage orbital velocity	(rad/sec)
ω_o	ball orbital velocity	(rad/sec)
ω_x	ball angular velocity component about the x axis	(rad/sec)
ω_y	ball angular velocity component about the y axis	(rad/sec)
ω_z	ball angular velocity component about the z axis	(rad/sec)
$\dot{\omega}_o$	first derivative of ω_o with respect to time	(rad/sec^2)
$\vec{\omega}$	angular velocity of ball in x, y, z coordinate system	(rad/sec)

*Where multiple units are indicated, the first units given are those associated with the computer program input and output.

SUBSCRIPTS

Symbol	Definition
B	refers to point where traction curve becomes nonlinear
C	refers to cage or conduction
N	refers to current iteration
R	refers to rolling or radiation
a, asp	denotes asperity effect
f	refers to fluid or flooded
i	denotes the i-th ball, i-th node, inner ring
j	denotes j-th node
k	index denoting a specific time interval
m	an index-denoting bearing component
o	denotes outer ring
s	refers to sliding, starvation effect, or shaft
t	refers to thermal effect
v	refers to free convection
w	refers to forced convection
x,y,z	denotes components of vector quantities with respect to x, y, and z coordinates
1,2	refers to bodies 1 and 2

I. INTRODUCTION

The computer program described herein, SHABERTH, "A Computer Program for the Steady State and Transient Analyses of Shaft Bearing Systems," is the third generation of S K F Computer Program AE72Y003. Program AE72Y003 was developed by Kellstrom (1) under U. S. Army Contract DAAD05-73-C-0011, sponsored by the Ballistics Research Laboratory at Aberdeen Proving Grounds. The original as well as the succeeding generations of the program consists of the following major subprograms.

The master program consists of the following major subprograms.

1) Bearing Analysis. These subprograms are largely based upon the methods of Harris, (2,3).

2) Three Dimensional Shaft Deflection Analysis developed by Norlander and Friedrichson. (See Appendix I 3).

3) Bearing Dimensional Change Analysis based on the methods of Timoshenko, (4), and adapted to the shaft-bearing-housing system by Crecelius, (5). (See Appendix I 2).

4) Generalized Steady State and Transient Temperature Mapping and Heat Dissipation Analyses based on the methods of Harris, (6), Fernlund, (7) and Andreason, (8).

Although the primary function of all three generati ns of the program is to predict general bearing performance characteristics, and the bulk of the coding reflects this emphasis, the steady state and transient heat dissipation and temperature mapping subprogram may be used on a stand alone basis to model the thermal behavior of any system which can be represented by discrete temperature nodes.

The differences between the successive generations of the program reflect the development and installation of improved bearing lubrication and friction models, improved analysis of the bearing cage and improvements in the program structure which increased the program versatility and solution procedures.

The first generation of the program used the Newtonian lubricated friction models developed by Harris (2, 3).

The second generation of the program which carries the designation AT74Y001 was created by Crecelius, Liu and Chiu under Air Force Contract No. F33615-72-C-1467 and Navy MIPR No. M52376-3-000007 and is documented by McCool, et al (9).* In that effort, with Program AE72Y003 as the basis, the ball bearing subprogram was modified to include new models as follows:

1) An EHD film thickness model that accounts for i) thermal heating in the contact inlet using a regression fit to results obtained by Cheng (10) and ii) lubricant film starvation using theoretical results derived by Chiu (11).

2) A new semi-empirical model for fluid traction in an EHD contact (9), is combined with an asperity load sharing model developed by Tallian (12) to yield a model for traction in concentrated contacts that reflects the state of lubrication as it varies from dry, through partial EHD to the full EHD regime.

3) A model for the hydrodynamic rolling and shear forces in the inlet zone of lubricated contacts accounting for the degree of lubricant film starvation, (9).

4) Normal and friction forces between a ball and a cage pocket are modelled in a way that accounts for the transition between the hydrodynamic and elasto-hydrodynamic regimes of lubrication (9).

5) A model for the effect on fatigue life of the ratio of the EHD plateau film thickness to the composite surface roughness, (9).

Additionally, models for temperature viscosity and pressure viscosity variation as functions of temperature given by Walther (13) and Fresco (14) respectively, were adopted.

Program AT74Y001 is capable of analyzing only a single axially loaded ball bearing. The program cannot be used to analyze a multi-bearing system. All other capabilities are present however.

---

*Due to the similarities between major segments of SHABERTH AT75Y004 and AT74Y001, many sections of (9) have been included in this text, without modification.

The basis for the present program, SHABERTH, was AT74Y001. The latent capability for the analysis of up to five ball and roller bearings subjected to general, (5 degrees of freedom) loading, has been utilized. The models added to AT74Y001 are used in the calculation of both the ball and roller bearing friction forces and frictional heat generation rates. The present program also includes a new model for the hydrodynamic rolling and slip forces in the inlet zone of lubricated line contacts, based on the work of Chiu, Ref. (15). Additionally, a cage model developed under NASA Contract No. NAS3-19739 Ref (15) has been added which allows the cage to move with up to three degrees of freedom versus the one degree of freedom permitted in Program AT74Y001. This cage model may be used in the analysis of both ball and roller bearings.

Under Air Force Contract No. F33615-76-C-2061 and Navy NAPTC MIPR No. N62376-76-MP-00005, the capabilities of SHABERTH were expanded to solve the combined set of multi-rolling element and cage quasidynamic equilibrium equations.

This exapnsion required changes in the concentrated contact asperity friction model as well as changes in the cage-rolling element and cage-ring interaction calculations. Additionally, the mathematical definition of the range of permitted variable values was made substantially more accurate.

SHABERTH is intended to be as general as possible with the following limits on system size.

Number of bearings supporting the shaft - five (5) maximum
Number of rolling elements per bearing - thirty (30) maximum
Number of temperature nodes used to describe the system - one hundred (100) maximum

The program structure is modular and has been designed to permit substitution of new mathematical models and refinements to the existing models as the needs and opportunities develop.

The third generation program, SHABERTH, exists as two versions, SHABERTH/SKF, SKF Program No. AT75Y004 and SHABERTH/NASA, SKF Program No. AT76Y001. The differences between the two versions reside in the calculation of the elastohydrodynamic (EHD) film thickness and traction forces which develop in the rolling element-raceway and rolling element-cage concentrated contacts. The calculation of these factors as performed in the SKF version is detailed herein. The details of the calculations performed by the NASA version are presented in Ref. (15).

2. PROBLEM FORMULATION AND SOLUTION

The purpose of the program is to provide a tool with which the shaft-bearing system performance characteristics can be determined as functions of system temperatures. These system temperatures may be a function of steady state operation or a function of time variant conditions brought on by a change in the system steady state condition. Such a change would be the termination of lubricant supply to the bearings and other lubricated mechanical elements.

The program is structured with four nested, calculation schemes as follows:

1. Thermal, steady state or traisient temperature calculations which predict system temperatures at a given operating state.

2. Bearing dimensional equilibrium which uses the bearing temperatures predicted by the temperature mapping subprograms and the rolling element raceway load distribution, predicted by the bearing subprograms, to calculate bearing diametral clearance at a given operating state.

3. Shaft-bearing system load equilibrium which calculates bearing inner ring positions relative to the respective outer rings such that the external loading applied to the shaft is equilibrated by the rolling element loads which develop at each bearing inner ring at a given state.

4. Bearing rolling element and cage load equilibrium which calculates the rolling element and cage equilibrium positions and rotational speeds based upon the relative inner-outer ring positions, inertia effects and friction conditions, which if lubricated, are temperature dependent.

The above program structure allows complete mathematical simulation of the real physical system. The program has been coded to allow various levels of program execution which prove useful and economical in bearing design studies.

These levels of execution are explained fully in Sections 3, 4, and 5.

The structure of the program and the nesting of the solution loops noted above can be seen clearly in the Program Flow Chart which is discussed in Appendix II 1.

The sections below present the systems of field equations which are solved in each of the nested calculation schemes. A more detailed discussion is contained in (1, 9 and 15).

2.1 Temperature Calculations

Subsequent to each calculation of bearing generated heat rates, either the steady state or transient temperature mapping solution scheme may be executed. This set of sequential calculations is terminated as follows:

1. For the steady state case, when each system temperature is within EPA ^{o}Centigrade of its previously predicted value, EPA is specified by the user. If it is zero or left blank, a default value of 1° Centigrade is used. This criteria implies that the steady state equilibrium conditions has been reached.

2. The transient calculation terminates when the user specified time up is reached or when one of the system temperatures exceeds 600°C.

2.1.1 Steady State Temperature Map

The mechanical structure to be analyzed is thought of as divided into a number of elements or nodes, each represented by a temperature. The net heat flow to node i from the surrounding nodes j, plus the heat generated at node i, must numerically equal zero. This is true for each node i, i going from 1 to n, n being the number of unknown temperatures.

After each calculation of bearing generated heat, which results from a solution of the shaft-bearing system portion of the program, a set of system temperatures is determined which satisfy the system of equations:

$$q_i = q_{oi} + q_{g\,i} = 0 \text{ for all temperature nodes } i \qquad (2.1)$$

where q_{oi} is the heat flow from all neighboring nodes to node i

$q_{g\,i}$ is the heat generated at node i. These values may be input or calculated by the shaft bearing program as bearing frictional heat

This scheme is solved with a modified Newton-Raphson method which successfully terminates when either of two conditions are met:

$$\frac{\Delta t_i}{t_i} \leq \text{EP2 for all nodes } i \qquad (2.2)$$

where Δt represents the Newton-Raphson correction to the temperature t at a given iteration such that, $t_{N+1} = t_N + \Delta t$ and N + 1, and N, refer to the next and current iteration respectively.

EP2 is a user specified constant. If EP2 is left blank or set to zero (0) a default value of 0.001 is used.

A second convergence criterion dependent upon EP2 is also used. In the system of equations, $q_{oi} + q_{\ell i} = 0$ for all nodes i, absolute convergence would be obtained if the right hand side (EQ) in fact reduced to zero (0). Usually a small residue remains at each node, such that $(q_{oi} + q_{\ell i}) = (EQ)i$.

The second convergence criterion is satisfied if

$$\sum_{i}^{n} \left[\frac{(EQ)_i^2}{n}\right]^{\frac{1}{2}} \leq 100 \times EP2 \qquad (2.3)$$

where n = number of equations in bearing solution

2.1.2 Transient Temperatures

In the transient case, the net heat q_i transferred to a node i heats the element. It is thus necessary for heat balance at node i that the following equations are satisfied.

$$\rho Cp_i \, V_i \, \frac{dt_i}{dT_i} = q_i \qquad (2.4)$$

where ρ = density
C_p = specific heat
V = volume of the element
t = temperature
T = time

The temperatures, t_{oi}, at the time of initiation $T - T_s$ are assumed to be knwon, that is

$$t_i(T_s) = t_{oi} \qquad i = 1, 2, \ldots, n \qquad (2.5)$$

The problem of calculating the transient temperature distribution in a bearing arrangement thus becomes a problem of solving a system of non-linear differential equations of the first order with certain initial values given. The equations are non-linear since they contain terms of radiation and free convection, which are non-linear with temperature as will be shown later. The simplest and most economical way of solving these equations is to calculate the rate of temperature increase at the time $T = T_k$ from equation 2.4 and then calculate the temperatures at time $T_k + \Delta T$ from

$$t_{k+1} = t_k + \frac{dt_k}{dT} \Delta T = t_k + \frac{q_k}{\rho C_p V} \Delta T \qquad (2.6)$$

If the time step ΔT used as program input is chosen too large, the temperatures will oscillate, and if it is chosen too small the calcualtion will be costly. It is therefore desirable to choose the largest possible time step that does not give an oscillating solution. The program optionally calculates such a time step. The step is obtained from the condition, (16)

$$\frac{dt_{i,k+1}}{dt_{i,k}} \geq 0 \qquad i = 1, 2, \ldots, n \qquad (2.7)$$

If this derivative were negative, the implication would be that the local temperature at node i has a negative effect on its future value. This would be tantamount to asserting that the hotter a region is now, the colder it will be after an equal time interval. An oscillating solution would result.

Differentiating equation (2.6) for node i, one has as condition (2.8),

$$\frac{dt_{i,k+1}}{dt_{i,k}} = 1 + \frac{\Delta T_i}{\rho_i C_{pi} V_i} \cdot \frac{dq_i}{dt_i} \quad 0, \qquad i = 1, 2, \ldots n \tag{2.8}$$

The derivative dq_i/dt_i is calculated numerically

$$\frac{dq_i}{dt_i} = \frac{q_i\ (t_i + \Delta t_i) - q_i(t_i)}{\Delta t_i} \tag{2.9}$$

For each node, the value of ΔT_i giving a value of zero to the right hand side of Eqn. (2.8) is calculated.

A value of ΔT rounded off to one significant digit smaller than the smallest of the ΔT_i given by Eqn. (2.8) is used.

If the transient thermal scheme is being used interactively with the bearing subprograms, the user must specify a small enough time step between calls to the bearing subprograms in order that the variation in bearing generated heats, with time, accurately reflects the physical situation. At first, a trial and error procedure will be required to effectively use the program in its mode, however, experience will increase the user's effectiveness.

2.1.3 Calculation of Heat Transfer Rate

The transfer of heat within a medium or between two media can occur by conduction, convection, radiation and fluid flow.

All these types of heat transfer occur in a bearing application as the following examples show.

1. Heat is transferred by conduction between inner ring and shaft and between outer ring and housing.

2. Heat is transferred by convection between the surface of the housing and the surrounding air.

3. Heat is transferred by radiation between the shaft and the housing.

4. When the bearing is lubricated and cooled by circulating oil, heat is transferred by fluid flow.

Therefore, in calculating the net flow to a node all the above-mentioned modes of heat transfer will be considered.

2.1.3.1 Generated Heat

There may be a heat source at node i giving rise to a heat flow to be added to the heat flowing from the neighboring nodes.

In the case that the heat source is a bearing, it may either be considered to produce known amounts of power, in which case constant numbers are entered as input to the program, or the shaft-bearing program may be used to calculate the bearing generated heat as a function of bearing temperatures.

2.1.3.2 Conduction

The heat flow $q_{ci,j}$ which is transferred by conduction from node i to node j, is proportional to the difference in temperature $(t_i - t_j)$ and the cross-sectional area A and is inversely proportional to the distance ℓ between the two points, thus

$$q_{ci,j} = \frac{\lambda A}{\ell} (t_i - t_j) \qquad (2.10)$$

where λ = the thermal conductivity of the medium.

2.1.3.3. Free Convection

Between a solid medium such as a metallic body and a liquid or gas, heat transfer is by free or forced convection. Heat transfer by free convection is caused by the setting in motion of the liquid or gas as a result of a change in density arising from a temperature differential in the medium. With free convection between a solid medium and air, the heat energy $q_{vi,j}$ transferred between nodes i and j can be calculated from the equation, (2.11)

$$q_{vi,j} = \alpha_v A \left| t_i - t_j \right|^d \cdot \text{SIGN}\ (t_i - t_j) \qquad (2.11)$$

where α_v = the film coefficient of heat transfer by free convection
A = the surface area of contact between the media
d = is an exponent, usually = 1.25, but any value can be specified as input to the program

$$\text{SIGN} = \begin{cases} 1 \text{ if } t_i \geq t_j \\ -1 \text{ if } t_k < t_j \end{cases}$$

The last factor is included to give the expression $q_{vi,j}$ a correct sign.

The value of α_v can be calculated for various cases, see Jacob and Hawkins, (16).

2.1.3.4 Forced Convection

Heat transfer by forced convection takes place when liquid or gas moves around a solid body, for example, when the liquid is forced to flow by means of a pump or when the solid body is moved through the liquid or gas. The heat flow $q_{wi,j}$ transferred by forced convection can be obtained from the following equation.

$$q_{wi,j} = \alpha_w A(t_i - t_j) \qquad (2.12)$$

where α_w is the film coefficient of heat transfer during forced convection. This value is dependent on the actual shape, the surface condition of the body, the difference in speed, as well as the properties of the liquid or gas.

In most cases, it is possible to calculate the coefficient of forced convection from a general relationship of the form,

$$N_u = aR_e^{\,b} p_r^{\,c} \qquad (2.13)$$

where a, b, and c are constants obtained from handbooks, such as (17). R_e and P_r are dimensionless numbers defined by

N_u = Nusselt's number = $\alpha_w L/\lambda$
L = characteristic length
λ = conductivity of the fluid
R_e = Reynold's number = $UL\,p/\eta$
U = characteristic speed
p = density of the fluid
η = dynamic viscosity of the fluid
P_r = Prandtl's number = $\eta C_p/\lambda$
C_p = specific heat

The program can use a value of the coefficient of convection, or let it vary with actual temperatures, the variation being determined by how the viscosity varies. Input can be given in one of four ways, for each coefficient.

Constant viscosity

1. Values of the parameters of equation (2.13) are given as input and a constant value of α_w is calculated by the program.

Temperature dependent viscosity

2. The coefficient α_w for turbulent flow and heating of petroleum oils is given by

$$\alpha_w = k_9 \cdot \{\eta(t)\}^{k_{10}} \qquad (2.14)$$

where k_9 and k_{10} are given as input together with viscosity at two different temperatures.

3. Values of the parameters of equation (2.13) are given as input. Viscosity is given at two different temperatures.

2.1.3.5 Radiation

If two flat parallel, similar surfaces are placed close together and have the same surface area A, the heat energy transferred by radiation between nodes i and j representing those bodies will be,

$$q_{Ri,j} = \varepsilon \sigma A [t_i + 273)^4 - (t_j + 273]^4 \qquad (2.15)$$

where ε is the surface emissivity. The value of the coefficient ε is an input variable and varies between 1 for a completely black surface and 0 for an absolutely clean surface. In addition, σ is Stefan-Boltzmann's radiation constant which has the value 5.76×10^{-8} watts/m^2-$(^oK)^4$ and t_i and t_j are the temperatures at points i and j.

Heat transfer by radiation under other conditions can also be calculated, (16). The following equation, for instance, applies

between two concentric cylindrical surfaces

$$q_{Ri,j} = \frac{\varepsilon\sigma A_i \left[(t_i + 273)^4 - (t_j + 273)^4\right]}{1 + (1-\varepsilon) \quad (A_i/A_e)} \tag{2.16}$$

where A_i is the area of the inner cylindrical surface
A_e is the area of the outer cylindrical surface

2.1.3.6 Fluid Flow

Between nodes established in fluids, heat is transferred by transport of the fluid itself and the heat it contains.

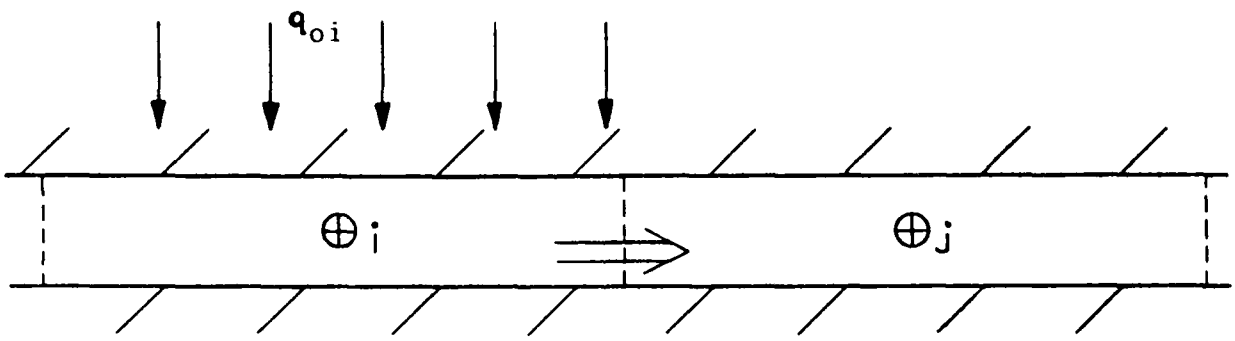

Figure 2.1 Convective Heat Transfer

Figure 2.1 shows nodes i and j at the midpoints of consecutive segments established in a stream of flowing fluid.

The heat flow $q_{ui,j}$ through the boundary between nodes i and j can be calculated as the sum of the heat flow q_{fi} through the middle of the element i, and half the heat flow q_{oi} transferred to node i by other means, such as convection.

The heat carried by mass flow is,

$$q_{fi} = \rho_i \, C_{p_i} \, V_i \, t_i = K_i t_i \tag{2.17}$$

where V_i = the volume flow rate through node i

The heat input to node i is the sum of the heat generated at node i (if any) and the sum over all other nodes of the heat transferred to node i by conduction, radiation, free and forced convection.

$$q_{oi} = q_{G,i} + \sum_{j} (q_{ci,j} + q_{vi,j} + q_{wi,j} + q_{Ri,j}) \qquad (2.18)$$

The heat flow between the nodes of Fig. 2.2 is then,

$$q_{ui,j} = q_{fi} + q_{oi}/2 \qquad (2.19)$$

If the flow is dividing between node i and j, Figure 2-2 then the heat flow is calculated from

$$q_{ui,j} = K_{ij} \; (q_{fi} + q_{oi}/2) \qquad (2.20)$$

where K_{ij} = the proportion of the flow at i going to the node j, o K_{ij} 1. K_{ij} is specified at input.

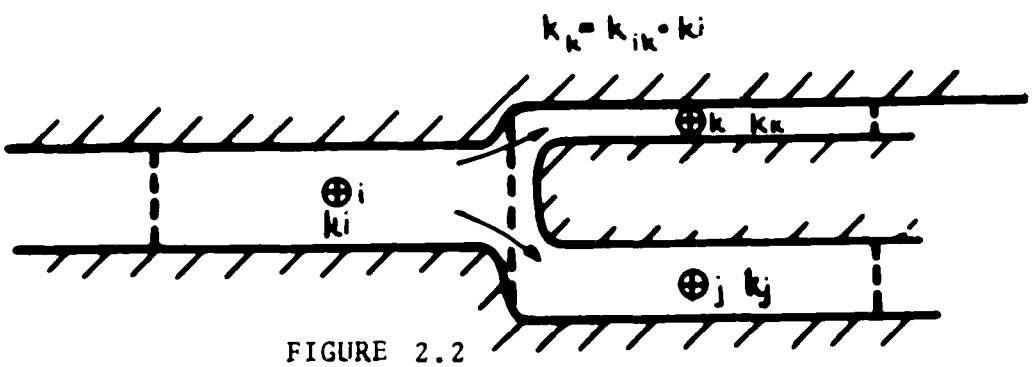

FIGURE 2.2
DIVIDED FLUID FLOW FROM NODE i

Figure 2.2 Divided Fluid Flow from Node i

2.1.3.7 Total Heat Transferred

The net heat flow rate to node i can be expressed as,

$$q_i = q_{G,i} + \sum_{j} (q_{ci,j} + q_{ui,j} + q_{vi,j} + q_{wi,j} + q_{Ri,j}) \qquad (2.21)$$

The summation should include all nodes j, both with unknown temperatures as well as boundary nodes, at which the temperature is known so long as they have a direct heat exchange with node i.

This expression is a non-linear function of temperatures because of the terms q_W and q_R. Therefore, the equations to be solved for a steady state solution are non-linear. The subprogram SOLVXX for solving non-linear simultaneous equations is used for this purpose.

2.1.4 Conduction Through a Bearing

As described in Section 2.1.3.2, the conduction between two nodes is governed by the thermal conductivity parameter λ of the medium through which conduction takes place. The value of λ is specified at input.

An exception is when one of the nodes represents a bearing ring and the other a set of rolling elements. In this case, the conduction is separately calculated using the principles described below.

2.1.4.1 Thermal Resistance

It is assumed that the rolling speeds of the rolling elements are so high that the bulk temperature of the rolling elements are the same at both the inner and outer races, except in a volume close to the surface. The resistance to heat flow can then be calculated as the sum of the resistance across the surface and the resistance of the material close to the surface.

The resistance Ω is defined implicitly by

$$\Delta t = \Omega \cdot q \tag{2.22}$$

where

Δt is temperature difference
q is heat flow

The resistance due to conduction through the EHD film is calculated as

$$\Omega_1 = (h/\lambda) \cdot A \tag{2.23}$$

where h is taken to be the calculated plateau film thickness
A is the Hertzian contact area at the specific rolling element-ring contact under consideration.
λ is the conductivity of the oil.

The geometry is shown in Figure 2.3(a). Asperity conduction is not considered.

So far, a constant temperature difference between the surfaces has been assumed. But during the time period of contact, the difference will decrease because of the finite thermal diffusivity of the material near the surface, Fig. 2.3(b).

To points at a distance from the surface this phenomenon will have the same effect as an additional resistance Ω_2 acting in series with Ω_1.

This resistance was estimated in (18) as,

$$\Omega_2 = \frac{1}{\lambda \ell_{re,i}} \left(\frac{\pi \psi}{2 b_i V}\right)^{\frac{1}{2}} \tag{2.24}$$

where ℓ_{re} = contact length, or in the case of an elliptical contact area, 0.8 times the major axis

λ = heat conductivity

ψ = thermal diffusivity = $\lambda / (\rho \cdot C_p)$

ρ = density

C_p = specific heat

b = half the contact width

V = rolling speed

The resultant resistance is

$$\Omega_{res} = \Omega_1 + \Omega_2 \tag{2.25}$$

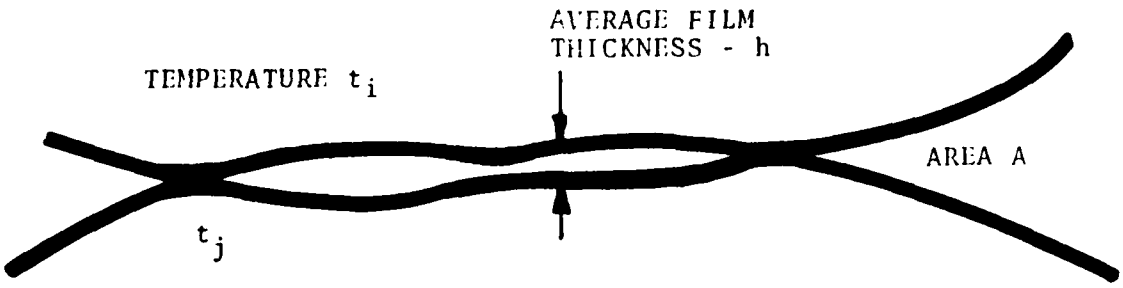

(a) Schematic Concentrated Contact

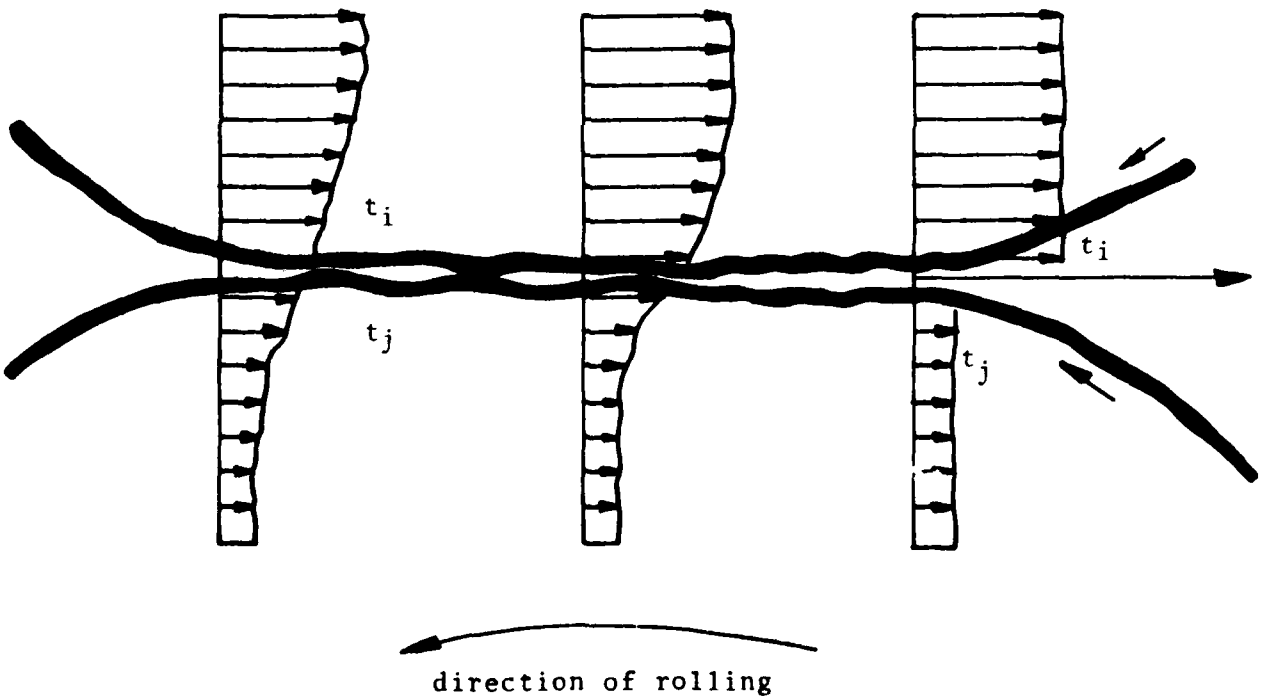

(b) Temperature Distribution at Rolling, Concentrated Contact Surfaces

FIGURE 2.3

CONTACT GEOMETRY AND TEMPERATURES

There is one such resistance at each rolling element. They all act in parallel. The resultant resistance, Ω_{res}, is thus obtained from

$$\frac{1}{\Omega_{res}} = \sum_{i=1}^{n} \frac{1}{\Omega_{res,i}} \tag{2.26}$$

2.2 Bearing Dimensional Change Analysis

The program calculates the changes in bearing diametral clearances according to the analysis described originally in (5) and herein in Appendix I 2, and expressed in generalized equation form as,

$$\Delta DCL = f\left\{(Fits)_m,\ t_i,\ \Omega_m,\ (Q_r)_m\right\},\ m = 1,\ 2 \tag{2.27}$$

for inner and outer rings respectively

$i = 1,2,3,4,5$ for shaft, inner ring, outer ring, housing and rolling element respectively

where: ΔDCL is the change in bearing diametral clearance
Fits are the cold mounted shaft and housing fits
t_i are the component temperatures
Ω_m refers to the ring rotational speeds
Q_r refers to the radial component of the minimum rolling element-race normal force.

A bearing clearance change criterion is satisfied when the change in bearing diametral clearance remains within a narrow, user specified range, for two successive iterations as follows:

$$\frac{|(\Delta DCL)_N - (\Delta DCL)_{N-1}|}{D} \leq \text{EPSFIT for all bearings} \qquad (2.28)$$

where: N denotes the most recent iteration and
N-1 denotes the previous iteration
D denotes the ball or roller diameter and
EPSFIT is a user specified value = .0001D

It should be noted that although ring rotational speeds, and initial, i.e. cold, shaft and housing fits are considered in the clearance change analysis, these two factors are fixed at input and remain constant through the entire solution. Although component temperatures may change as a consequence of the thermal solution, temperatures remain constant through a complete set of clearance change iterations. As a result, only the change in bearing load distribution affects the change in bearing clearance within a set of clearance change iterations.

2.3 Bearing Inner Ring Equilibrium

The bearing inner ring equilibrium solution is obtained by solving the system:

$$(\vec{F}_b)_i - (\vec{F}_s)_i = 0 \text{ for all bearings, } i \qquad (2.29)$$

where: $\vec{F}_b$ denotes a vector of bearing loads and moments resulting from rolling element/race forces and moments.

$$(\vec{F}_b)_i = \begin{bmatrix} F_{bxi} \\ F_{byi} \\ F_{bzi} \\ \hline M_{byi} \\ M_{bzi} \end{bmatrix} \begin{matrix} \text{Forces} \\ \\ \text{Moments} \end{matrix} \qquad (2.30)$$

If the bearing solution considers friction, $\vec{F}_b$ is comprised of the rolling-element race friction forces as well as the normal forces.

If the bearing solution is, at the user's option, frictionless, F_b is comprised only of rolling element/race normal contact forces.

$(\vec{F}_s)_i$ denotes a similar vector of loads, exerted on the inner ring by the shaft. The calculation of $(\vec{F}_s)_i$ is presented in Appendix I 3.

$$(\vec{F}_s)_i = \begin{bmatrix} F_{sxi} \\ F_{syi} \\ F_{szi} \\ \hline M_{syi} \\ M_{szi} \end{bmatrix} \begin{matrix} \text{Forces} \\ \\ \text{Moments} \end{matrix} \qquad (2.31)$$

The variables in this system of equations are the bearing inner ring deflections Δ_b and the shaft displacements $\vec{\Delta}$ at all bearing locations. The bearing loads may be expressed as a function of the inner ring deflections.

$$\vec{F}_b = \vec{F}_b\,(\vec{\Delta}_b) \qquad (2.32)$$

The deflection $\vec{\Delta}_b$ of a bearing is described by two radial deflections δ_y and δ_z, two angular deflections θ_y and θ_z and one axial deflection δ_x. The axial deflection is assumed to be the same for all bearings on a shaft, i.e.

The solution scheme is ended when

$$\frac{\delta(\vec{\Delta})_{ij}}{(\vec{\Delta})_{ij}} \leq \begin{cases} \text{EPS1 (frictionless)} \\ \text{EPS2 (friction)} \end{cases} \tag{2.37}$$

i = 1,...(Number of bearings)
j = 1,5 - for the 3 linear and two angular deflections at each bearing

If for some i or j, $(\vec{\Delta})_{ij} = 0$, Eq. (2.38) is used in place of (2.37)

$$\frac{\delta(\vec{\Delta})_{ij}}{(0.001 \times \text{NBRG})} \leq \begin{cases} \text{EPS1 (frictionless)} \\ \text{EPS2 (friction)} \end{cases} \tag{2.38}$$

NBRG denotes the number of bearings in the system.

EPS1 and EPS2 are used depending on whether the bearing solutions are frictionless or include friction, respectively. If the bearing deflections are extremely small, computer-generated numerical inaccuracies may prevent convergence according to the above criteria although a perfectly good solution has been obtained. To overcome this problem, the iteration is terminated if all angular deflections are less than 2×10^{-6} radians and all linear deflections are less than 5×10^{-8} inches. Any one of the above criteria imply that inner ring equilibrium is satisfied.

2.4 Bearing Quasi-Dynamic Solution

The bearing quasi-dynamic solution is obtained through a two-step process:

1. Elastic Solution - considering rolling element contrifugal force.

2. Elastic and Quasi-dynamic Solution*

*Quasi-dynamic equilibrium is used to connote that the true dynamic equilibrium terms containing first derivatives of the ball rotational speed vectors and the second derivatives of rolling element position vectors with respect to time are replaced by numerical expressions which are position rather than time dependent.

2.4.1 Rolling Element Equilibrium Equations

The equations which define rolling element quasi-dynamic force equilibrium take the form

$$\sum_m \left[\int_{-a_m}^{a_m} (\vec{Q}_m + \vec{f}_m)dt + \vec{F}_m \right] + \vec{F} = 0 \qquad (2.39)$$

m = 1-3 refers to the outer, inner and cage rolling element contacts respectively

where: $\vec{Q}_m$ is the vector normal load per unit length of the contact. See Appendix I 4.

$\vec{f}_m$ is the vector of friction force per unit length of the contact. See Appendices I 5 and I 6.

$\vec{F}$ is the vector of inertia and drag forces. See App. I 6 and I 7

t is a coordinate along the contact, perpendicular to the direction of rolling (usually the major axi)

a is half the contact length. See Ref. (1).

$\vec{F}_m$ is the vector sum of the hydrodynamic forces acting on the rolling element at the m-th contact. See Appendix I 6.

Rolling element moment equilibrium is defined by:

$$\sum_m \left[\int_{-a_m}^{a_m} \vec{r}_m \times (\vec{Q}_m + \vec{f}_m)dt \right] + \vec{r}_m \times \vec{F}_m + \vec{M}_I = 0 \qquad (2.40)$$

$\vec{Q}_m, \vec{f}_m, \vec{F}_m, \vec{a}_m$, and t are defined above, $\vec{M}_I$ is a vector of inertia moments. For the definition of M_I, refer to Appendix I 7.

$\vec{r}_m$ is a vector from the rolling element center to the point of contact, see Appendix I 4.

The solution to the equation sets represented (2.39) and 2.40) generate the necessary data to calculate bearing fatigue life. See Appendix I 9.

In the frictionless elastic solution $\vec{F}_m$ and $\vec{f}_m = 0$. Additionally, the only rolling element inertia term considered in the frictionless solution is centrifugal force. As a consequence, only the axial and radial force equilibrium equations are solved for each ball. For each roller, the radial force equilibrium and the tilting moment about the Z axis of Fig. 2.4 is solved. A dummy equation for axial force equilibrium is included in the solution matrix which keeps the roller centered

FIGURE 2.4

Bearing Inertial (XYZ) and Rolling Element (xyz), Coordinate Systems

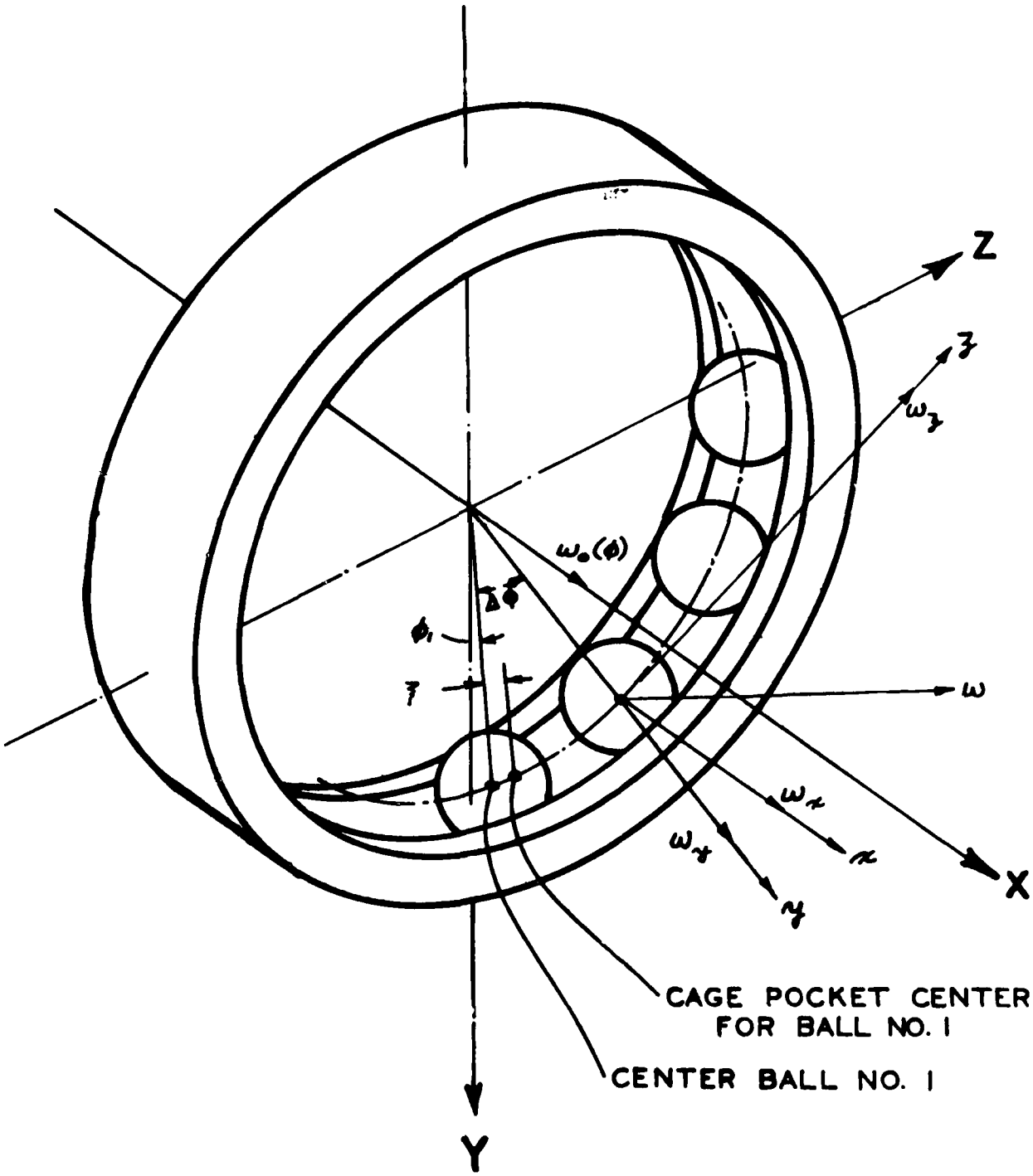

with respect to the outer race. The cylindrical roller bearing considered by the program cannot carry axial loading.

The friction solution determines ball quasi-dynamic equilibrium for six degrees of freedom. A roller is permitted four degrees of freedom. The rolling-element variables in this solution are x_1, Y_1, ωx, ωy, ωz, and ωo.

where x_1 is the rolling element axial position relative to the outer race. For a roller, this is a dummy variable.
y_1 is the rolling element radial position relative to the outer race.
$\omega x, \omega y, \omega z$ are the orthogonal rolling element rotational speeds relative to the cage speed, about the x, y and z axes and ωo is the rolling element orbital speed. For the roller, ωz is a dummy variable.

The variables x_1 and y_1 are the ball variables in the frictionless solution. The variables in the roller frictionless solution are x_1, a dummy, Y_1 and $\Theta z = \tan^{-1} (\omega y/\omega x)$.

2.4.2 Cage Equilibrium Equations

The cage equations and cage-rolling element interactions are not considered when the friction forces are omitted from the rolling element equilibrium equations.

The number of degrees of freedom given to the cage is one, if the cage will tend to rotate concentrically with respect to the ring on which it is riding. This condition is determined as a function of the rolling element orbital speed variation and prevails with most roller bearings and with ball bearings subjected only to axial loading. In both cases, orbital speed variation is often inconsequential. Also, single degree of freedom is allowed when the cage is rolling element riding. The single degree of freedom corresponds to a small angular rotation about the bearing axis, measured with respect to rolling element 1. The angular displacement is converted to a linear dimension by a multiplication by the bearing pitch diameter and is noted in Fig. 2.4 as γ. When a single degree of freedom is permitted, the sum of moments acting on the cage about the bearing x axis is required to be zero. This moment equation considers the cage-rolling element normal and friction forces as well as the torque generated at the cage-ring surface.

If there is significant rolling element orbital speed variation, the cage is permitted to move to an eccentric position with respect to the land on which it is piloted. Two additional degrees of freedom are required to describe the eccentric position. These are the cage center of mass radial displacement, e, and the angular displacement of the center of mass, with respect to the bearing Y axis, θ c', see Figures 2-5 and 2-6. These radial and angular displacement variables are determined when the sum of forces acting on the cage, resolved along the bearing Y and Z axes, reduce to zero. The rolling element-cage normal and friction forces as well as the pressure

FIGURE 2-5

Inner Ring-Cage Land Contact Geometry

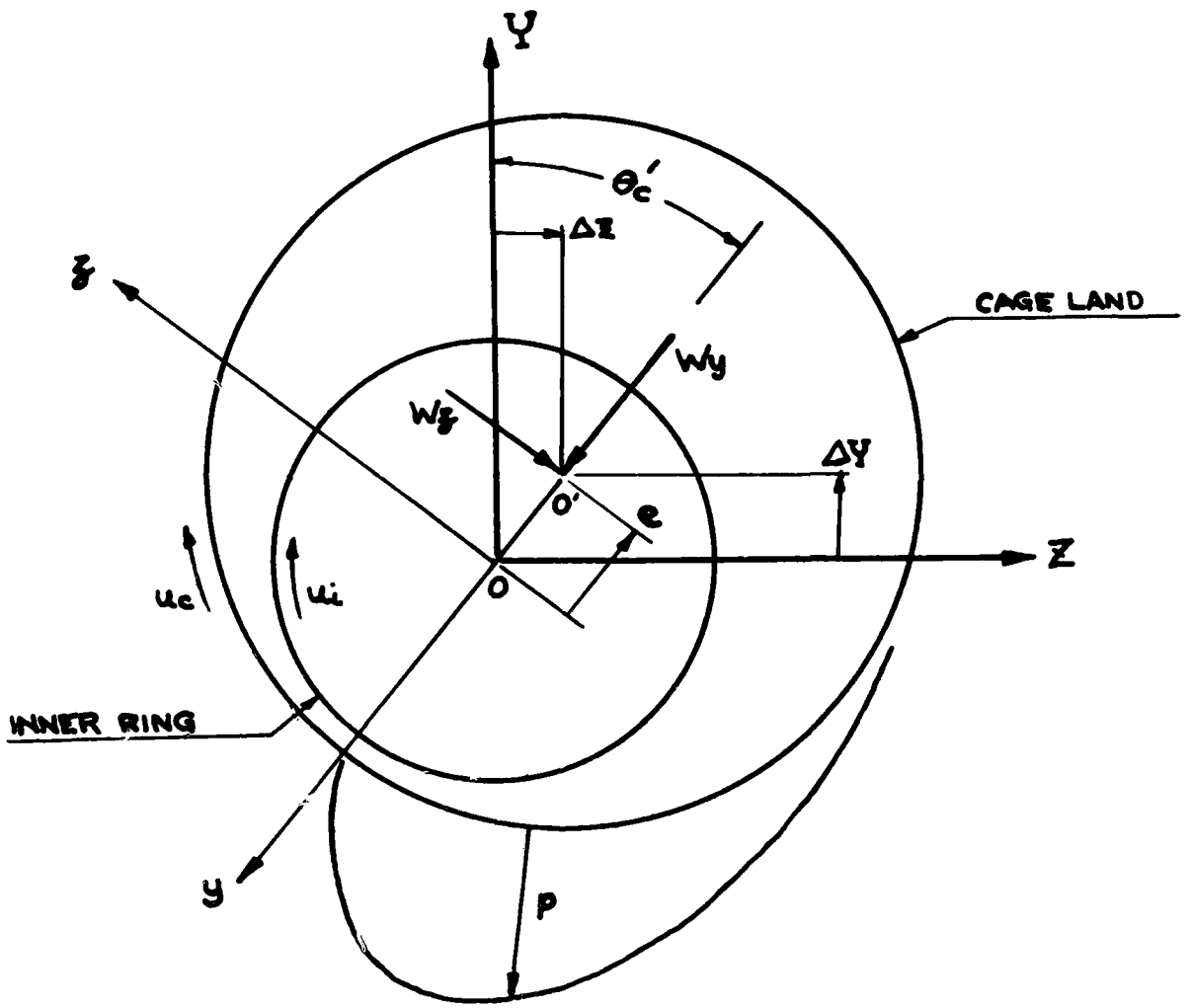

$$\theta_c = \theta_c' + \pi$$

FIGURE 2-6

Outer Ring-Cage Land Contact Geometry

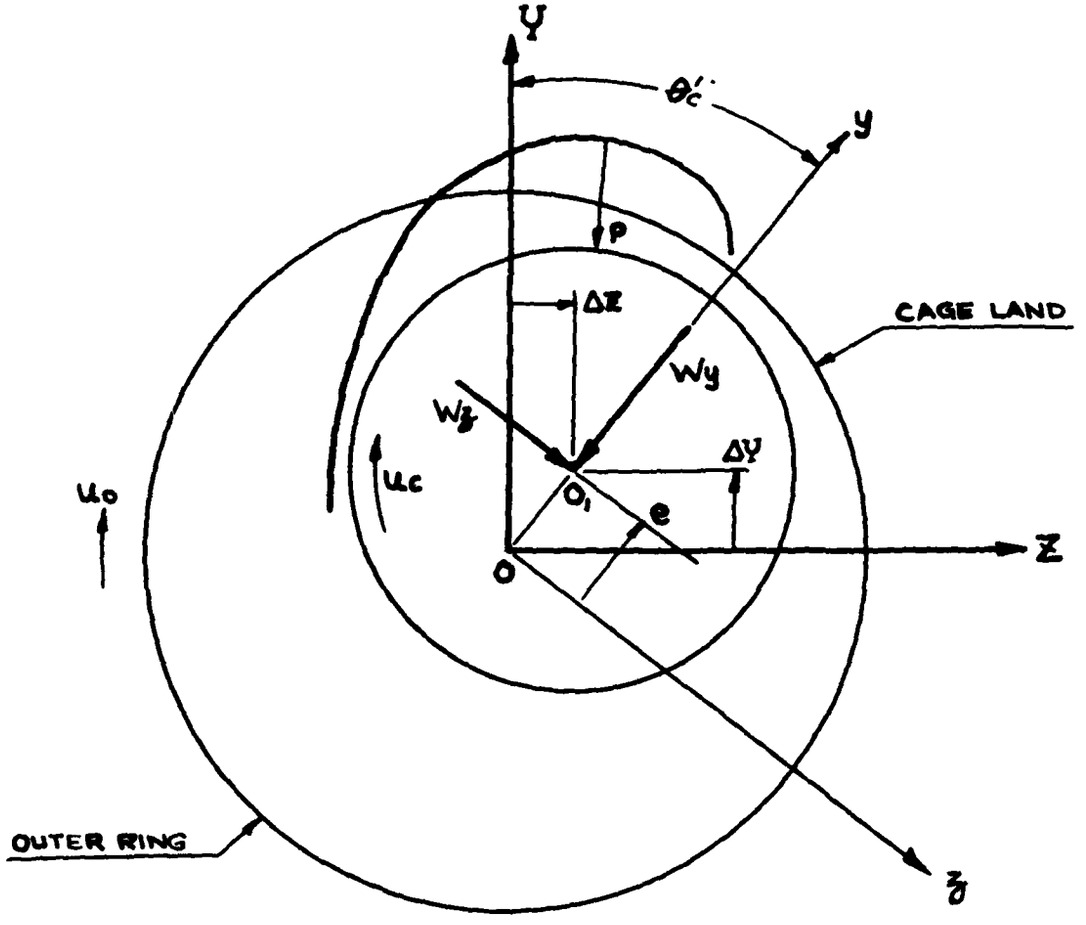

$\theta_c = \theta_c'$

buildup between the cage and its piloting surface are considered in the equilibrium equations. The effect of the cage mass is neglected.

Figure 2-7 depicts the cage pocket normal and friction forces acting on a rolling element which are considered in the cage equibrium solution. These forces are functions of the rolling speeds ω_x and ω_y and the contact geometry are calculated in the x,y,z frame. The forces exerted on the cage due to the i-th rolling element are, in the XYZ frame of reference:

$$
\begin{aligned}
M_{Xi} &= -(F_{y1} + F_{y2})_i r + (P_1 - P_2)_i R_m \\
F_{Yi} &= -(F_{y1} - F_{y2})_i \cos \phi_i - (P_1 - P_2)_i \sin \phi_i \\
F_{Zi} &= (F_{y1} - F_{y2})_i \sin \phi_i + (P_1 - P_2)_i \cos \phi_i
\end{aligned}
\tag{2.41}
$$

when the forces of Eq. (2.41) are summed over all of the rolling elements, and the total added to the cage land contact forces, the cage equilibrium equations for the three degree of freedom model are obtained as:

$$
\begin{aligned}
M_X = 0 &= (M_{Xi}) + M_{cX} \\
F_Y = 0 &= (F_{Yi}) + F_{cY} \\
F_Z = 0 &= (F_{Zi}) + F_{cZ}
\end{aligned}
\tag{2.42}
$$

where M_{Xi}, F_{Yi} and F_{Zi} are defined for each rolling element by Eq. (2.41), M_{cX} is the cage land friction torque, F_{cY} and F_{cZ} are the cage land hydrodynamic forces.

Within SHABERTH, Eq. (2.42) which defines cage equilibrium, are solved simultaneously with the set of all ball or roller quasidynamic equilibrium equations.

Details for calculating the rolling element/cage pocket forces and the cage land/ring land forces are presented in Appendix I 9.

The ball bearing friction solution is thus obtained by solving 6Z+(1 or 3) equations where Z is the number of rolling elements. The ball bearing frictionless solution is obtained by solving 1,(Z/2) (Z/2+1) or Z sets of 2 equations, depending upon the number of rolling elements in the bearing and the degree of load symmetry which prevails. The various symmetry conditions are explained below.

The roller bearing friction solution contains 4Z+(1 or 3) equations and the frictionless solution contains Z/2, Z/2+1 or Z sets of three equations again depending upon the number of rolling elements and whether or not load symmetry exists.

FIGURE 2-7

Cage Pocket Normal and Friction Forces
Affecting Equilibrium

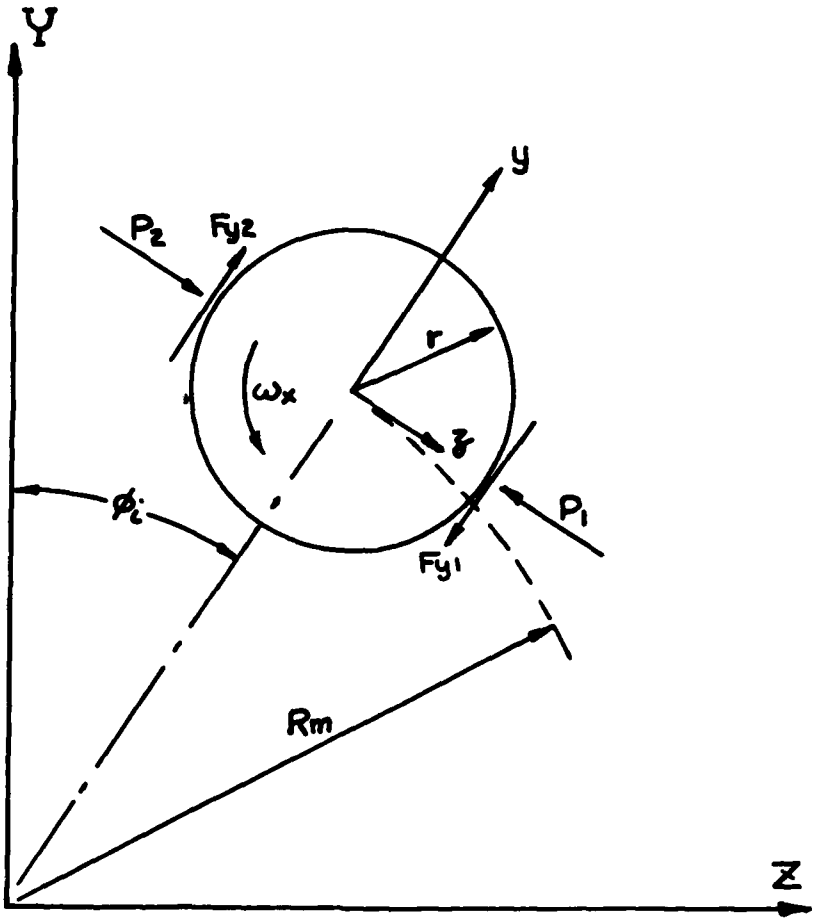

2.4.3 Load Symmetry Conditions

The various load symmetry conditions are as follows.

Axial symmetry is utilized if, for a ball bearing the load is axial only, then only one set of two equations is solved for the frictionless case. Six ball and one cage equilibrium equations are solved when friction is included. All balls are assumed to behave identically.

Radial load symmetry is utilized if the non-axial shaft loading is comprised of only radial components parallel to the Y axis and moment components parallel to the Z axis and the position of the first rolling element is on the Y axis, then symmetry exists, only half the rolling elements need be considered if the number of rolling elements is even and one half plus one need be considered if the number is odd. Because of inertia terms, radial load symmetry can only be utilized in the frictionless solution.

If load symmetry is not present, then Z sets of two (ball bearing) or Z sets of three (roller bearing) equations must be solved to obtain the frictionless solution.

2.4.4 Bearing Quasidynamic Solution Criteria

As with the steady state temperature mapping scheme, the Newton-Raphson scheme in subprogram SOLVXX is used to solve the sets of equations for each bearing. The iteration scheme terminates when either:

$$\left| \frac{\Delta X_{iN}}{X_{iN-1}} \right| \underset{i=1\ldots n}{\leq} \begin{cases} \text{EPS1} & \text{frictionless} \\ \text{EPS2} & \text{friction} \end{cases} \tag{2.43}$$

or

$$\left(\frac{\sum_{i=1}^{n} EQ_i^2}{n} \right)^{\frac{1}{2}} \leq 100 \text{ X} \begin{cases} \text{EPS1} & \text{frictionless} \\ \text{EPS2} & \text{friction} \end{cases} \tag{2.44}$$

Experience has shown that the second criteria is usually responsible for terminating the solution. However, when rolling element loads are extremely large, on the order of 10^5 Newtons, it becomes difficult to reduce the equation residues to less than 10 Newtons. In those instances, the first criteria usually terminates the iteration scheme.

3. PROGRAM INPUT

3.1 Types of Input Data

A complete set of input data comprises data of four distinct categories. Within these categories, cards which convey specific kinds of information are referred to as card types. Depending on the complexity of the problem, the input data set may contain none, one or several cards of a given type. The categories are listed below.

I. Title Cards
A title card plus a second card which provides the program control information for the shaft-bearing solution.

II. Bearing Data Cards
A set of up to sixteen (16) card types, each set describing one bearing in the assembly. All bearings must be so described. The card sets must be input sequentially in order of increasing distance from a selected end of the shaft.

III. Thermal Data Cards
A set of up to nine (9) card types to describe the thermal model of the assembly.

IV. Shaft Data Cards
A set of three (3) card types to describe the shaft geometry, bearing locations on the shaft and shaft loading

If the program is being used to predict the performance of a bearing assembly, cards from all four sets must be included in the runstream. If the program is being used to thermally model a mechanical system wherein no bearing heat generation rates are required, and therefore, no bearing calculations need be performed, the cards from sets II and IV are omitted.

The review of required input information which follows is broken into the four sets of data categories given above, with special emphasis on program control data.

The input data instructions are given in Appendix II 2, and are for the most part self explanatory. They are laid out in the format of an eighty column data card. A description of the variables is given in the input instruction forms.

The units used for input data are as follows:

Linear Dimensions - (mm)
Angles - (degrees)
Surface Roughness - (microns)
Bearing Angular Mounting Errors - (radians)
Rotational Speeds - (RPM)
Force - (Newtons) (N)
Moments - (N-mm)
Pressure, Elastic Modulus - (N/mm^2)
Density - (gm/cm^3)
Kinematic Viscosity - (cs)
Temperature - (degrees centigrade) (^oC)
Coefficient of Thermal Expansion - ($^oC^{-1}$)
Thermal Conductivity - (Watts/m/^oC)

3.2 Data Set I - Title Cards

3.2.1 Title Card 1

This card should contain the computer run title and any information which might prove useful for future identification. The full eighty (80) columns are available for this purpose. The title will appear at the top of each page of Program output.

3.2.2 Title Card 2

This card provides the control information for the shaft bearing solution.

Item 1: Shaft Speed in rpm, GOV (1). All bearings have the same shaft, i.e. inner ring speed.

Item 2: Number of Bearings on the shaft (NBRG), a minimum of zero is permitted if no bearing solution is being sought. A maximum of five is permitted.

Item 3: Print Flag (NPRINT), NPRINT equal to zero is normal and will result in no intermediate or debug output. With a value of one, a low level intermediate print is obtained at the end of each shaft bearing iteration. The values of the variables, the inner ring displacements (DEL), and the equation residues are printed.

At the end of each bearing iteration, wherein the rolling element and cage equilibrium equations are solved, an error parameter is printed which has the value:

Error Parameter = X_N/X_{N-1}

X_N is the change in the variable X specified at iteration N.

X_{N-1} is the value of the variable specified at the previous iteration.

The Error Paremeter is calculated for each of the bearing variables, but only the largest one is printed.

Additionally, at the end of each Clearance Change iteration, the clearance change error parameter is printed. This error is defined by Eq. 2.28.

If NPRINT is set at 2, all of the above information is printed. Additionally, the variable values and residue values are printed for each iteration of the rolling element and cage equilibrium solution.

Item 4: ITFIT controls the number of iterations allowed to satisfy the bearing clearance change iteration scheme. If ITFIT is set to zero (0), or left blank, the clearance change portion of the program is not executed. If a position integer is input, the clearance change scheme is utilized with a maximum iteration limit of five (5). If a negative interger is input, the scheme is used with a maximum iteration limit equal to the absolute value of the negative integer.

Item 5: ITMAIN limits the number of iterations attempted during the solution of the shaft and bearing inner ring equilibrium problems, i.e., establishing the equilibrium of bearing reactions and applied shaft loads. If ITMAIN is left blank, set to zero, or to a positive integer, then (15) iterations are premitted. If ITMAIN is set to a negative integer, the number of iterations is limited to the absolute value of that integer.

Item 6: GOV(2) or EPSFIT is the convergence criterion for the diametral clearance change portion of the analysis. As mentioned under item 3 above, this error parameter is defined by Eq. 2.28.

The iteration scheme is terminated when the error parameter is less than the input value of EPSFIT. If EPSFIT is left balnk or is set to zero (0), the program default value of 0.0001 is used.

Items 7 & 8: Main loop accuracy for frictionless elastic (EPS1) and friction solution (EPS2). These accuracy values control the accuracy of the shaft bearing deflection solution as well as the quasi-dynamic solution of the component dynamics (cf. Section 3). If EPS1 and EPS2 are left blank or set to zero (0), default values of 0.001 and 0.0001 respectively are used.

Item 9: IMT, if set to 1, the Material properties for both bearing rings and the rolling elements are to be input on card types B 11 through B 19. If IMT is zero or blank, the rings and rolling elements are assumed to be steel. Card types B 11 through B 14 are required only if the change in bearing diametral clearance is to be calculated.

Item 10: NPASS controls the level of the bearing solution

0 Elastic Contact Forces are calculated. No lubrication or friction effects are considered.

1 Elastic Contact Forces are calculated. Lubrication and friction effects are considered using raceway control (ball bearing) or epicyclic (roller bearing) assumptions to estimate rolling element and cage speeds.

2 Inner Equilibrium is satisfied considering only the Elastic Contact Forces. Using the inner ring positions thus obtained, rolling element and cage equilibrium are determined considering friction.

3 Complete Solution. The inner ring, rolling element and cage equilibrium is determined considering all elastic and friction forces.

3.3 Data Set II - Bearing Data

Most of the input instructions are self-explanatory. Where certain items are deemed to require more explanation than given in the input data format instructions, they are treated on an individual basis by card type and item number.

Most of the bearing input data is read into a two dimensional array named "BD," which has the dimensions (1830, 5). For each of the five bearings permitted on a shaft, a total of 1830 pieces of data may be stored. Denoting BD(I,J), I represents a specific piece of bearing data, J represents the bearing number. The bearing input data of Data Set II occupies the first 106 locations of the 1830 allocated. On the input data format sheets, the designation BD(I) where I-1...106, denotes the location within the BD array where each piece of input data is stored.

3.3.1 Card Type 1 - Bearing Type and Material Designations

Item 1: Bearing type, columns 1-10 must be specified, left justified, i.e., "B" or "C" in column 1. This format must be followed since the Program recognition of bearing type, (ball bearing or cylindrical roller bearing), is derived from reading the "B" or "C" in the first column of this card.

Item 2 & 3: Columns 11-30 and 31-50, "Steel designations," inner and outer rings, respectively. The alphameric-literal description of the steel types such as "M-50" or "AISI 52100" is input.

Items 4 & 5: Columns 51-60 and 61-70, the numbers input for items 4 (inner ring) and 5 (outer ring) are used to account for improved materials and multiply the raceway fatigue lies as determined by Lundberg-Palmgren methods. Typical life factor values for modern steels are in the neighborhood of 2.0 to 3.0. If the ASME Publication Life Adjustment Factors for Ball and Roller Bearings, is referenced by the user, the Material Factor D and the Material Process Factor E should be used multiplicatively as inputs for items 4 and 5. Additionally, if the user is accustomed to using a lubricant life multiplier he must also multiply the material factor by the lubricant life multiplier. The program considers EHD film thickness and RMS surface roughness but generates a life multiplier having a maximum value of 1 and a minimum of 0.479, i.e. Lube-Life Factor Programmed only serves to reduce predicted Fatigue Life.

Item 6: Columns 71-78, "Orientation angle of the first rolling element." (ø1) (degrees). Refer to Fig. (2.4). The quasi-dynamic rolling element bearing problem has an infinite number of solutions which fall within a narrow envelope having a periodic shape. The solution obtained is a function of the rolling elemént positions relative to the bearing system coordinate axes. ø1 = 0, places a rolling element on the Y axis and is the choise customarily made. ø1 can be desig-

nated as any value $0 \leq \phi \frac{360}{Z}$ where Z is the number of rolling elements. For each different value assigned to ø1, a different, although similar, bearing solution will be obtained. To take advantage of bearing symmetry and the computer time savings which result, ø1 must be specified as zero or left blank.

Item 7: Column 80, a signal, termed the crown drop flag, which specifies for a cylindrical roller bearing, whether the roller-race crown drops will be calculated, or read directly. If item 7 is blank or zero, the crown drops are calculated based on the roller-race crown radius, and effective flat length input information. If the crown drop flag is other than zero or balnk, the non-uniform separation of the roller and raceway must be specified at the center of each slice into which the roller-raceway effective contact length is divided. The slice widths are identical. The number of slices is input as item 7 card type B4. The non-uniform roller-raceway separation is input on card types B5 and B6.

3.3.2 Card Type B2 - Bearing Geometry and Outer Ring Speed

Item 1, 2 and 5 need no explanation, however, items 3 and 4 require substantial explanation as they apply to the various types of ball bearings.

3.3.2.1 Ball Bearing Geometry

Through the proper specification of the diametral clearance and contact angle, the Program can properly handle deep grove, split inner, and angular contact ball bearings.

The deep groove ball bearing requires the specification of zero contact angle and either the operating diametral clearance Pd or the off-the-shelf diametral clearance, if the dimensional change analysis is utilized.

The angular contact bearing is fully described through specification of the contact angle which obtains under a gauge, axial load. However, this method of input does not accurately define the system if there is more than one angular contact supporting the shaft and at least one of those bearings has its grooves offset in the direction opposite to the other bearings and if the shaft is capable of axial and/or radial play. In other words, if what are known as angular contact ball bearings are mounted such that some diametral shaft play is permitted, an auxilliary angle as well as the diametral play must be specified at input. The angle input is not the

manufacturer's designated contact angle, α, but an auxilliary angle, α_o, the calculation for which shall be demonstrated.

Refer to Figure 3.1. The manufacturer's contact angle is calculated as follows:

$$\alpha = \cos^{-1} \left[\frac{2A-Pd}{2A}\right] \tag{3.1}$$

$$A = r_o + r_i - D \tag{3.2}$$

where: r_o and r_i are the outer and inner raceway groove radii respectively

D is the ball diameter

Under a gauge axial load α is obtained at both inner and outer raceways for each ball. Under this condition, the outer and inner raceways are axially offset an amount s_α.

$$s_\alpha = A \sin\alpha \tag{3.3}$$

When angular contact ball bearings are mounted with some diametral play, the grooves are offset an amount S_{α_o} such that $S_{\alpha_o} < S_\alpha$. The diametral play which obtains at this condition is Sd. This diametral play is usually known by the engineer or designer and is usually required to allow some forgiveness when thermal gradients are encountered. Assuming that the user has the values for α, r_o, r_i, D and S_{α_o} then:

$$\alpha_o = \tan^{-1} \left[\frac{S_{\alpha_o}}{A - \frac{Pd}{2}}\right] \tag{3.4}$$

where: Pd and A may be calculated from Eqs. (3.1) and (3.2).

The manufacturer might be able to provide the value of S_{α_o} at the Sd value of interest. If not, the following equation may be solved for α_o.

FIGURE 3-1

Angular Contact Ball Bearing

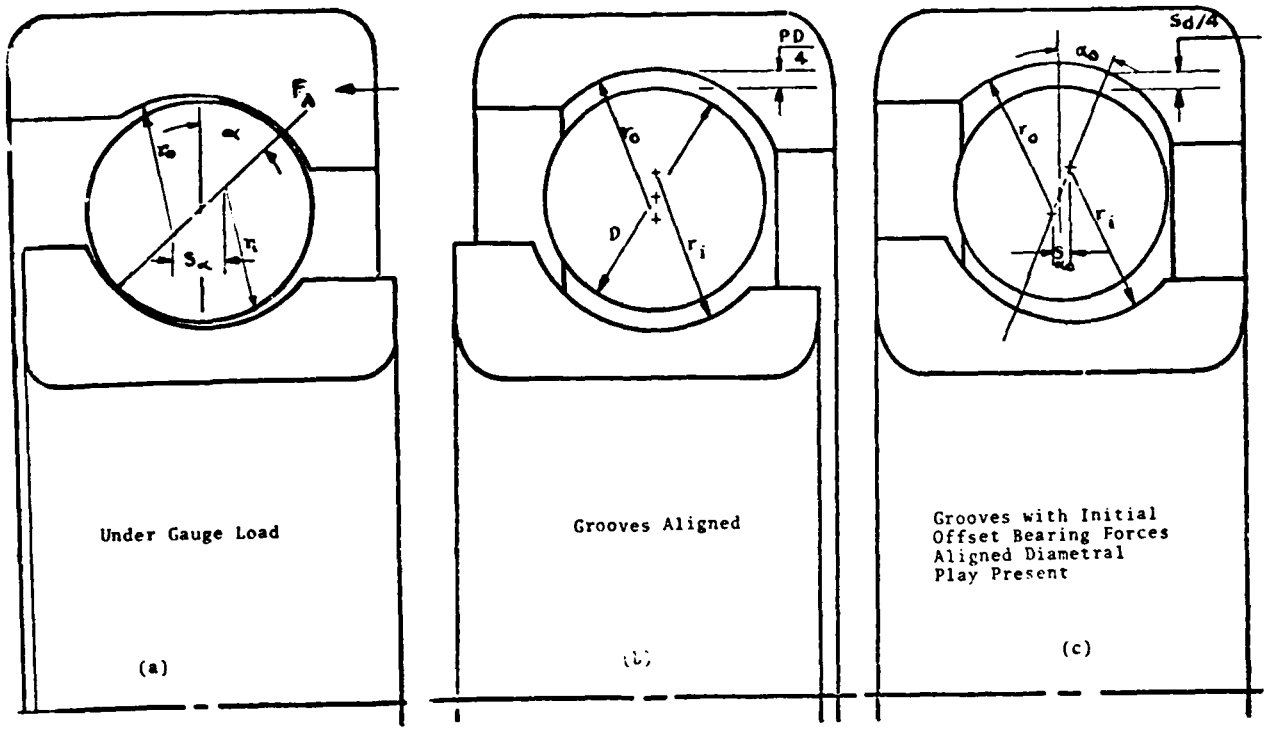

$$\frac{Sd}{2} \cos^2 \alpha_o - A \cos\alpha_o + A - \frac{Pd}{2} = 0 \qquad (3.5)$$

Note: $S\alpha_o$ should be less than $S\alpha$ and α_o should be less than α.

Equation (3.6) is derived by developing two expressions for the radial separation (A_r) of the outer and inner raceway curvature centers.

$$Ar = A - \frac{Pd}{2}$$

$$Ar = (A - \frac{Sd}{2}\cos\alpha_o) \cos\alpha_o \qquad (3.6)$$

$$A - \frac{Pd}{2} = A \cos\alpha_o - \frac{Sd}{2}\cos^2\alpha_o$$

In order that the Program properly handle split inner ring ball bearings an auxilliary angle and diametral play must be input. Referring to Figure 3.2, the auxilliary angle α_o and diametral play Sd must be determined and input. Typically, the values of D, r_o, α_s and Sd' are known. Pd and Sd may be calculated as follows:

$$Pd = Sd' + (2ri-D) (1-\cos\alpha_s) \qquad (3.7)$$

$$Sd = \left[Pd - 2A (1-\cos\alpha_o)\right] / \cos^2\alpha_o \qquad (3.8)$$

The unloaded half of the inner ring must be removed from consideration and the ball moved such that its center lies on the line connecting the origins of r_i and r_o and positioned such that the auxilliary clearance Sd/4 exists at both the inner and outer raceways. The auxilliary angle is

$$\alpha_o = \tan^{-1} \left[\frac{(r_i - D/2) \sin\alpha_s}{r_o - D/2 - Sd'/2 + (r_i - D/2) \cos\alpha_s} \right] \qquad (3.9)$$

FIGURE 3-2

Split Inner Ring Ball Bearing Geometry

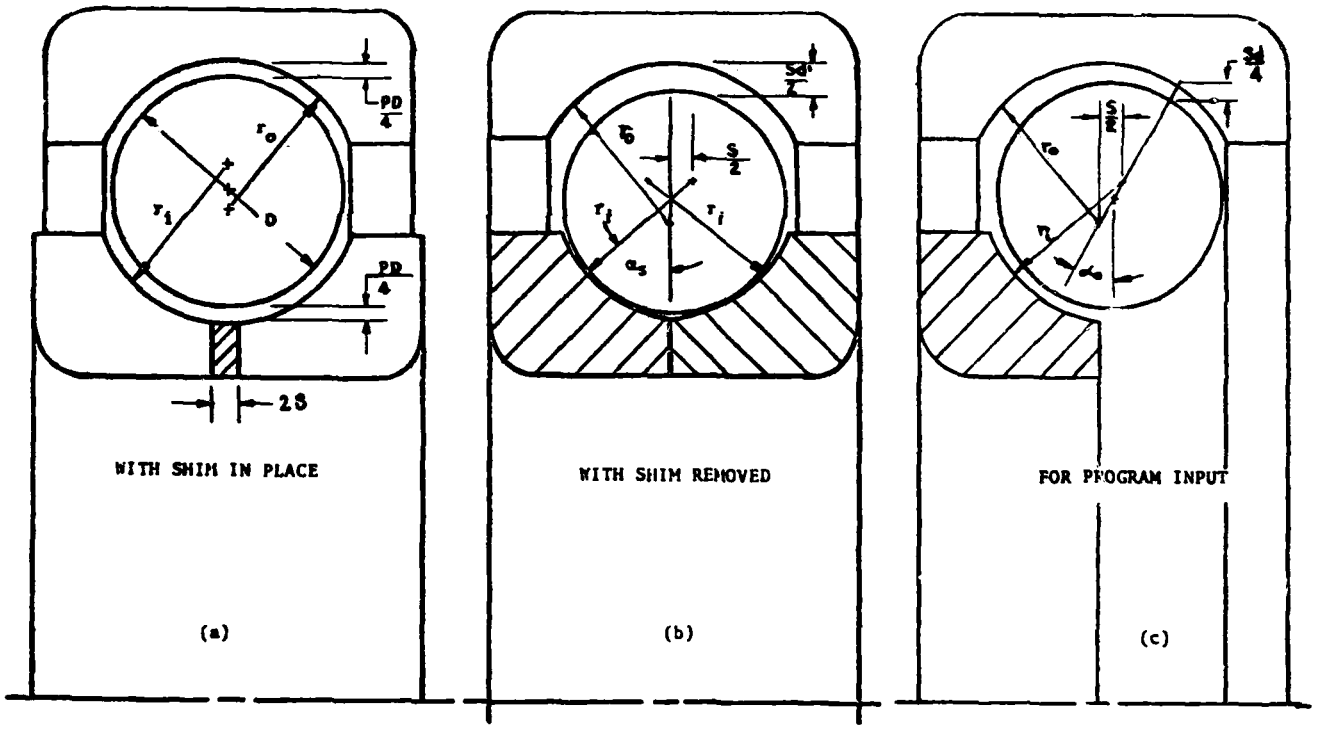

The angle associated with each ball bearing must be specified with the correct sign. A positive contact angle allows the bearing to accept a positively directed axial load transmitted by the shaft.

3.3.3 Card Type B3 - Rolling Element Geometry

These data are self explanatory. Although space has been set aside for the specification of roller end radius and roller included angle, this has been done for future considerations and are not used by the program. The items may be left blank.

3.3.4 Card Type B4 - Raceway and Roller Raceway Contact Geometry

3.3.4.1 Ball Bearing

Items one and two refer to the outer and inner raceway curvatures respectively where curvature is defined as the cross groove radius divided by the ball diameter. Typical values range from 0.515 to 0.57.

3.3.4.2 Roller Bearing Contact Geometry Data

All items are used to define the roller-race contact geometry, see Fig. 3.3 "Flat length" and "Crown Radius" are used to calculate roller-race separation along the roller profile if this information is not specifically input. See Item 7 of the Bearing Data title card and Bearing Data Cards B5 and B6.

Items 1 and 4 "Effective Contact Length" refer to the longest possible length which can obtain at a roller-race contact. Typically, this is the roller total length less the corner radii. If, however, the raceway undercuts are exceptionally large so that the tract width is smaller than the effective roller length then the tract width should be input.

Item 7 refers to the number of slices into which the roller raceway contact may be divided. A maximum value of twenty is permitted a default value of two is used if Item 7 is blank or zero. Each slice is the same width.

3.3.5 Roller-Raceway Non-Uniform Profile Definition

3.3.5.1 Card Type B5 - Inner Roller Raceway Contact

These cards are used to input the inner and outer race roller-race separation along the roller profile. With the high points of the roller and race in contact, i.e. with all clearance between roller and raceway removed. These cards must be omitted if item 7 of the Bearing Data Title card is zero or blank.

FIGURE 3.3

Roller-Race Lamination Showing Relative Approach (δn) and Crown Drop (δc)

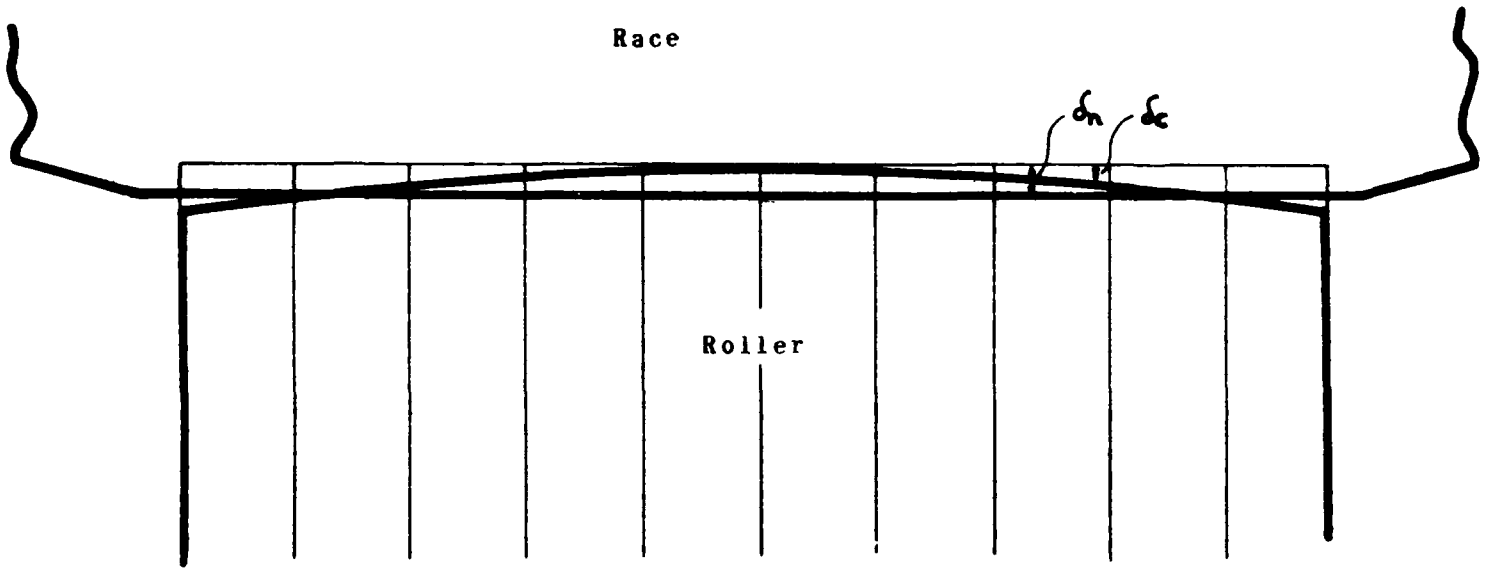

3.3.6 Card Type B6 - Outer Roller Raceway Contact

Same as Card Type B5.

3.3.7 Card Type B7 - Raceway-Rolling Element Surface Data

Items 1 through 6 define the statistical surface micro-geometry parameters of the rollers and raceways. Items 1 through 3 require the input of center line average CLA surface roughness. Within the program CLA values are converted to RMS by multiplying by 0.9.

Items 4 through 6 are RMS values of the slopes measured in degrees of the surface asperities as measured in a traverse across the groove for rings, longitudinally for rollers and in any arbitrary direction for balls. Typical values for raceway and rolling element surfaces are 1 to 2 degrees. This card is omitted if item 10 of title card 2 is zero or blank.

3.3.8 Card Type B8 - Cage Data

This card is omitted if item 10 of the title card 2 is zero or blank. These data are self explanatory. Note that the cage weight is an input item. The weight, however, is not used in any calculation. It is included only for future consideration of cage stability predictions.

3.3.9 Card Type B9 - Shaft and Housing Fit Dimensions

These cards are to be included only if the change in bearing diametral clearance with operating conditions is to be calculated, i.e. if item 4 ITFIT on the Bearing Title Card 2 is non-zero. On Card Type B9, tight interference fits bear a positive sign and loose fits, a negative sign.

Items 3 and 6 on Card No. 9 are termed the shaft and housing effective widths, respectively. The value specified for these effective widths may be as great as twice the ring width.

Use of an effective width is an attempt to account for the greater radial rigidity of a shaft than the ring that is pressed on to it, owing to the fact that the shaft deflects over a distance that extends beyond the ring width. In the program, the calculated internal pressure on the ring due to

its interference fit with the shaft, is distributed over the shaft effective width and this (lower) pressure is used in computing the shaft deflection. Using double the actual width as the effective width is customary.

3.3.10 Card Type B10 - Shaft Housing Fit Dimensions

These items are self explanatory, and are used to describe equivalent ring sections, see Fig. I 2.1.

3.3.11 Card Type B11

This card defines the elastic modulus for the shaft, inner ring, rolling element, outer ring, and housing, respectively. This card is to be included only if the change in bearing diametral clearance with operating conditions is to be calculated, i.e., if item 4 ITFIT on the Bearing Title Card is non-zero.

3.3.12 Card Type B12

This card defines the Poisson's ratio for the shaft, inner ring, rolling element, outer ring, and housing, respectively. This card is to be included only if the change in bearing diametral clearance with operating conditions is to be calculated, i.e., if item 4 ITFIT on the Bearing Title Card is non-zero.

3.3.13 Card Type B13

This card defines the density for the shaft, inner ring, rolling element, outer ring, and housing, respectively. This card is to be included only if the change in bearing diametral clearance with operating conditions is to be calculated, i.e., if item 4 ITFIT on the Bearing Title Card is non-zero.

3.3.14 Card Type B14

This card defines the coefficient of thermal expansion for the shaft, inner ring, rolling element, outer ring, and housing, respectively. This card is to be included only if the change in bearing diametral clearance with operating conditions is to be calculated, i.e., if item 4 ITFIT on the Bearing Title Card is non-zero.

3.3.15 Card Type B15 - Lubrication and Friction Data

This card is omitted if item 10 of title card 2 is zero or blank.

Items 1 and 2

These items are the amounts by which the combined thickness of the lubricant film on the rolling track and rolling element is increased during the time interval between the passage of successive rolling elements, from whatever replenishment mechanisms are operative. Items 1 applies to the outer and Item 2 to the inner race-rolling contacts, respectively. If Item 1 is zero or blank, the mode of friction is assumed to be dry.

At the present time, the magnitude of the inner and outer raceway replenishment layers has not been correlated to lubricant flow rate, lubricant application methods and bearing size and speed factors. At this point then, the user is forced to establish proper values for the replenishment layer thickness. As a rough guide, the following suggestions are made.

1. To avoid starvation, the replenishment layer thicknesses should be one or two times the EHD film thickness which develops in the rolling element raceway contacts.

2. Because of centrifugal force effects, intuition suggests that the outer raceway replenishment layer should be several times thicker than that prescribed at the inner raceway.

Item 3, XCAV, describes the percentage of the bearing cavity, estimated by the user to be occupied by the lubricant. $0 \leq XCAV \leq 100$.

As with the replenishment layer thicknesses, the amount of free lubricant should be able to be correlated with lubricant flow rate, lubricant application methods and bearing size and speed factors. At this time, such correlations do not exist. XCAV values of approximately one percent are recommended at this point.

Item 4 is the coefficient of coulomb friction applicable for the contact of asperities. If Items 1 and 2 are zero, then Item 4 serves as the coulomb friction coefficient which prevails in all contacts.

3.3.16 Card Type B16

This card is omitted if Item 10 title card 2 is zero or blank or if Item 1 card 15 is zero or blank which implies dry friction.

This card specifies the lubricant type. If Item 1, NCODE is 1, 2, 3, or 4, the Program uses preprogrammed lubricant properties as presented in Table 1, and no further information is required.

TABLE 1

PROPERTIES OF FOUR LUBRICANTS

LUBRICANT NO.	LUBRICANT TYPE	KINEMATIC VISCOSITY 37.78°C (100°F)	(cs) 98.89°C (210°F)	DENSITY @15.56°C (60°F) gm/cm^3	THERMAL CONDUCTIVITY W/m/°C	THERMAL COEFF. OF EXPAN. 1/°C* 10^{-4}
1	Mineral Oil	64.0	8.0	0.88	0.116	6.336
2	MIL-L-7808G	17.8	3.2	0.95	0.152	7.092
3	C-Ether	25.4	4.13	1.20	0.119	7.470
4	MIL-L-23699	28.0	5.1	1.01	0.152	7.452

NCODE	Lubricant
1	A specific mineral oil
2	A MIL-L-7808G
3	C-Ether
4	A MIL-L-23699

NCODE may also be specified as negative (-1 to -4), in which case, the traction characteristics of the respective lubricant NCODE noted above are used but the actual properties specified by Items 2 through 7 override the hard coded data. This option is most useful in specifying various mineral oils i.e. NCODE = -1.

3.4 Data Set III - Thermal Model Data

Appendix I 1 has been included to aid the user in data preparation and calculation of heat transfer coefficients required at input.

3.4.1 Card Type 1

Card type 1 is a control card. If no temperature map is to be calculated, this card is to be included as a blank card followed by a Type 2 card for each bearing on the shaft. Card Type 1 contains control input for both steady state and transient thermal analyses. It is not intended, however, that both analyses be executed with the same run.

Item 1: The highest node number (M). The temperature nodes must be numbered consecutively from one (1) to the highest node number. The highest node number must not exceed one hundred (100).

Item 2: Node Number of the Highest Unknown Temperature Node (N). This number should equal the total number of unknown node temperatures. It is required that all nodes with unknown temperatures be assigned the lowest node numbers. The nodes which have known temperatures are assigned the highest numbers.

Item 3: Common Initial Temperature (TEMP)^{o}C: The temperature solution iteration scheme requires a starting point, i.e., guesses of the equilibrium temperatures. Card Type 3 allows the user to input guesses of individual node temperatures. When a node is not given a specific initial temperature, the temperature specified as Item 3 of Card Type 1 is assigned.

Item 4: Punch Flag (IPUNCH): If the Punch Flag is not zero (0) or blank, the system equilibrium temperature along with the respective node numbers will be punched according to the format of Card T3. This option is useful if, for instance, the user makes a steady state run with lubrication, and then wishes to use the resultant temperature as the initiation point for a transient dry friction run in order to assess the consequence of lubricant flow termination.

Item 5: "Output Flag" (IUB). If the "Output Flag" is not zero, the bearing program output and a temperature map will be printed after each call to the shaft bearing solution scheme. This printout will allow the user to observe the flow of the solution and to note the interactive effects of system temperatures and bearing heat generation rates. Since the temperature solution is not mathematically coupled to the bearing solution, the possibility exists that the solution may diverge or oscillate. In such a case, study of the intermediate output produced by the "Output Flag" option may provide the user with better initial temperature guesses that will effect a steady state solution.

Item 6: "Maximum Number of Calls to the Shaft Bearing Program" (IT1). IT1 is the limit on the number of Thermal-Shaft-Bearing iterations, i.e., the external temperature equilibrium calculation. The user must input a non-zero integer such as 5 or 10 in order for the Program to iterate to an equilibrium condition. If IT1 is left blank or set to zero (0) or 1, shaft bearing performance will be based on the initially guessed temperatures of the system. The temperatures printed out will be based on the bearing generated heats. It is unlikely that an acceptable equilibrium condition will be achieved. However, the temperatures which result may provide better initial guesses, for a subsequent run, than those specified by the user.

IT1 also serves as a limit on the transient temperature solution scheme, by limiting the number of times the shaft-bearing solution scheme is called. Each call to the shaft-bearing scheme will input a new set of bearing heats to the transient temperature scheme until a steady state condition is approached or until the transient solution time up limit is reached.

Item 7: "Absolute Accuracy of Temperatures for the External Thermal Solution" (EP1). In the steady state thermal solution scheme, each calculation of system temperatures occurs after a call to the shaft-bearing scheme which produces bearing generated heats. After the system temperatures have been calculated for each iteration, using the internal temperature solution scheme, each node temperature is checked against the nodal temperature at the previous iteration.

If $\{t_{(N)i} - t_{(N-1)i}\} \leq$ EP1 for all nodes i then equilibrium has been achieved and the iteration process stops.

Item 8: "Iteration Limit for the Internal Thermal Solution" (IT2). After each call to the shaft-bearing program, the internal temperature calculation scheme is used to determine the steady state equilibrium temperatures based on the calculated set of bearing heat generation rates. If the program is used to calculate the temperature distribution of a non bearing system, it is the internal temperature scheme which is employed. If IT2 is left blank or set to zero, the number of internal iterations is limited to twenty (20).

Item 9: "Accuracy for Internal Thermal Solution" (EP2). The use of EP2 is explained in Section 2.1.1. If EP2 is left blank or set to zero (0), a default value of 0.001 is used.

Item 10: "Starting Time" (START) is a time T_s at which the transient solution begins; usually set to zero (0).

Item 11: "Stopping Time" (STOP) is the time in seconds at which the transient solution terminates, T_f. The transient solution will generate a history of the system performance which will encompass a total elapsed time of

$$(T_f - T_s) \text{ seconds}$$

Item 12: "Calculation Time Step" (STEPIN). The transient internal solution scheme solves the system of equations

$$t_{k+1} = t_k + \frac{q_k}{\rho C_p V} \Delta T \tag{3.10}$$

$$\Delta T = \text{STEPIN}$$

The user may specify STEPIN. If left blank or set to zero (0), the Program calculates an appropriate value for STEPIN using the procedure described in Section 2.1.2.

Item 13: "Time Interval Between Printed Temperature Maps" (TTIME) seconds. The user must specify the length of time which will elapse between each printing of the temperature map. The interval will always be at least as large as the "calculation timestep" (STEPIN).

Item 14: "Time Interval Between Calls of the Shaft Bearing Portion of the Program" (BTIME). BTIME will always have a value larger than or equal to (STEPIN) even if the user inadvertently inputs a shorter interval. Computational time savings result if BTIME is greater than STEPIN, however, accuracy might be lost.

3.4.2 Card Type 2

Card Type T2 is required, one card for each bearing if no thermal analysis is being performed. The temperature data is used within the shaft-bearing analysis portion of the program to fix temperature dependent properties of the lubricant in which case the inner race, outer race and lubricant bulk cavity temperatures are used. The assembly component temperatures at each bearing location are used in the analysis which calculates the change in bearing diametral clearance from "off the shelf" to operating conditions.

Item 9: "Flange" temperature is not currently used in the analysis. It simply provides for future consideration of tapered roller bearings.

3.4.3 Card Type 3

In the steady state analysis this card is used to input initial guesses of individual nodal temperatures for unknown nodes as well as the constant temperatures for known nodes, such as ambient air and/or an oil sump.

In the transient analysis, Card Type T3 is used to input the nodal temperatures of all nodes at (START) = T_S i.e., at the initiation of the transient solution.

3.4.4 Card Type 4

With this card, node numbers are assigned to the components of each bearing, one card per bearing. With this information, the proper system temperatures are carried into each respective bearing analysis. The inner race and inner ring node numbers may or may not be the same at the user's discretion. Similarly, the outer race and outer ring node numbers may or may not be the same.

3.4.5 Card Type 5

The shaft bearing system analysis accounts for frictional heat generated at four locations in the bearing, i.e., at the inner race, the outer race, between the cage rail and ring land, and in the bulk lubricant due to drag. The heat generated at the hydrodynamic cage-rolling element contact is added to the bulk lubricant. Heat generated at the flange is not presently considered. This card allows the heat generated to be distributed equally to two nodes. For instance, the heat generated at the inner race-rolling element contact should be

distributed half to the rolling element and half to the inner race. The heat developed between the cage and inner ring land may be distributed half to the inner ring and half to the cage if a cage node has been defined, otherwise, half to the bulk lubricant.

3.4.6 Card Type 6

This card specifies the node numbers and the heat generation rate for those nodes where heat is generated at a constant rate such as at rubbing seals or gear contacts.

3.4.7 Card Type 7

This card type is used to input the numerical values of the various heat transfer coefficients which appear in the equations for heat transfer by conductivity, free convection, forced convection, radiation and fluid flow. Up to ten coefficients of each type may be used. Separate values of each type of coefficient are assigned an index number via card T7 and in describing heat flow paths (Card Type T8 below) it is necessary only to list the index number by which heat transfers between node pairs.

Incides 1-10 are reserved for the conduction coefficient λ, 11-20 for the free convection parameters, 21-30 for forced convection, 31-40 for emissivity and 41-50 for fluid flow (product of specific heat, density and volume flow rate).

As an example, for heat transfer by conduction with coefficient λ of 53.7 watts/M^{o}C one could prepare a card type T7 with the digit 1 punched in column 10 and the value 53.7 punched in the field corresponding to card columns 11-20. If a conduction coefficient of 46.7 were applicable for certain other nodes in the system, one could punch an additional card assigning index No. 2 to the value λ = 46.7 by punching a "2" in card column 10 and 46.7 anywhere within card columns 11-20.

Rather than inputting constant forced convection coefficients, optionally, these coefficients can be calculated by the program in oen of three ways. If the calculation option is exercised a pair of cards is used in place of a single card containing a fixed value of α. The contents of the pair of cards depends upon which of the three optional methods are used.

Option 1) is independent of temperature but is calculated as a function of the Nusselt number which in turn is a function of the Reynolds number Re, the Prandtl number P_r as follows, (cf. {17})

$$\alpha = \lambda_{oil}/LN_u \tag{3.11}$$

$$N_u = aR_e^b P_r^c \tag{3.12}$$

where λ_{oil} is the lubricant conductivity, L is a characteristic length (with a unit of meters) and K, a, b and c are constants.

Option 2) α is a function only of fluid dynamic viscosity and viscosity is temperature dependent.

$$\alpha = c\eta^d \tag{3.13}$$

where c and d are constants

Option 3) α is a function of the Nusselt, Reynolds and Prandtl numbers, and viscosity is temperature dependent.

3.4.8 Card Type 8

Thic card defines the heat flow paths between pairs of nodes. Every node must be connected to at least one other node, i.e., two or more independent node systems may not be solved with a single Program execution.

The calculation of heat transfer areas is based on lengths, L_1 and L_2 input using Card Type T8. Additionally, the type of surface for which the area is being calculated is indicated by the sign assigned to the heat transfer coefficient index. If the surface is cylindrical or circular, the index should be positive, if the surface is rectangular the index should be input as a negative integer.

In the case of radiation between concentric axially symmetric bodies, L_3 is the radius of the larger body. For radiation between two parallel flat surfaces or for conduction between nodes, L_3 is the distance between them.

Fluid flow heat transfer accounts for the energy which the fluid transports across a node boundary. Along a fluid node at which convection is taking place, the temperature varies. The nodal temperature which is output is the average of the fluid temperature at the output and input boundaries. If the emerging temperature of the fluid is of interest, it is necessary to have a fluid node at the fluid outlet. At this axiliary node, only fluid flow heat transfer occurs and the fluid temperature would be constant throughout the node. Thus, the true fluid outlet temperature will be obtained.

Conduction of heat through a bearing is controlled by index 51. The actual heat transfer coefficient which contains a conductivity, area and a path length term is calculated in the bearing portion of the program. The term is based upon an average outer race and inner race rolling element contact.

3.4.9 Card Type 9

This card inputs data required to calculate the heat capacity of each node in the system. This card type is required only for a transient analysis.

3.5 Data Set IV - Shaft Input Data

The Shaft-bearing analysis requires all loading to be applied to the shaft. The loads applied to each bearing are a product of the shaft-bearing solution. There is no need for the user to solve the statically determinant or indeterminant system for bearing loads. Even if a single bearing is being analyzed, with the applied load acting through the center of the bearing, data for a dummy shaft must be supplied.

In the analysis, the housing is assumed to be rigid. Provision has been allowed to input data for housing radial and angular spring characteristics. However, this has been done for future consideration of an elastic housing and is therefore currently unavailable.

The shaft input data consists of three card types:

1. Shaft Geometry and Elastic Modulas Data
2. Bearing Position and Mounting Error Data
3. Shaft Load Data

3.5.1 Card Type 1

This card type is used to describe shaft geometry at up to twenty locations along the shaft. The user must place his shaft in a cartesian coordinate system with the end of the shaft at the origin and with the shaft lying along the X-axis.

The shaft may have stepwise and linear diameter variations. The stepwise variations require a single card which specifies different diameters immediately to the left and right of the relevant X shaft coordinate. The shaft analysis assumes a linear diameter variation if on two successive cards, i.e. two successive X coordinates, the diameters to the right of the location differ from the diameters to the left of the location

of the following card. Complex shaft geometries may be approximated with a set of linear diameter variations spaced at close intervals.

If an Elastic Modulus is not specified at the designated input location, the modulus of steel is assumed, 204083 N/mm2.

3.5.2 Card Type 2

This card type locates the bearing inner ring on the shaft in the X-Y and X-Z planes. For a ball bearing, the X coordinate specified locates the inner ring center of curvature. For cylindrical roller bearings, the X coordinate locates the center of the inner race roller path.

In addition to specifying bearing location, the Type 2 card is also used to specify housing radial and angular mounting errors. As mentioned previously, space has been reserved for inputting housing radial and angular spring characteristics, however, these characteristics are not used in the system analysis.

Two sets of Type 2 cards may be required. The first set is always required and defines housing alignment errors in the shaft X-Y plane. The second set defines the housing alignment errors in the shaft X-Z plane and is required only if non zero errors exist for the particular bearing in question.

The first set of Type 2 cards must contain a card for each bearing.

3.5.3 Card Type 3

Type 3 cards are used to specify shaft loading at a given X coordinate. Loading may be applied in the x-y and x-z planes, thus requiring two distinct sets of Type 3 cards. Applied loads may have the form of concentrated radial forces, concentrated moments, linearly distributed radial forces and concentrated axial loads which may be eccentrically applied. If an axial load is eccentrically applied, the moment which results must not be separately calculated and input as a concentrated moment.

Variations in distributed radial loads are handled at input just as shaft linear diameter variations are handled.

Note that each set of Type 3 cards must be followed by a blank card.

Also, note that in order for symmetry conditions (see section 2.4.2) to be considered the second type 3 card must be void of any loading data.

4. COMPUTER PROGRAM OUTPUT

4.1 Introduction

The Program Output is intended to provide the engineer or designer with a complete picture of the shaft-bearing system performance.

In addition to the calculated output data, the input data is listed, thus producing a complete record of the computer run.

A sample set of program output is included for reference as Appendix II 3 and represents an NPASS=2 solution for a two bearing system comprised of a 209 size cylindrical roller bearing, a single 110 mm bore angular contact ball bearing operating at 10,000 rpm under a thrust load of 2,000 lbs. (8,896 Newtons) with MIL-L-23699 lubricant and a 6220 size split inner ring angular contact ball bearing operating at 15000 RPM under shaft loads of 8896 Newtons axial, 2248 Newtons radial and a moment load of 4000 Newton millimeters. The bearings are lubricated with an MIL-L-7808G lubricant.

The first seven pages of output essentially consists of a summary of the input data categorized into bearing, cage, steel, lubricant, fit temperature and shaft geometry and loading data.

For four specific lubricants, see Table 1, the relevant lubricant data has been coded into the Program. In this case, the lubricant input information consists only of a single number which designates the particular lubricant but the relevant information for the lubricant is printed in the input data list.

Except as just noted, the actual results of calculations are printed under the headings "Bearing Output" and "Rolling Element Output."

Key output items are discussed briefly below.

4.2 Bearing Output

4.2.1.1 Linear and Angular Deflections

These deflections refer to the bearing inner ring relative to the outer ring and are defined in the inertial coordinate system of Figure 2.4. The bearing deflections are not necessarily equal to the shaft displacements since the bearing outer ring radial or angular mounting errors may be specified as non-zero input.

4.2.1.2 Reaction Forces and Moments

These values reflect bearing reactions to shaft applied loading and outer ring mounting errors.

When the bearing inner ring has achieved an equilibrium position, the summation of all bearing reaction loads should numerically equal the shaft applied loading. When the level of solution indicated by "NPASS" = 2 is employed, as discussed in Section 5, differences between shaft applied and bearing reaction loads will exist but will typically be less than 10%.

This difference is a consequence of friction forces contributing to the reaction loads whereas the inner ring equilibrium position has been determined considering elastic contact forces only.

4.2.2 Fatigue Life Data

The L_{10} fatigue life of the outer and inner raceways as well as the bearings are presented. The bearing life represents the statistical combination of the two raceway lives. These lives reflect the combined effects of the lubricant film thickness and material life factors. The lubricant film thickness life factor is described in detail in Section 3.

4.2.2.1 h/sigma

The ratio h/σ, also referred to as Λ, is printed for the most heavily loaded rolling element. The variable h, represents the EHD plateau film thickness with thermal and starvation effects considered. The variable σ, represents the composite root mean square surface roughness of the rolling element and the relevant raceway.

4.2.2.2 Life Multipliers

4.2.2.2.1 Lubrication - This life multiplier is a function of h/σ at each concentrated contact and is in the form of a derating factor. Its value ranges from 0.479 for $h/\sigma = 0$ to 1.0 at $h/\sigma \geq 4$. Since the lubricant life multiplier is decremental the normal multiple of 3 used for thick film lubrication must be multiplied by the material life factor normally used and this product should be specified at input. This subject is covered in more detail in Section 3.3.1.

4.2.2.2.2 Material - This output simply reflects the input value. Again, it is covered in Section 3.3.1.

4.2.3 Temperatures Relevant to Bearing Performance

These temperatures fully describe the temperature conditions which affect the performance of a given bearing. If one of the temperature mapping options is used, the temperatures printed reflect the results of the particular option. If, neither temperature option was used, the list is simply a repeat of the input data. Note that there are separate temperatures for outer and inner raceway and ring temperatures. The raceway temperature is used to determine lubricant properties. The ring temperatures are used in the bearing dimension change analysis. The raceway and ring temperatures may be the same value.

4.2.4 Frictional Heat Generation Rate and Bearing Friction Torque

4.2.4.1 Frictional Heat Generation Rate

The various sources of frictional heat generated within the bearings are listed. The values printed for "OUTER RACE, OUTER RINGS, INNER RACE, INNER RINGS, R.E. DRAG AND R.E.-CAGE" represent the sum of the generated heats for all rolling elements. Additionally, the heats printed for the outer and inner raceways plus the rolling element-cage, reflect the friction developed outside the concentrated contacts, i.e., the HD friction as well as the EHD friction developed within the concentrated contacts. The raceway data also include any heat generated as a consequence of asperity contacts. "R.E. DRAG" should be interpreted as the heat resulting from lubricant churning as the rolling elements plow through the air-oil mixture. Items 2 and 4 relevant to rolling element-flange contacts are present for future program expansion.

4.2.4.2 Torque

The torque value is calculated as a function of the total generated neat and the sum of the inner and outer ring rotational speeds. The intent is to present a realistic value of the torque required to drive the bearing. Under conditions of inner ring rotation, the torque value reflects the torque required to drive the inner ring. The inner ring torque includes that fraction of torque required to impart an angular velocity to the lubricant in the bearing. A considerable portion of the lubricant will come to rest within the housing and not at the outer ring. Thus, the measured outer ring torque may not equal the torque at the inner ring.

4.2.5 EHD Film and Heat Transfer Data

4.2.5.1 EHD Film Thickness

These values refer to the calculated EHD plateau film thickness at both contacts of the most heavily loaded rolling element and include the effects of the thermal and starvation reduction factors.

4.2.5.2 Starvation Reduction Factor

These factors give for the inner and outer ring contacts, the reduction in EHD film thickness ascribable to lubricant film starvation according to the methods of Chiu, (11).

These factors pertain to the EHD film thickness for both the inner and outer race contacts of the most heavily loaded rolling elements, but are applied to the respective inner and outer race film thickness for each rolling element in the bearing.

4.2.5.3 Thermal Reduction Factor

These factors are calculated according to the methods of Cheng, (10) and pertain to the EHD film thickness for both the inner and outer race contacts of the most heavily loaded rolling elements, but are applied to the respective inner and outer race film thickness for each rolling element in the bearing.

4.2.5.4 Meniscus Distance

These factors are calculated according to the methods of Chiu, (11) and pertain to the EHD film thickness for both the inner and outer race contacts of the most heavily loaded

rolling elements, but are applied to the respective inner and outer race film thickness for each rolling element in the bearing.

4.2.5.5. Raceway-Rolling Element Conductivity

These data reflect the amount of heat transfer between rolling element and raceway for each degree centigrade difference between the two components. These data reflect the average of all outer and inner contacts, respectively.

4.2.6 Fit and Dimensional Change Data

4.2.6.1 Fit Pressures

These data refer to the pressures built up as a consequence of interference fits between shaft and inner ring and housing and outer ring. Pressures are presented both for the standard cold-static condition (16°C) and at operating conditions.

4.2.6.2 Speed Giving Zero Fit Pressure (Between the Shaft and Inner Ring)

This is a calculated value based upon operating conditions and provides a measure of the adequacy of the initial shaft fit.

4.2.6.3 Clearances

"Original" refers to cold unmounted clearance which is specified at input if the diametral clearance change analysis is executed. "Change" refers to the change in diametral clearance at operating conditions relative to the cold unmounted condition. A minus sign indicates a decrease in clearance. "Operating" refers to the clearance at operating conditions. For all types of ball bearings, the decrease in clearnace can be combined with the initial diametral clearance, and the free operating contact angle at operating conditions may be calculated. Note that the change in clearance should be compared against the diametral play of the split inner ring ball bearing in order to determine if the possibility for three point contact exists. The Program does not account for three point contacts even though the change in clearance might suggest that three point contact is obtained.

4.2.7 Lubricant Temperatures and Physical Properties

The lubricant properties, particularly the dynamic viscosity and to a lesser degree, the pressure viscosity coefficient, are heavily temperature dependent. These factors enter the EHD film thickness calculation and the HD and EHD friction models. The lubricant is assumed to be at the same temperature as the relevant raceway. As noted elsewhere, these temperatures may be either input directly or calculated by the Program.

The physical properties printed are self-explanatory. The units are enumerated.

4.2.8 Cage Data

4.2.8.1 Cage-Land Interface

The cage data indicates the performance parameters at the interface between the cage rail and the ring land on which the cage is guided. The torque, heat rate and separating force require no explanation. The eccentricity ratio defines the degree to which the cage approaches the ring on which it is guided at the point of nearest approach. The radial displacement of the cage relative to the bearing axis is divided by one half the cage-land diametral clearnace. An eccentricity ratio of one indicates cage-land contact. A ratio of zero indicates that the cage rotation is concentric with the bearing axis.

Only the cage-land and rolling element pocket forces are considered in determining the cage eccentricity. The cage weight and centrifugal force which result from the eccentricity, although available, are not considered in the analysis. The omission of these considerations helps reduce convergence problems.

4.2.8.2 Cage Speed Data

Cage speed data presents the comparison between the cage speed calculated based upon the quasidynamic equilibrium considerations and the speeds calculated with raceway control theory for ball bearings and the epicyclic speeds of the roller bearing components.

4.3 Rolling Element Output

4.3.1 Rolling Element Kinematics

4.3.1.1 Rolling Element Speeds

All of the rolling element speeds tend to vary from position to position when the bearing is subjected to combined loading.

The total rolling element speed is with reference to the cage and represents the vector sum of the three orthogonal components.

4.3.1.2 Speed Vector Angles

The rolling element speed vector angles, Arctan ($\omega y/\omega x$) and Arctan ($\omega z/\omega x$) are presented in order to show a clearer picture of the predicted ball kinematics. The ball speed vector tends to become parallel with the bearing X axis with increasing shaft speed and decreasing contact friction.

4.3.2 Rolling Element Raceway Loading

4.3.2.1 Normal Forces

The normal forces acting on each rolling element are printed. The rolling element race normal forces are self-explanatory. The cage force is calculated only when the friction solution is employed and is always directed along the rolling element Z axis. If the rolling element orbital speed is positive, a positive cage force indicates the the cage is pushing the rolling element, tending to accelerate it. Cage force is a function of rolling element position within the cage pocket. Its magnitude is derived using hydrodynamic lubrication assumptions, when the distance between the rolling element and cage web is large, and EHD assumptions when the separation is of the order of the EHD film thickness or when rolling element-cage web interference exists.

4.3.2.2 Hertz Stress

The stress printed represents the maximum normal stress at the center of each ball race contact or at the most heavily loaded slice of the roller raceway contact.

4.3.2.3 Load Ratio Q_{asp}/Q_{tot}

If the EHD film thickness is small compared to the RMS composite rolling element-race surface roughness, the rolling element-race normal load will be shared by the EHD film and asperity contacts. The load ratio reflects the portion of the total load carried by the asperities.

4.3.2.4 Contact Angles

A ball bearing, subject to axial loading, misalignment or mounted such that the inner ring is always displaced axially relative to the outer rings, (i.e., a duplex set of angluar contact ball bearings) will have non-zero contact angles. At low ball orbital speeds, the inner and outer race angles will be substantially the same. At high speeds, ball centrifugal force will cause the outer race contact angle to be less than the inner race angle.

4.4 Thermal Data

As in the case for bearing output, all of the input data is printed. The calculated output data is presented in the form of a temperature map in which a node number and the respective node temperature appear. The appearance of the steady state and transient temperature maps are identical. The transient temperature map also includes the time (T) at which the temperature calculations were made.

4.5 Shaft Data

These data simply reflect the input information.

4.6 SHABERTH Error Messages

4.6.1 Introduction

For various reasons, SHABERTH execution may terminate before the desired results have been achieved. This section is intended to give insight to the user as to the nature of the problem which caused termination.

In some instances, error messages are printed and execution proceeds. These messages indicate that in one of the internal iterative loops, a particular solution failed to converge to the desired accuracy. These messages should be taken as caution signals to the user to check the results carefully. In particular, compare the calculated bearing reaction forces against the applied shaft loading. If these results check to within 10 percent with an NPASS = 2 solution and to within 1 percent with an NPASS = 3 solution, the solutions should be sufficiently accurate.

Additional means of evaluating solution accuracy are presented in section 4.6.10.

4.6.2 From ALLT - Message: "STEADY STATE SOLUTION WITH (EP1) DEGREES ACCURACY WAS NOT OBTAINED AFTER (IT1) ITERATIONS." Explanation: This message pertains to the thermal equilibrium solution in which bearing generated heat and system temperatures must be consistent.

4.6.3 From AXLBOJ - Message: "ERROR MESSAGE, KX = (IER) SINGULAR SET OF SHAFT EQUATIONS." Explanation: This message indicates an error in the input data which describes the shaft.

4.6.4 From DAMPCO - Message: "THE NUMBER OF EQUATIONS CALCULATED BY SUMMING THE NUMBER OF EQUATIONS IN EACH SUBSET IS (NTOT). THIS DOES NOT EQUAL THE TOTAL NUMBER OF EQUATIONS SPECIFIED (N) AN ERROR EXISTS AND EXECUTION TERMINATES." Explanation: If the nonlinear equations are comprised of M independent subsets, then N must equal the summation of NSIZE(K) = 1,M.

$$NTOT = \sum_{K=1}^{K=M} NSIZE(K) \tag{4.1}$$

In SHABERTH M is always 1 and NSIZE(1) is N. This message should thus never be written.

4.6.5 From EHDSKF - Message: "AN IMPROPER LUBRICANT TYPE CODE HAS BEEN PASSED TO EHD SKF. EXECUTION TERMINATES." Explanation: Coming into EHD SKF N must have an integer value 1, 2, 3 or 4, a test has shown that 1>N>4.

4.6.6 From INTFIT - Message: "SINGULAR MATRIX ON TIGHT SHAFT FIT." Message: "SINGULAR MATRIX ON LOOSE SHAFT FIT." Explanation: These messages indicate bad data entering INTFIT.

4.6.7 From SHABE - Message: "AFTER (ITFIT) ITERATIONS, ERRMAX = (ERRMAX) WHILE THE REQUIRED FIT ACCURACY WAS (ERFIT)." Explanation: The bearing diametral clearance change analysis did not converge in ITFIT iterations. Either increase the number of iterations or set the number to -2 for a good approximate solution.

4.6.8 From SONRI - Message: "SINGULAR SET OF EQUATIONS, NPASS = (NPASS)." Explanation: This message pertains to shaft equilibrium solution and has never been known to occur.

4.6.8.1 From SONRI - Message: "THE RELATIVE ACCURACY EPS HAS NOT BEEN OBTAINED AFTER IT ITERATIONS IN ROUTINE SONRI." Explanation: This message indicates that shaft bearing inner ring equilibrium has not been achieved within the specified number of iterations. This may occur under light loading.

4.6.9 From STARFC - Message: "***IN STARFC/ROOTI*** ROOT OF F(X) DOES NOT EXIST BELOW HO." Explanation: The iterative solution for the meniscus distance for a rolling element raceway contact has not converged. This occurs only when the specified replenishment layers are extremely thin.

4.6.10 From SOLVXX

The majority of the error messages printed by SHABERTH will be printed from SOLVXX, indicating that SOLVXX has been unable to fully solve a particular set of nonlinear equations. Within SHABERTH failure has never occurred during the solution of a set of steady state thermal equations. Failure does occur, however, in the solution of the bearing quasidynamic set of rolling element and cage equations. The major portion of this section should be read with this in mind.

4.6.10.1 Message: "ONLY (NDER) EQUATIONS WERE FOUND TO VARY WITH X(J), ND(J) WERE EXPECTED." THE DIFFERENCES EQ (X+DX) - EQ(X) + DIFF(I)" IF DIFF(I) IS LESS THAN SF8*EQ(I), THEN EQ(I) IS NOT CONSIDERED TO VARY WITH X SF8 = (SF8)." "FOR THE FOLLOWING EQUATIONS THE DIFFERENCES ARE BIG ENOUGH" (C(N*J-N+I), I = 1, COUNT. Explanation: The matrix of partial derivatives calculated within SHABERTH must have at least N, nonzero diagonal elements. It is possible to specify a minimum number of nonzero elements greater than one, for each variable with the use of the array ND. If that minimum number is not obtained, the above set of error messages is printed. In SHABERTH, only the diagonal elements are required.

4.6.10.2 Message: "**** ERROR MESSAGE FROM THE EQUATION SOLVING ROUTINE AT ITERATION LOOP (LOOP) ****."

One of the four following situations has occurred. Situations 1. and 2. have never been known to occur; 3. and 4., however, have, and are explained.

1. "SINGULAR SET OF EQUATIONS," IER = 1.
2. "DIVERGENCE HAS OCCURRED 10 CONSECUTIVE ITERATIONS," IER = 2.
3. "THE LIMIT FOR NUMBER OF ITERATIONS IS REACHED," IER = 3.

This message (No. 3) indicates that the solution accuracy is not as good as desired. To achieve the required accuracy, the problem might be rerun with the iteration limit increased. This is accomplished at solution level NPASS = 2, through changing the "20" in CALL BEAR statement in "SHABE" from 20 to a larger number. At solution level NPASS = 3, the "30" in the CALL BEARC statement in SONRI must be increased to a larger number.

Prior to making these Program changes, however, the magnitudes of the equation residues should be examined in the same manner as suggested above. The solution may be sufficiently good, as discussed in 4 below, so that further computations are unnecessary.

4. "THIS IS THE BEST WE CAN DO. IT MAY BE USABLE." IER = 4.

This message indicates that computation has stopped before the desired results have been obtained. Fifty attempts have been made to increment the variable values without finding a set of increments which would reduce the equation residues.

After failing at these numerous attempts to improve the solution, it is concluded that the best solution has been achieved and that further changes to the variables will serve only to increase the equation residues. (In this discussion equation values and residue values are synonomous.) It is believed that this situation arises when large changes in variable values introduce small changes in equation values, i.e. when the force versus variable function has a very shallow slope.

When the differences in equation values are of the same order of magnitude as the numerical accuracy of the particular computer being used, these kinds of convergence problems can be expected.

It is possible that when this "BEST WE CAN DO" message is printed, that even though the solution is not as accurate as desired, it may be sufficiently accurate to be usable. The accuracy can be assessed by comparing the magnitude of the equation residue to the magnitude of the individual terms which comprise the equation. Since most convergence problems arise in the quasi-dynamic equilibrium solution of the rolling element and cage equations, the method of assessing the accuracy of this set of equations shall be addressed.

As noted earlier, the set of equations used to define the quasidynamic problem is comprised of (6Z + Mcage) equations where Z is the number of rolling elements and Mcage is the number of degrees of freedom (1 or 3) assigned to the cage. To assess the accuracy of the solution, the magnitude of the equation residue should be compared to the magnitude of the components which make up the equation. The residue values are printed under the heading "CORRESPONDING EQ-VALUES." The residues are printed in a six per line format such that the residues pertaining to a given element are all on one line. These six values represent the following six equilibrium equations:

1) $\Sigma F_x = 0$ 2) $\Sigma F_y = 0$ 3) $\Sigma F_z = 0$

4) $\Sigma M_x = 0$ 5) $\Sigma M_y = 0$ 6) $\Sigma M_z = 0$

Equations 1 and 2 are dominated by the normal raceway contact forces and the rolling element centrifugal force. Compared to the magnitude of these forces the residues of ΣF_x and ΣF_y are usually very small and thus acceptable. The remaining four equilibrium equations, however, have as their major terms, various components of the friction forces which act upon the element. Large values of these residue values are a manifestation of an unstable

operating condition, where the instability is defined qualitatively in terms of large change in component and raceway relative speeds producing small changes in internal bearing forces. The shallow slopes of these "Force vs. Relative Speed Functions" promote dynamic and numerical instabilities.

The ΣF_z equation should be examined for each rolling element. Typically this may be done by inspection with close comparison and calculations made for only one or two elements.

The three cage equilibrium equations are:

1) $\Sigma M_x = 0$ 2) $\Sigma F_y = 0$ 3) $\Sigma F_z = 0$

If only one cage equation is considered, it is equation 1); if more than one is considered, all three are used.

The components of these equations are the rolling element cage normal and friction forces as well as the cage-ring normal and friction forces. Magnitudes of the components of these forces and moments are printed as part of the output. Thus, comparison of components against residues is straight forward after converting to a consistent set of units. Residues are in English while the output is in metric units.

It should be noted that in those solutions in which the cage has only one degree of freedom, that the cage interaction with the rolling elements has only minor impact upon the rolling element dynamics. Therefore, a relatively large residue for the cage equation is not terribly significant. The rolling element ΣF_z equations should be the basis for the judgement as to whether a solution is good enough.

Although the message "THIS IS THE BEST WE CAN DO. IT MAY BE USABLE" may be written during a steady state temperature calculation scheme, numerical instabilities in those schemes are rather uncommon. None have been experienced with this program after three years of operation.

The following data are printed subsequent to printing messages 1 through 4 above.

RELATIVE ACCURACY (ERREL) ITERATION.

LIMIT (ITEND), NUMBER OF UNKNOWNS (N) ABSOLUTE ACCURACIES EXA(J).

DAMPING FACTORS 1-5 OTHER STEP FACTORS 6-10 (SF), MAXIMUM STEP FACTORS (SMX(J), J=1,N).

CORRECTIONS OF THE X-ES FROM SMQ D(J), J=1,N.

NUMBER OF DERIVATIVES EXPECTED FOR EACH X ND(J), J=1,N

X=VALUE X X(J), J=1,N.

CORRESPONDING EQ-VALUES EQ(J), J=1,N.

5. GUIDES TO PROGRAM USE

The Computer Program is a tool. As with any tool, the results obtained are at least partially dependent upon the skill of the user. Certainly, the economics of the Program usage are highly dependent upon the user's technical need and discriminate use of Program options.

Some general guides for efficient use of the Program are listed below:

1. Attempt to use the lowest level of solution possible. For instance, if the prime object of a given run is to obtain bearing fatigue lives, execute only the elastic solution (NPASS = 0). If an estimate of bearing frictional heat is required, execute the low level friction evaluation (NPASS = 1). Execute the friction solution (NPASS = 2) only if rolling element and cage kinematics are of interest. Execute the highest level of solution (NPASS = 3) if kinematics are of interest and the bearing reaction loads deviate substantially from the shaft applied loading, i.e., a deviation greater than ten percent.

2. Attempt to input bearing operating diametral clearance rather than calculate it. Or, execute the diametral clearance change analysis once for a group of similar runs and use the output from the first run as input to the subsequent runs omitting the clearance change analysis.

3. Attempt to input accurate operating temperatures rather than calculate them.

4. The more non-linear the problem, the more computer time required to solve it. In the bearing friction solution, large coefficients of friction seem to increase the degree of non-linearity. In the thermal solutions, if possible, eliminate non-linearities by omitting radiation terms and by using constant rather than temperature dependent free and forced convection coefficients.

5. In the transient thermal solution, space the calls to the shaft-bearing solution (BTIME) to as large an interval as prudently possible. Be careful, however, too long an interval will produce large errors in heat rate predictions.

6. In the steady state thermal analysis, attempt to estimate nodal temperatures on a node-by-node basis. Nodes which are heat sources should have higher temperatures than the surrounding nodes.

The above suggestions are intended to encourage the use of the Program on a cost-effective basis. The intent is not to discourage the use of important program capabilities, but to emphasize how the program should be most effectively used.

It is suggested that the user take a simple, axially loaded ball bearing problem and execute the program through the full range of options beginning with a frictionless solution proceeding to the three levels of friction solution with a low (0.01) and high (0.1) friction coefficient. The diametral clearance change analysis and the thermal solutions should also be executed on an experimental basis. This exercise will provide the user with some insight into economics of the Program usage on his computer as well as the results obtained from various levels of solution of the same problem.

It is also suggested that a constant user of the program should study the hierarchical Program flow chart, Appendix II 1, along withe the Program listing to gain an appreciation of the program complexity and the flow of the problem solution. The Program is comprised of many small functional subroutines. Knowledge of these small elements may allow the user to more easily piece together the philosophy of the total problem solution.

SHABERTH is intended to be used for the analysis of a multi-bearing system. It may, however, be used to analyze single bearings, mounted on dummy shafts under certain conditions of limited applied loading. These loading conditions are outlined and explained below as they apply separately for ball and cylindrical roller bearings.

Ball Bearings

Of major value is the capability of SHABERTH to treat, in a simple, economic manner, ball bearings subjected to axial loading only. Use of the program in this manner is recommended.

SHABERTH is not recommended for the solution of a single ball bearing subjected to radial load only. The Program attempts to satisfy axial and angular equilibrium as well as radial. A ball bearing is elastically very soft in those directions which causes mathematical instabilities during the solution scheme. This makes the Program uneconomical for this particular situation.

Whereas the use of SHABERTH to solve single radially loaded ball bearing problems is not recommended, because of economics, the solution of a single, radially and axially loaded problem is impossible. The impossibility arises because a moment reaction will develop when a ball bearing is subjected to both radial and axial loading. In order for the user to solve this problem he must specify at input the bearing reaction moment. The user must know the answer to a portion of the problem before he can begin to solve it.

Cylindrical Roller Bearing

A single, cylindrical roller bearing may be subjected to radial loading or combinations of radial and moment loading. When SHABERTH is used in this manner, it is important that bearing misalignments be specified indirectly through specification of a non-zero applied moment. If a radial load and an initial outer ring misalignment are specified along with a zero applied amount, SHABERTH will attempt but will be unable to solve the problem since it will be impossible to equilibrate the non-zero reaction moment, resulting from the offset, against the zero applied moment.

The cylindrical roller bearing cannot accept applied axial loading and thus when a single cylindrical roller bearing is being examined, the applied axial load must be specified to be zero.

When a single cylindrical roller bearing is being examined all loading should be referred to the X-Y plane in order to take advantage of the symmetry of load distribution among rolling elements.

LIST OF REFERENCES

1. Kellstrom, M.. "A Computer Program for Elastic and Thermal Analysis of Shaft Bearing Systems," S K F Report No. AL74P014, submitted to Vulnerability Laboratory, U. S. Army Ballistic Research Laboratories, Aberdeen Proving Ground, MD, under Army Contract DAAD05-73-C-0011.

2. Harris, T., "An Analytical Method to Predict Skidding in High Speed Roller Bearing," ASLE Transactions, 9, 1966, pp. 229-441.

3. Harris, T. A., "An Analytical Method to Predict Skidding in Thrust Loaded Angular Contact Ball Bearings," Journal of Lubrication Technology, Trans. ASME, Series F, Vol. 93, No. 1, 1971, pp. 17-24.

4. Timoshenko, Strength of Materials Part II Advanced Theory and Problems, 3rd Edition, D. VanNostrand Co., Inc., 1958.

5. Crecelius, W. J. and Milke, D., "Dynamic and Thermal Analysis of High Speed Tapered Roller Bearings Under Combined Loading," Technical Report NASA CR 121207.

6. Harris, T. A., "How to Predict Bearing Temperature Increases in Rolling Bearings," Product Engineering, pp. 89-98, 9th December 1963.

7. Fernlund, I. and Andreason, S., "Bearing Temperatures Calculated by Computer," The Ball Bearing Journal No. 156, March 1969.

8. Andreason, S., "Computer Calculation of Transient Temperatures," The Ball Bearing Journal, No. 160, March 1970.

9. McCool, J. I., et al, "Technical Report AFAPL-TR-75-25, "Influence of Elastohydrodynamic Lubrication on the Life and Operation of Turbine Engine Ball Bearings - Bearing Design Manual," S K F Report No. AL75P014 submitted to AFAPL and NAPTC under AF Contract No. F33615-72-C-1467, Navy MIPR No. M62376-3-000007, May 1975.

10. Cheng, H. S., "Calculation of EHD Film Thickness in High Speed Rolling and Sliding Contacts," MTI Report 67-TR-24 (1967).

11. Chiu, Y. P., "An Analysis and Prediction of Lubricant Film Starvation in Rolling Contact Systems," ASLE Transactions, 17, pp 23-35 (1974).

12. Tallian, T. E., "The Theory of Partial Elastohydrodynamic Contacts," Wear, 21, pp 49-101 (1972).

13. McGrew, J. M., et al, "Elastohydrodynamic Lubrication Preliminary Design Manual," Technical Report AFAPL-TR-70-27, pp 20-21, November 1970.

14. Fresco, G. P., et al, "Measurement and Prediction of Viscosity-Pressure Characteristics of Liquids," A Thesis in Chemical Engineering Report No. PRL-3-66, Department of Chemical Engineering College of Engineering, The Pennsylvania State University, University Park, Pennsylvania.

15. Crecelius, W. J., Heller, S., and Chiu, Y. P., "Improved Flexible Shaft-Bearing Thermal Analysis with NASA Friction Models and Cage Effects," S K F Report No. AL76P003, February 1976.

16. Jakob, M. and Hawkins, G. A., "Elements of Heat Transfer," 3rd Ed., John Wiley & Sons, Inc., 1957.

17. Kent's Mechanical Engineering Handbook-Power Volume, John Wiley & Sons, Inc., 12th Ed., 1960, Chapter 3, p. 20.

18. Burton, R. A., and Staph, H. E., "Thermally Activated Seizure of Angular Contact Bearings," ASLE Trans. 10, pp. 408-417 (1967).

19. Liu, J. Y., Tallian, T. E., McCool, J. I., "Dependence of Bearing Fatigue Life on Film Thickness to Surface Roughness Ratio," ASLE Preprint 74AM-7B-1 (1974).

20. Archard, J. and Cowking, E., "Elastohydrodynamic Lubrication at Point Contact," Proc. Inst. Mech. Eng., Vol. 180, Part 3B, 1965-1966, pp. 47-56.

21. Dowson, D. and Higginson, G., "Theory of Roller Bearing Lubrication and Deformation," Proc. Inst. Mech. Eng., London, Vol. 177, 1963, pp. 58-69.

22. Loewenthal, S. H., Parker, R. J., and Zaretsky, E. V., "Correlation of Elastohydrodynamic Film Thickness Measurements for Fluorocarbon, Type II Ester and Polyphenyl Ether Lubricants," NASA Technical Note D-7825, National Aeronautics and Space Administration, Washington, D.C., November 19, 1974.

23. McCool, J. I., et al, "Interim Technical Report on Influence of Elastohydrodynamic Lubrication on the Life and Operation of Turbine Engine Ball Bearings," S K F Report No. AL73P014, submitted to AFAPL and NAPTC under AF Contract No. F33615-72-C-1467, Navy MIPR No. M62376-3-000007, October, 1973.

24. Allen, C. W., Townsend, D. P., and Zaretsky, E. V., "New Generalized Rheological Model for Lubrication of a Ball Spinning in a Nonconforming Groove," NASA Technical Note D-7280, National Aeronautics and Space Administration, Washington, D.C., May 1973.

25. Lundberg, G. "Cylinder Compressed Between Two Plane Bodies," SKF Internal Report 1949-08-02.

26. Nayak, P. R., "Random Process Model of Rough Surfaces," Journal of Lubrication Technology, 93, pp. 398-407 (1971).

27. McCool, J. I., et al, "Interim Technical Report on Influence of Elastohydrodynamic Lubrication on the Life and Operation of Turbine Engine Ball Bearings," SKF Report No. AL73P014, submitted to AFAPL and NAPTC under AF Contract No. F33615-72-C-1467, Navy, MIPR No. M62376-3-000007, October 1973.

28. Johnson, K. L., and Cameron, R., "Shear Behavior of EHD Oil Film at High Rolling Contact Pressure," The Institution of Mech. Engr. Tribology Group, Westminster, London WEI (1968).

29. Smith, R., et al, "Research on Elastohydrodynamic Lubrication of High Speed Rolling-Sliding Contacts, Air Force Aero Propulsion Laboratory, Wright Patterson AFB, Ohio Technical Report AFADC-TR-71-54 (1971).

30. Floberg, L., "Lubrication of Two Cylindrical Surfaces Considering Cavitation," Report No. 14 Chalmers University of Technology, Gothenburg, (1966).

31. Snidle, R. W. and Archard, J. K., "Lubrication at Elliptical Contacts," Symposium on Tribology Convention, Gothenburg Institute of Mechanical Engineering, 1969.

32. Pinkus, O., and Sternlicht, B., "Theory of Hydrodynamic Lubrication," McGraw-Hill Book Company, Inc., New York, N.Y. 1961 p. 48.

33. Lundberg, G. and Palmgren, A., "Dynamic Capacity of Rolling Bearings" Acta Polytechnica, Mechanical Engineering Series 1. Proceedings of the Royal Swedish Academy of Engineering, Vol. 7, No. 3, 1947.

34. Lundberg, G. and Palmgren, A. "Dynamic Capacity of Roller Bearings" Proceedings of the Royal Swedish Academy of Engineering Vol. 2, No. 4, 1952.

35. Knudsen, J. G., and Katz, D. L., Fluid Dynamics and Heat Transfer, McGraw-Hill Book Company, New York, New York, pp. 311-315.

APPENDIX I 1

HEAT TRANSFER INFORMATION

APPENDIX I 1

HEAT TRANSFER INFORMATION

I 1.1 BACKGROUND

The temperature portion of SHABERTH is designed to produce temperature maps for an axisymmetric mechanical system of any geometrical shape. The mechanical system is first approximated by an equivalent system comprising a number of elements of simple geometries. Each element is then represented by a node point having either a known or an unknown temperature. The environment surrounding the system is also represented by one or more nodes. With the node points properly selected, the heat balance equations can be set up accordingly for the nodes of unknown temperature. These equations become non-linear when there is convection and/or radiation between two or more of the node points considered. The problem is, therefore, reduced to solving a set of linear and/or non-linear equations for the same number of unknown nodal temperatures. It is obvious that the success of the approach depends largely on the physical subdivision of the system. If the subdivision is too fine, there will be a large number of equations to be solved; on the other hand, if the subdivision is too crude, the results may not be reliable.

In a system consisting of rolling bearings, for the sake of simplicity, the elements considered are usually axially symmetrical, e.g., each of the bearing rings can be taken as an element of uniform temperature. For an element which is not axially symmetrical, its temperature is also assumed to be uniform and its presence is assumed not to distort the uniformity in termpature of a neighboring element which is axially symmetrical. That is, the non-symmetrical element is represented by an equilvalent axially symmetrical element with approximately the same surface area and material volume. This kind of approximation may seem to be somewhat unrealistic, but with properly devised equivalent systems, it can be used to solve complicated problems with results satisfying some of the important engineering requirements.

The computer program can solve the heat-balance equations for either the steady state or the transient state conditions and produce temperature maps for the mechanical system when the input data are properly prepared.

I 1.2 BASIC EQUATIONS

I 1.2.1 Heat Conduction

The rate of heat flow $q_{ci,j}$(W) that is conducted from node i to node j may be expressed by,

$$q_{ci,j} = \frac{\lambda_{ij} A_{ij}}{L_{ij}} (t_i - t_j) \qquad \text{I 1.1)}$$

t_i and t_j are the temperatures at i and j, respectively, $A_{i,j}$ the area normal to the heat flow, (m^2) L_{ij} the distance (m) and λ_{ij} the thermal conductivity between i and j, (W/m^oC).

Assuming that the structure between point i and j is composed of different materials, an equivalent heat conductivity may be calculated as follows:

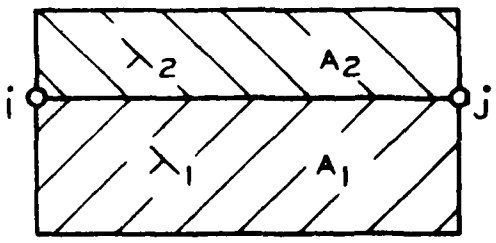

Fig. I 1.1 Parallel Conduction

$$\lambda_{ij} = \frac{\lambda_1 A_1 + \lambda_2 A_2}{A_{ij}}$$

$$A_{ij} = A_1 + A_2$$

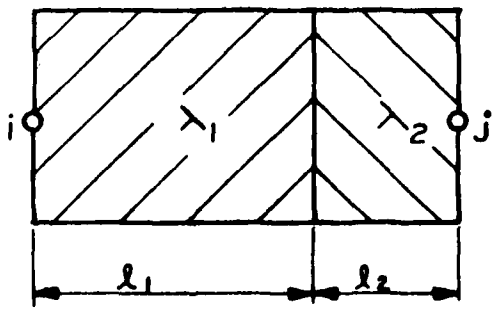

Fig. I 1.2 Series Conduction

$$\lambda_{ij} = \frac{\ell_{ij}}{\ell_1/\lambda_1 + \ell_2/\lambda_2}$$

$$\ell_{ij} = \ell_1 + \ell_2$$

The calculation of the areas will be discussed in Section I 1.2.5

I 1.2.2 Convection

The rate of heat flow that is transferred between a solid structure and air by free convection may be expressed by

$$q_{vi,j} = \alpha_{i,j} A_{i,j} \left| t_i - t_j \right|^{1.25} \cdot \text{SIGN}\ (t_i - t_j) \qquad \text{(I 1.2)}$$

where

$$\text{SIGN} = \begin{cases} 1, \text{ if } (t_i - t_j) \geq 0 \\ -1, \text{ if } (t_j - t_i) < 0 \end{cases}$$

in which

$$\alpha_{ij} = \begin{cases} 2.5 \cdot 10^{-2}\ \text{W/m}^2 - (\text{degC})^{1.25} & \text{for hot surfaces facing upward and cold surfaces facing downward} \\ 1.4 \cdot 10^{-2}\ \text{W/m}^2 - (\text{degC})^{1.25} & \text{for hot surfaces facing downward and cold surfaces facing upward} \\ 1.8 \cdot 10^{-2}\ \text{W/m}^2 - (\text{degC})^{1.25} & \text{for vertical surfaces} \end{cases}$$

For other special conditions, α_{ij} must be estimated by referring to heat transfer literature.

The rate of heat flow that is transferred between a solid structure and a fluid by <u>forced convection</u> may be expressed by

$$q_{ni,j} = \alpha_{i,j} A_{i,j} (t_i - t_j) \qquad \text{(I 1.3)}$$

in which $_{ij}$ is the heat transfer coefficient.

Now, with $\alpha = \alpha_{ij}$, introduce the Nusselt number

$$N_u = \frac{\alpha L}{\lambda} \qquad \text{(I 1.4)}$$

the Reynolds number

$$R_e = \frac{UL}{\nu} \qquad \text{(I 1.5)}$$

and the Prandtl number

$$P_r = \frac{\rho \nu c_p}{\lambda} \qquad \text{(I 1.6)}$$

where

L is a characteristic length which is equal to the diameter in the case of a cylindrical surface and is equal to the plate length in case of a flat surface.

U is a characteristic velocity which is equal to the difference between the fluid velocity at some distance from the surface and the surface velocity (m/sec)

λ is the fluid thermal conductivity ($W/M^{o}C$)

ν is the fluid kinematic viscosity (M^2/sec)

ρ is the fluid density (kg/m^3)

c_p is the fluid specific heat ($J/kg^{o}C$)

For given values of R_e and P_r, the Nusselt number N_u and thus, the heat transfer coefficient may be estimated from one of the following expressions:

Laminar flow along a flat plate: $R_e < 2300$

$$N_u = 0.323 \sqrt{R_e} \cdot \sqrt[3]{P_r} \qquad \text{(I 1.7)}$$

Laminar flow of a liquid in a pipe:

$$N_u = 1.36 \sqrt[3]{R_e \cdot P_r \left(\frac{D}{L}\right)} \qquad \text{(I 1.8)}$$

where D is the pipe diameter and L the pipe length

Turbulent flow of a liquid in a pipe:

$$N_u = 0.027 \cdot R_e^{0.8} \cdot \sqrt[3]{P_r} \qquad \text{(I 1.9)}$$

Gas flow inside and outside a tube:

$$N_u = 0.3\ R_e^{0.57} \qquad \text{(I 1.10)}$$

Liquid flow outside a tube:

$$N_u = 0.6\ R_e^{0.5} \cdot P_r^{0.31} \qquad \text{(I 1.11)}$$

Forced free convection from the outer surface of a rotating shaft

$$N_u = 0.11 \left[0.5\ R_e^{2} \cdot P_r\right]^{0.35} \qquad \text{(I 1.12)}$$

where the Reynolds number R_e is developed by the shaft rotation.

$$R_e = \frac{\omega \pi D^2}{\nu} \qquad \text{(I 1.13)}$$

in which ω is the angular velocity (rad/sec)
D is the roll diameter (m)

The average coefficient of forced convection to the lubricating oil within a rolling contact bearing may be approximated by,

$$\alpha = 0.0986 \left\{ \frac{N}{\nu} \left[1 \pm \frac{D \cos(\beta)}{d_m} \right] \right\}^{\frac{1}{2}} \lambda (P_r)^{1/3} \qquad \text{(I 1.14)}$$

using + for outer ring rotation
- for inner ring rotation

in which N is the bearing operating speed (rpm)
D is the diameter of the rolling elements (mm)
d_m is the bearing pitch diameter (mm)
α is the bearing contact angle (degrees)

I 1.2.3 Fluid Flow

The rate of heat flow that is transferred from fluid node i to fluid node j by fluid flow is

$$q_{fi,j} = \rho \dot{V}_{ij} \; C_p \; (t_i - t_j) \qquad \text{(I 1.15)}$$

V_{ij} is the volume rate of flow from i to j. It must be observed that the continuity of mass requires the following equation to be satisfied

$$\Sigma \dot{V}_{ij} = 0 \qquad \text{(I 1.16)}$$

provided the fluid density is constant. The summation should be extended over all nodes i within the fluid which have heat exchange with node j by fluid flow.

I 1.2.4 Heat Radiation

The rate of heat flow that is radiated to node j from node i is expressed by

$$q_{Ri,j} = \sigma_{i,j} \left\{ (t_i+273)^4 - (t_j+273)^4 \right\} \qquad \text{(I 1.17)}$$

where

$T_j = t_j + 273.16$

$T_i = t_i + 273.16$

and the value of the coefficient $\delta_{i,j}$ depends on the geometry and the emissivity or the absorptivity of the bodies involved.

For radiation between large, parallel and adjacent surfaces of equal area, $A_{i,j}$ and emissivity, $\varepsilon_{i,j}$, $\delta_{i,j}$ is obtained from the equation

$$\delta_{i,j} = \varepsilon_{i,j} \ \sigma A_{i,j} \qquad \text{(I 1.18)}$$

where σ, the Stefan-Boltzmann constant, is

$$\sigma = 5.76 \cdot 10^{-8} \ W/m^2/(degK)^4$$

For radiation between concentric spheres and coaxial cylinders of equal emissivity, $\varepsilon_{i,j}$, $\delta_{i,j}$ is given by the equation

$$\delta_{ij} = \frac{\varepsilon_{i,j} \sigma_{i,j}}{1 + (1 - \varepsilon_{i,j}) \frac{A_{i,j}}{A^*_{i,j}}} \qquad \text{(I 1.19)}$$

where σ is as above $A_{i,j}$ is the area of the enclosed body and $A^*_{i,j}$ is the area of the surrounding body, i.e. $A_{i,j} \quad A^*_{i,j}$.

Expressions for $\sigma_{i,j}$ that are valid for more complicated geometries or for different emissivities may be found in the heat transfer literature.

I 1.2.5 <u>Calculation of Areas</u>

In the case of heat transfer in the axial direction $A_{i,j}$ is given by the equation (I 1.3)

$$A_{i,j} = 2\pi r_m \cdot \Delta r \qquad \text{(I 1.20)}$$

Referring to the input instructions, Section 5, but recalling L must be input in mm not m.

$$L_1 = r_m = \frac{r_1 + r_2}{2} \qquad \text{(I 1.21)}$$

$$L_2 = \Delta r = r_2 - r_1 \qquad \text{(I 1.22)}$$

In the case of heat transfer in the radial direction, $A_{i,j}$ is obtained from the expression

$$A_{i,j} = 2\pi r_m \cdot H; \; L_1 = r_m; \; L_2 = H$$

and similarly for the radiation term above

$$A^*_{i,j} = 2\pi r^*_m H$$

$$L_3 = r^*_m$$

$$L_2 = 2H$$

in which H is the length of the cylindrical surface; where heat is conducted between i and j, r_m is given by the same equation as above (Fig. I 1.3(d)); where heat is convected between i and j, r_m is the radius of the cylindrical surface (Fig. I 1.3(c)); where heat is radiated between i and j, r_m is the radius of the enclosed cylindrical surface and r_m^* the radius of the surrounding cylindrical surface (Fig. I 1.3(d)).

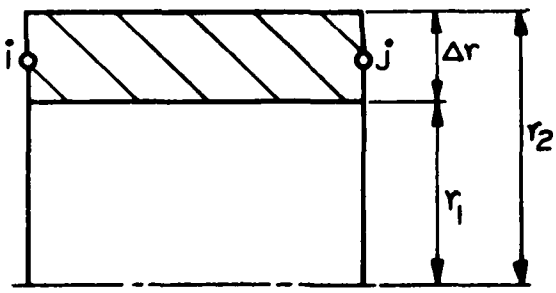

Fig. I 1.3 (a)

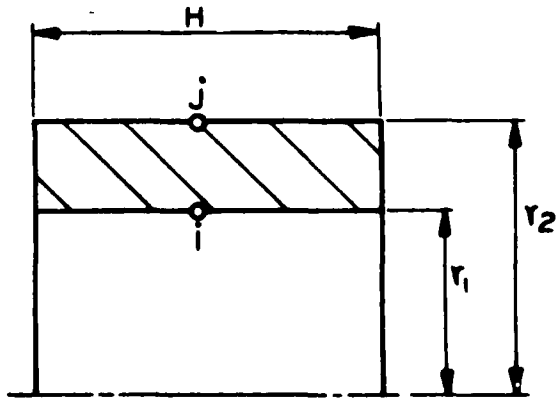

Fig. I 1.3 (b)

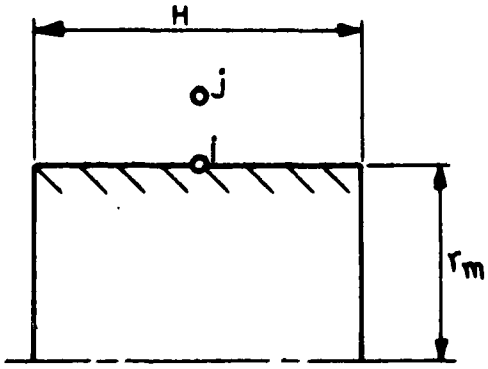

Fig. I 1.3(c)

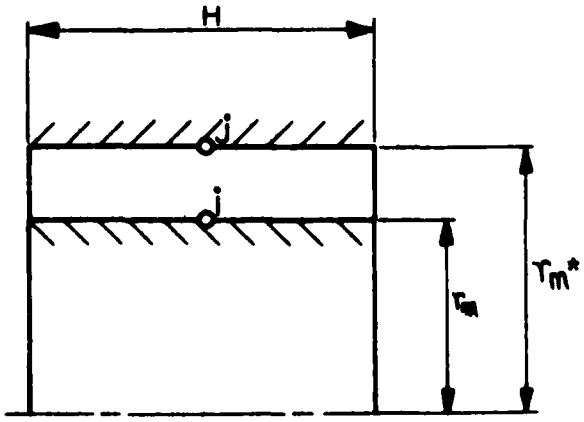

Fig. I 1.3(d)

I 1.3 Transient Analysis

For the transient analysis, all of the data pertaining to the node-to-node heat transfer coefficients must be provided by the input. Additionally, the volume and the specific heat at each node is required. For metal nodes, this input is striaghtforward. However, when fluid flow is being considered, there is no easy way to approximate the fluid nodal volume in a free space such as the bearing cavity. However, through use of the Program, the user's ability to make appropriate estimates will improve.

APPENDIX I 2

BEARING DIAMETRAL CLEARANCE CHANGE ANALYSIS, FROM COLD UNMOUNTED TO MOUNTED OPERATING CONDITIONS

APPENDIX I 2

BEARING DIAMETRAL CLEARANCE CHANGE ANALYSIS, FROM COLD UNMOUNTED TO MOUNTED OPERATING CONDITIONS*

I 2.1 INTRODUCTION

As a bearing is taken from the shelf, mounted in a housing and on a shaft, turned up to speed and subjected to operating loads and temperature, the diametral clearance of the bearing will change. To accurately analyze the performance of a bearing, its operating clearance must be known. An analysis has been developed to account for the following effects:

1. Temperature changes and gradients.
2. Initial and operating shaft and housing fits.
3. Rotation induced, ring radial growth.
4. Uniform radial components of the rolling element-raceway normal loads.

The basis for the major portion of this analysis is taken from Timoshenko, {4}. The bearing rings are treated as thick walled circular cylinders of constant wall thickness subjected to the action of uniformly distributed internal and external pressure.

The external pressure arises in the case of the outer ring from a press fit into the bearing housing. The internal pressure on the outer ring arises from the discrete rolling element loads which are regarded as uniform internal pressure acting on the outer ring. Similarly for the inner ring the press fit on the shaft provides a uniform internal pressure and the rolling element loads are regarded as a uniform external pressure. Fig. I 2.1 show the idealized sections used in the analysis.

*This Appendix is based upon the original work {5}

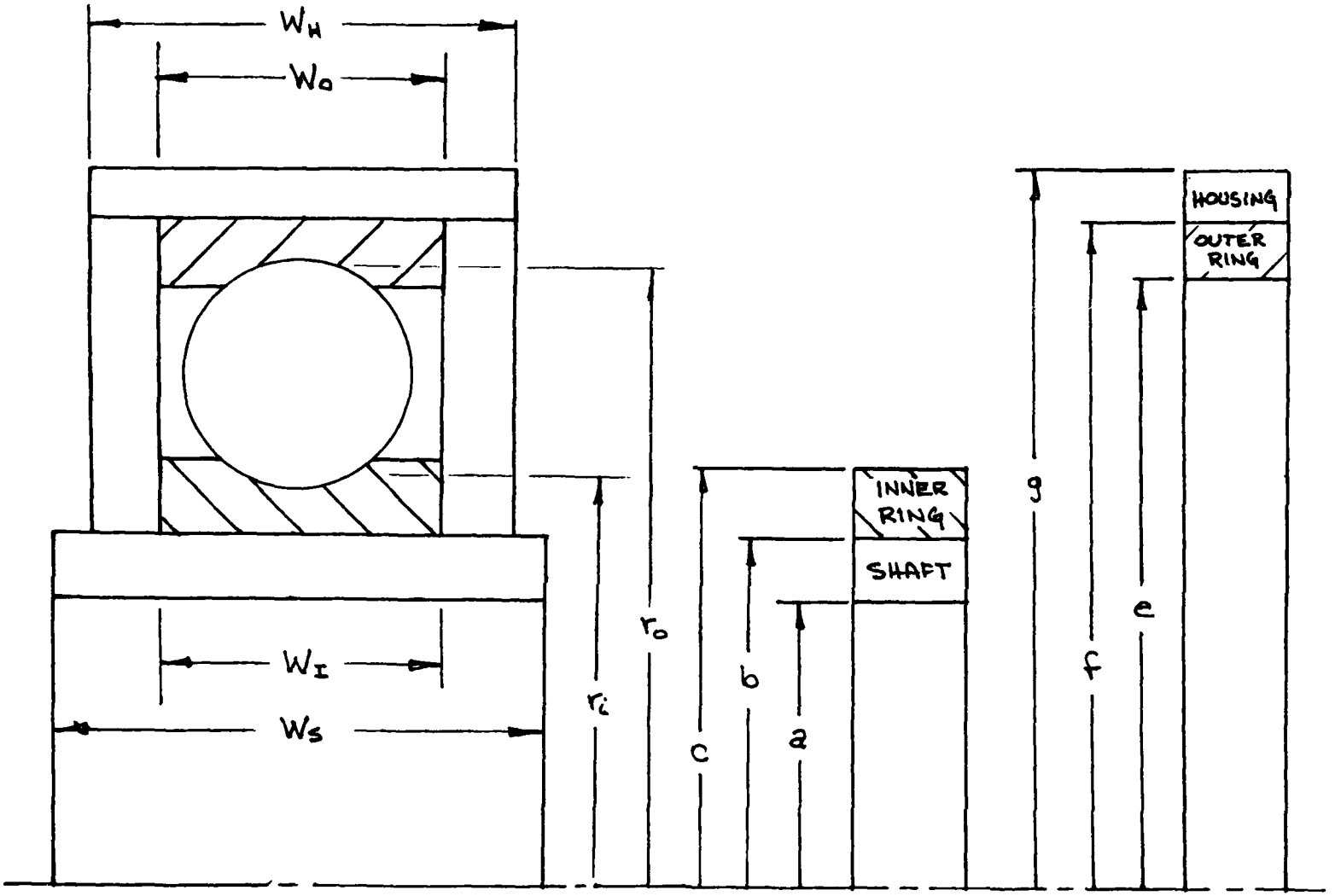

FIG. I 2.1 BEARING ASSEMBLY EQUIVALENT SECTIONS

I 2.2 BEARING SHAFT AND HOUSING EQUIVALENT SECTIONS

Timoshenko's analysis requires that a ring be fully defined by specification of only internal and external radii. If two concentric rings are pressed together the analysis assumes that the rings are of equal width. Perhaps the outside surface of the actual inner ring section cannot be defined by a single radius. However, an equivalent radius may be found such that the cross sectional areas of the real and equivalent rings are equal.

A second significant dimension associated with both the outer and inner rings is the radius of the rolling element path at each section. Ultimately, it is the change in these path radii, in addition to a change in the rolling element diameter, which permit a change in the bearing diametral clearance.

The bearing diametral clearance change problem requires the solution to similar problems for both the inner ring-shaft (shaft) and the outer ring-housing (housing) sections. To help eliminate repetition and cumbersome subscripting, only the shaft section will be covered thoroughly. Differences in analysis which occur at the housing section will be noted.

I 2.3 INTERNAL AND EXTERNAL EQUIVALENT PRESSURES

Both the shaft and housing sections are represented by two rings The rings may or may not be in intimate contact. Intimate contact occurs when due to any of several factors, the outside radius of the inside ring is greater than the inside radius of the outer ring. A pressure is developed at that interface, which tends to expand the outside ring and collapse the inside ring. Although the pressure acting on the actual interfering surfaces is identical, the use of equivalent geometric sections requires the

use of equivalent pressure, such that the calculated pressure acting to collapse the inside ring will not be identical to the pressure acting to expand the outside ring.

The equivalent pressure concept allows the effect of unequal component widths to be considered.

The effect of unequal inner ring and shaft width is taken into account by the factor X which applies to the pressure where, referring to Fig. I 2.1

$$0.5 \leq \left(X_s = \frac{W_I}{W_s} \right) \leq 2. \qquad \text{(I 2.1)}$$

$$0.5 \leq \left(X_H = \frac{W_O}{W_H} \right) \leq 2. \qquad \text{(I 2.2)}$$

Where W denotes the element width and the subscripts I, O, S and H refer to inner, outer, shaft and housing respectively.

The equivalent pressures acting on the shaft and housing are thus

$$P_{S_o} = X_s \; P_{I_i} \qquad \text{(I 2.3)}$$

$$P_{H_i} = X_H \; P_{O_o} \qquad \text{(I 2.4)}$$

P_{S_o} denotes the pressure on the shaft O.D. as related to the pressure on the inner ring P_{I_i}, P_{H_i} and P_{O_o} are similarly defined. The pressures (P) in Eq. (I 2.3 and I 2.4) are non-zero only if an interference fit exists at the section in question. An interference fit may exist under cold mounted conditions but due to thermal gradients and high speed rotation, clearance may develop at operating conditions.

To account for the elastic effect of the uniform radial components of the rolling element loads on the ring dimensions, an equivalent inner ring external pressure and outer ring internal pressure are calculated based on the minimum radial component of the rolling element loads, such that for the inner ring;

$$P_{I_o} = \frac{Z\,(Q_{Ij} \cos \alpha_{Ij})_{min}}{2\pi C\, W_I} \qquad \text{(I 2.5)}$$

where Z is the total number of rolling elements

$(Q_{Ij} \cos \alpha_{Ij})_{min}$ is the smallest rolling element raceway radial load component at the inner raceway

W_I is the inner ring total width, or one half the total width if the inner ring is split.

An expression corresponding to Eq. (I 2.5) can be developed for the internal pressure acting to expand the outer ring. In fact P_{IO} will exist only when the applied load is predominantly axial or when the bearing is preloaded, but the internal pressure acting on the outer ring, P_{oi}, will always exist to some extent, as a result of rolling element centrifugal force.

I 2.4 TEMPERATURE EFFECTS

Temperature effects at operating conditions are considered in two ways. A bulk effect based on the radii to the rolling paths (R) is calculated from Eq. (I 2.6)

$$\delta = R \lambda \bar{t} \qquad \text{(I 2.6)}$$

where

δ - is the change in rolling path radius

λ - is the component coefficient of thermal expansion,

$\bar{t}$ - is the difference between the component effective temperature and 68°F.

A similar expression may be written for the change in roller diameter.

The second effect of temperatures is the change in interference fit from cold to operating conditions such that the interference fit as a result of the initial fit and the temperature difference between the two components can be calculated. Cold (293°K, (68°F)), shaft and housing fits (F_{cold}) are input to the analysis. A positive value reflects an interference fit. The analysis neglects asperity crushing. The fit $(F_{hot})_s$ at operating temperature is given by

$$(F_{hot})_s = (F_{cold})_s + 2b(\lambda_s t_{s_1} - \lambda_i t_{i_1}) \quad \text{(I 2.7)}$$

(F_{hot}) is the fit considering operating temperatures.

I 2.5 RING RADIAL DISPLACEMENT CONSIDERING SURFACE PRESSURES

At this point we consider the problem of evaluating thick walled cylinder, (ring) radial displacements as a function of the ring radial dimensions, physical properties, and uniform internal and external pressures. Timoshenko develops Eq. (I 2.8) for determining the ring/radial displacement (δ), as a function of a general radius (r) to any point within the ring when considerations of ring rotation are omitted.

$$\frac{d^2\delta}{dr} + \frac{1}{r}\frac{d\delta}{dr} - \frac{\delta}{r^2} = 0 \quad \text{(I 2.8)}$$

The general solution of this equation is

$$\delta = K_1 r + \frac{K_2}{r} \quad \text{(I 2.9)}$$

The expression for normal stress in the ring is given by:

$$\sigma_r = \frac{E}{1-\nu}\left[K_1(1+\nu) - K_2\left(\frac{1-\nu}{r^2}\right)\right] \quad \text{(I 2.10)}$$

The constants of integration K_1 and K_2 can be determined from Eqs. (I 2.11 and I 2.12) which make use of the boundary conditions at the inner and outer surfaces of the ring. Note that the dimensions of inner ring section are used in Eq. (I 2.11 and I 2.14). These equations, however, are general expressions and are valid for all rings,

$$(\sigma_r)_{r=c} = -P_{I_o} = \frac{E_I}{1-\nu_I^2}\left[K_1(1+\nu_I) - K_2\left(\frac{1-\nu_I}{c^2}\right)\right] \quad \text{(I 2.11)}$$

$$(\sigma_r)_{r=b} = -P_{I_i} = \frac{E_I}{1-\nu_I^2}\left[K_1(1+\nu_I) - K_2\left(\frac{1-\nu_I}{b^2}\right)\right] \quad \text{(I 2.12)}$$

Where E and ν are the modulus of elasticity and Poisson's ratio respectively. The negative sign associated with P_{I_o} and P_{I_i} reflect the sign convention, wherein a positive normal stress indicates tension. Solving Eqs. (I 2.11-12) for K_1 and K_2 and substituting the results into Eqs. (I 2.9 and I 2.10) gives the general expressions for normal stress and radial deflection as functions of the internal and external pressures acting on the ring:

$$\sigma_r = \frac{b^2 P_{I_i} - c^2 P_{I_o}}{c^2 - b^2} - \frac{c^2 b^2 (P_{I_i} - P_{I_o})}{r^2 (c^2 - b^2)} \quad \text{(I 2.13)}$$

$$\delta_{IR} = \left(\frac{1-\nu_I}{E_I}\right)\frac{r b^2 P_{I_i} - c^2 P_{I_o}}{c^2 - b^2} + \frac{1+\nu_I}{r E_I}\left[\frac{b^2 c^2 (P_{I_i} - P_{I_o})}{(c^2 - b^2)}\right] \quad \text{(I 2.14)}$$

Using the appropriate dimensions and pressures, Eq. (I 2.14) can express the inward displacement of the shaft and the outward displacement of the inner ring when assembled with an interference fit F_{HOT}.

$$\delta_{Ib} - \delta_{sb} = F_{HOT} \quad \text{(I 2.15)}$$

$$\delta_{Ib} = \frac{(1-\nu_I)}{E_I} b\left(\frac{b^2 P_{I_i} - c^2 P_{I_o}}{c^2 - b^2}\right) + \frac{(1+\nu_I)}{b E_I}\left[\frac{b^2 c^2 (P_{I_i} - P_{I_o})}{(c^2 - b^2)}\right] \quad \text{(I 2.16)}$$

$$\delta_{sb} = \frac{-b P_{s_o}}{E_s}\left[\frac{a^2 + b^2}{b^2 - a^2} - \nu_s\right] \quad \text{(I 2.17)}$$

P_{si} and P_{Ho} are assumed zero. Using Eq. (I 2.5) to obtain P_{Io}, the following expression may be developed for P_{Ii} which accounts for all variables in the interference fit problem except for the effect of high speed rotation.

$$P_{Ii} = \frac{F_{HOT} + 2\left(\frac{1-\nu_I}{E_I}\right)\left(\frac{bc^2 P_{Io}}{c^2-b^2}\right)}{\left(\frac{1-\nu_I}{E_I}\right) b\left(\frac{b^2+c^2}{c^2-b^2}\right) + \frac{bX}{E_s}\left(\frac{a^2+b^2}{b^2-c^2} + \nu_s\right)} \qquad \text{(I 2.18)}$$

Note, P_{Ii} may not be negative, i.e. the effect of fitting one ring on another cannot result in placing the common surfaces in tension.

Having determined P_{Ii} and P_{Io} Eq. (I 2.14) may be used to determine $\delta_{IR}(F,t,Q)$ by replacing the general radius (r) with the radius to the roller path, R. $\delta_{IR}(F,t,Q)$ is defined as the change in rolling path radius resulting from:

- F · The initial fit
- t · The change in fit resulting from a temperature gradient
- Q · The effect of the rolling element load.

I 2.6 RING ROTATION

We must now examine the effect on the rolling path which results from high speed rotation. If the rotational speed is less than 100 rpm, the rolling path radius is assumed to be unaffected.

Timoskenko presents Eq. (I 2.19) to define ring displacement δ in terms of a general radius (r), the weight density of the ring material, (ρ), and the ring angular velocity (Ω)

$$\frac{d^2\delta}{dr^2} + \frac{1}{r}\frac{d\delta}{dr} - \frac{\delta}{r^2} + (1-\nu^2)\frac{\rho\Omega^2 r}{gE} = 0 \qquad \text{(I 2.19)}$$

Using the notation;

$$N = (1-\nu^2)\frac{\rho\Omega^2}{gE} \qquad \text{(I 2.20)}$$

the general solution to Eq. (I 2.19) may be written:

$$\delta = -N\frac{r^3}{8} + K_1 r + \frac{K_2}{r} \qquad \text{(I 2.21)}$$

The general expression for the normal stress is given by:

$$\sigma_r = \frac{E}{(1-\nu^2)}\left[\frac{\nu-3}{8}Nr^2 + (1-\nu)K_1 - (1-\nu)K_2\frac{1}{r^2}\right] \qquad \text{(I 2.22)}$$

Using Eqs. (I 2.21 and I 2.22) and the principle of superposition, the effects of ring rotation can be considered. In this case, superposition allows a set of integration constants K_1 and K_2 to be calculated for a ring based on a change in pressure (P^*) at the internal and external surfaces. Eq. (I 2.22) may be written for the four specific surfaces of the shaft section as follows;

Inner Ring External Surface

$$-P_{I_o}^* = \frac{E_I}{1-\nu_I}\left[\frac{\nu_I-3}{8}N_I c^2 + (1+\nu_I)K_{1I} - (1-\nu_I)K_{2I}\frac{1}{c^2}\right] = 0 \qquad \text{(I 2.23)}$$

Inner Ring Internal Surface

$$-P_{I_i}^* = \frac{E_I}{1-\nu_I}\left[\frac{\nu_I-3}{8}N_I b^2 + (1+\nu_I)K_{1I} - (1-\nu_I)K_{2I}\frac{1}{b^2}\right] \qquad \text{(I 2.24)}$$

Shaft External Surface

$$-P_{s_o}^* = \frac{E_s}{1-\nu_s}\left[\frac{\nu_s-3}{8}N_s b^2 + (1+\nu_s)K_{1s} - (1-\nu_s)K_{2s}\frac{1}{b^2}\right] \qquad \text{(I 2.25)}$$

Shaft Internal Surface

$$-P_{s_i}^* = \frac{E_s}{1-\nu_s}\left[\frac{\nu_s-3}{8}N_s a^2 + (1+\nu_s)K_{1s} - (1-\nu_s)K_{2s}\frac{1}{a^2}\right] = 0 \qquad \text{(I 2.26)}$$

From Eq. (I 2.3)

$$P_{s_o}^* = X\,P_{I_i}^* \qquad \text{(I 2.27)}$$

An additional useful relationship derived from Eq. (I 2.21) defines the difference δ^* between the inner ring and shaft

displacement at their common surface, as a result of their rotational speed, in terms of the four integration constants of Eq. (I 2.23 - I 2.26).

$$\delta^* = K_{1I}\, b + \frac{K_{2I}}{b} - N_I \frac{b^3}{8} - K_{1S}\, b - \frac{K_{2S}}{b} + N_S \frac{b^3}{8} \qquad \text{(I 2.28)}$$

Under press fit conditions $\delta^* = 0$.

We will now examine the application of Eq. (I 2.23 - I 2.26) in determining the ring behavior as a function of rotational speed.

The following conditions might be encountered:

1. A tight fit remains tight
2. A tight fit loosens
3. A loose fit remains loose
4. A loose fit tightens

For all four conditions, $P_{Si}^* = 0$ and $P_{IO}^* = 0$, i.e. it is assumed that no change in pressure occurs at the internal surface of the shaft or the external surface of the inner ring resulting from ring rotation. Also Ω_I and Ω_S are identical. All four of the integration constants K_{1I}, K_{2I}, K_{1S} and K_{2S} are unknowns. Also, either the change in pressure P_{Ii}^* or the rotational speed Ω embodied in N_I and N_S are additional unknowns.

Now the formulations of Eq. (I 2.23 - I 2.28) are presented which are required to solve each of the four conditions.

I 2.6.1 <u>SITUATION 1 AND 2, INITIALLY TIGHT FIT</u>

In addition to the integration constants, P_{Ii}^* is the unknown, where P_{Ii}^* is the change in inner ring internal pressure resulting from the rotational speed. If P_{Ii}^* is less than P_{Ii} from Eq. (I 2.18), situation 1 is realized. The operating fit pressure is the difference between P_{Ii} and P_{Ii}^* and the fit remains tight. The resulting radial displacement at the inner ring rolling path is given by:

$$\delta_\Omega = -N_I \frac{R^3}{8} + K_{1I}\, R + \frac{K_{2I}}{R} \qquad \text{(I 2.29)}$$

and the total change in the rolling path radius at the inner ring is

$$\delta_{TOT} = \delta_{(F,Q)} + \delta_{\xi} + \delta_{\Omega} \qquad \text{(I 2.30)}$$

δ_{ξ} is the change in rolling path radius which occurs as a result of a temperature change from 68°F.

If P_{Ii}^{*} is greater than P_{Ii} the solution to the problem requires several additional steps. Eq. (I 2.23), must be re-solved to determine the rotational speed, Ω_{TL} at which the change in fit pressure is just equal to the initial fit pressure and $\delta^{*} = 0$. This rotational speed is termed the tight fit speed limit and is subscripted with the letter (TL). Using the integration constants thus determined and Eq. (I 2.21), δ_{TL} may be determined.

Note, the subscripts in parenthesis should be interpreted as follows: The first subscript refers to the state of the initial fit (T-tight) or (L-loose), the second subscript refers to the rotational speeds (T-Total) or (L-Limit). For instance, U_{TL} refers to the change in inner ring rolling path radius due to the rotational speed at which the initially tight shaft fit is lost.

After determining U_{TL} Eqs. (I 2.23 - I 2.26) are resolved twice for the four integration constants, with P_{Ii}^{*} set to zero. First, for the full rotational speeds, yielding U_{TL} and then for the tight fit speed limit, yielding U_{LL}. This is accomplished by changing the values of N_I and N_s through a change in the value of Ω in Eq. (I 2.20). Utilizing super-position, the change in rolling path radius resulting from rotation is given in Eq. (I 2.31).

$$\delta_{\Omega} = \delta_{TL} + (\delta_{LT} - \delta_{LL}) \qquad \text{(I 2.31)}$$

Eq. (I 2.31) is presented graphically in Fig. I 2.2. Then is calculated from Eq. (I 2.30).

FIGURE I 2.2

Ring Radial Expansion vs. Rotational Speed Squared

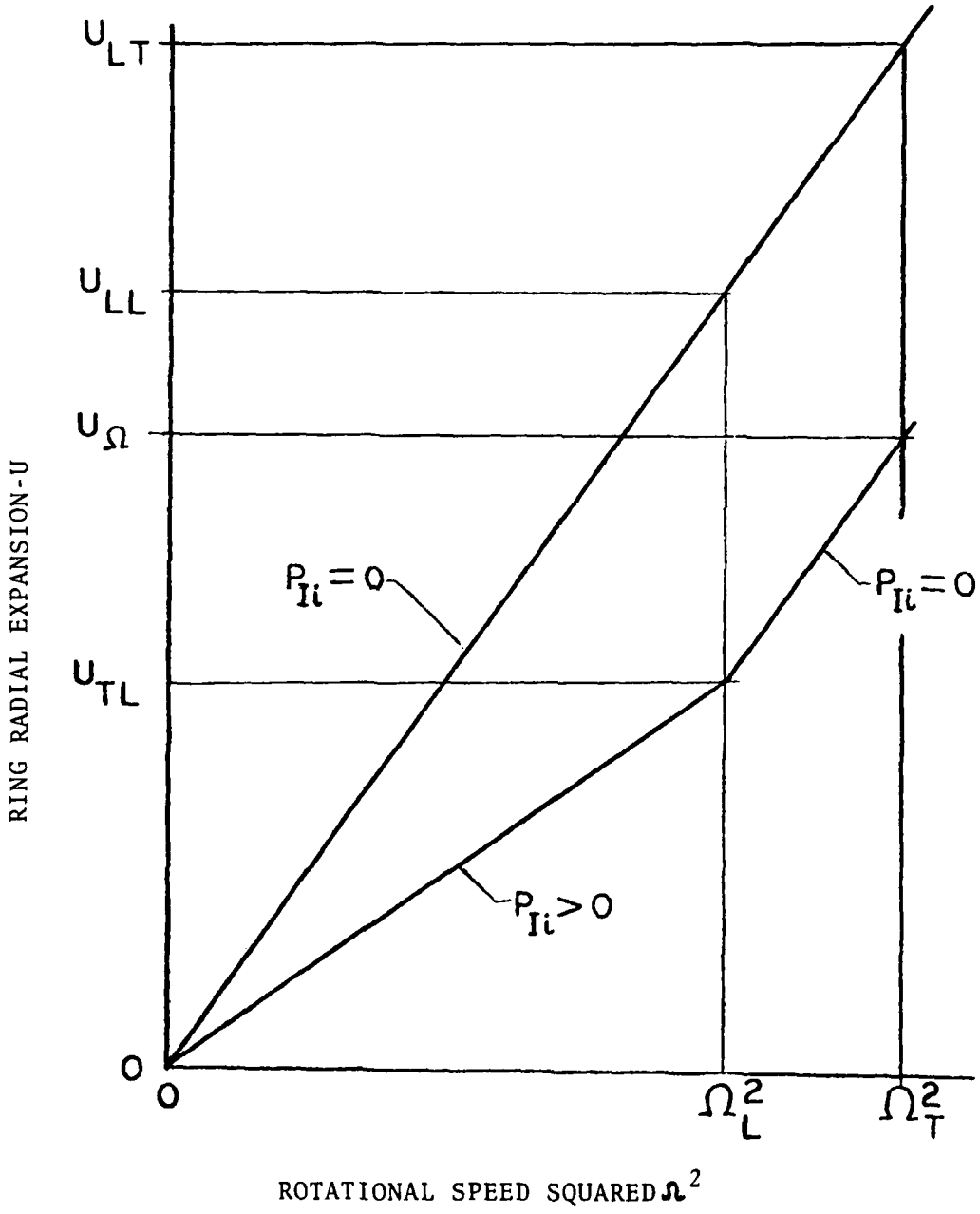

I 2.6.2 SITUATIONS 3 AND 4 INITIALLY LOOSE FIT

The integration constants K_{1I}, K_{2I}, K_{1S}, and K_{2S} are unknowns. P_{Ii}^*, P_{Io}^*, P_{Si}^* and P_{So}^* are all set to zero, and only Eqs. (I 2.23 - I 2.26) are solved. Using the integration constants thus obtained, Eq. (I 2.28) is solved for δ^*. If $\delta^* < |F_{HOT}|$ where F_{HOT} is negative, the loose fit remains loose at operating conditions. The constants K_{1I} and K_{2I} are used to calculate U_Ω. Using Eq. (I 2.30), U_{TOT} is calculated. If $\delta^* > |F_{HOT}|$, the shaft has expanded further under the effects of rotation than the inner ring, and the initially loose fit becomes tight. This requires additional solutions to Eqs. (I 2.23 - I 2.26).

δ^* is set equal to F_{HOT} and the equations are solved for the integration constants plus the speed at which the initially loose fit becomes tight Ω_{LL}. Using the integration constants K_{1I} and K_{2I} along with Eq. (I 2.32), δ_{LL} is determined. Eq. (I 2.23 - I 2.28) are again resolved twice at Ω_{LL} and Ω_{LT} for P_{Ii} and the integration constants, after setting δ^* to zero. δ_{TL} and δ_{TT} can be obtained by from eq. (I 2.29) using the two sets of integration constants . The operating fit pressure is then given by;

$$P_{Ii} = P_{Ii\,TT}^* - P_{Ii\,TL}^* \qquad \text{(I 2.32)}$$

$$\delta_\Omega = \delta_{LT} + (\delta_{TT} - \delta_{TL}) \qquad \text{(I 2.33)}$$

and Eq. (I 2.30) is used to determine δ_{TOT}. Where δ_{TOT} represents the total change in the radius to the rolling path of the section as the bearing is taken off the shelf at 68°F, mounted on the shaft, subjected to load and rotated up to operating speed.

I 2.7 BEARING DIAMETRAL CLEARANCE

The preceeding sections dealt primarily with the shaft-inner ring section. However, the equations presented are valid for all four of the assembly sections. For both sections, a value is determined for δ_{TOT}, cold fit pressure, operating fit pressure and the speed at which an initially tight fit loosens.

As noted earlier, Eq. (I 2.6) can be used to determine this change in rolling element diameter such that:

$$2\delta_{RT} = D(\lambda \bar{t})_R \qquad \text{(I 2.34)}$$

The change in bearing diametral clearance is given by

$$\Delta P_d = 2\left[\delta_{HTOT} - \delta_{STOT} - 2\delta_{Rt}\right] \qquad \text{(I 2.35)}$$

The bearing operating diametral clearance equals the initial clearance plus the change in clearance ΔP_d

APPENDIX I 3

ELASTIC SHAFT ANALYSIS

APPENDIX I 3

ELASTIC SHAFT ANALYSIS *

I 3.1 COORDINATE SYSTEM, LOAD AND GEOMETRY CONSIDERATIONS

The shaft subprogram calculates the deflection characteristics of a general shaft in two planes, one plane at a time, by solving the differential equation for the deflection curve of the shaft,

$$\frac{d^2Y}{dX^2} = -\frac{M(X)}{EI(X)} \qquad \text{(I 3.1)}$$

where M = moment
E = modulus of elasticity
I = moment of inertia

The coordinates X and Y are shown in Fig. I 3.1

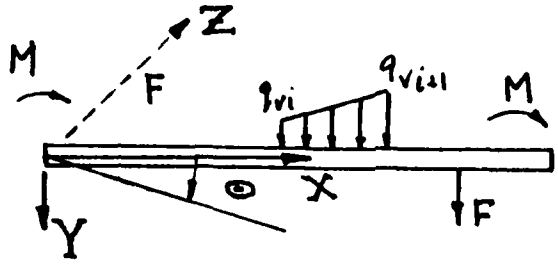

Figure I 3.1 Shaft Coordinate System and Shaft Loading

The shaft load may consist of concentrated loads, moments, or linearly varying distributed loads, Fig. I 3.1. The shaft may be hollow, and the inner and outer diameters may vary stepwise or linearly, Fig. I 3.2

Figure I 3.2 Shaft Schematic Showing Stepwise and Linear Diameter Variation

*This Appendix is based upon the original work {1}

The shaft may be supported by bearings at up to five locations. The bearings may take force and/or moments and they may be initially displaced $(\delta_{y0}, \Theta_{z0})$.

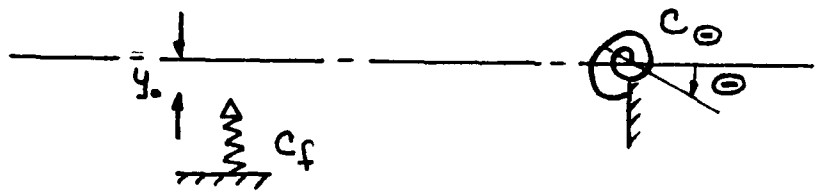

Figure I 3. Schematic-Shaft Supports

The bearing subprograms calculate the reaction forces and moments on the shaft from the bearings as functions of bearing deflections. The bearing deflections can be looked upon as shaft support displacements, (δ_y, Θ).

I 3.2 SHAFT BEARING EQUATIONS

The shaft reaction at any location i is calculated as the shaft reaction, F_{0i}, at i when all additional displacements of the shaft supports are zero, plus the additional reactions at i caused by all additional displacements, or bearing deflections:

$$F_i = F_{0i} + \sum_{j=1}^{N_b} \frac{\partial F_i}{\partial \Theta_{zj}} \cdot \Theta_{zj} + \sum_{j=1}^{N_b} \frac{\partial F_i}{\partial \delta_{yi}} \delta_{yi} \qquad \text{(I 3.2)}$$

The reactions F_0 are calculated using the shaft program with the given initial displacements and spring constants. The constant derivatives $dF/d\Theta$ and $dF/d\delta$ are calculated by introducing one initial displacement at a time. If the bearing mounts are rigid, i.e. spring constants are zero, then the reaction at location i depends only on the deflections at i-1, i, and i+1. The other derivatives are zero. The present program uses the shaft program this way, and has not yet been extended to include all derivatives. Thus the influence of housing elasticity is not taken into account.

I 3.3 METHOD OF SOLUTION

The object is to calculate the shaft deflections and slopes at the bearing locations along the shaft. The shaft may be arbitrarily loaded and have arbitrarily varying cross-section. The supports may take force or moment load, they can be initially displaced. These deflections and slopes are found by going through the following steps:

Step 1. Take away all supports (support and bearing are synonomous) except two. In the following, these two supports are called the initial supports. In the steps to follow, slopes, deflections and initial displacements refer to a coordinate system with the X-axis along the center-line of the unloaded shaft when it is supported by the initial supports. The relation between this coordinate system and the original system is given by the coordinates δ_{y_0} and Θ_{z_0} of the left end of the shaft as defined in the original coordinate system.

The problem is now statically determinate and the reactions of the initial supports are calculated.

Step 2. Define a new coordinate system. Fix the left end of the shaft in that system so that deflection and slope are zero at that end. Let the load acting on the shaft still be the external load plus the reactions from the initial supports as calculated in Step 1.

Since these reactions were obtained from equilibrium equations of the shaft, there is no reaction at the fixed end. Therefore, all shaft loads are known and the moment M of the shaft can be calculated at any section X

from an equation of equilibrium of the shaft to the left of the section. The slopes and deflections are calculated from the Moment-Area theorems by numerical integration of the following equations.

$$\Theta(X) = \int_0^X \frac{M(x)}{EI(x)}\,dx \qquad \text{(I 3.3)}$$

$$\delta(X) = \int_0^X \frac{M(x)(X-x)}{EI(x)}\,dx \qquad \text{(I 3.4)}$$

Step 3. Put the shaft back on the initial supports and correct the slopes and deflections accordingly. The resulting calculated slopes and deflections are in the following denoted by Δ_c.

Step 4. The reaction forces and moments, here called F_i at all supports except the initial supports are now introduced. Their magnitude is determined from the condition that the deflection at each support location goes back to zero + initial displacement, Δ_o .

$$F_i \cdot \beta_{ii} + \cdots + F_i \beta_{ii} + \cdots + F_{N_b} \beta_{N_b i} = -\Delta_{ci} - \Delta_{oi} \qquad \text{(I 3.5)}$$

where

β are influence coefficients

β_{ij} is the deflection or slope at location i from a unit force or moment at location j.

The influence coefficients are obtained by introducing a unit force or moment at one support at a time and then calculating the deflections and slopes starting from Step 2.

There is one equation for each of the n bearings except the two initial supports. The linear system of equations

can be written

$$A \cdot F = B \qquad \text{(I 3.6)}$$

where A is a matrix $N_b \times N_b$

$$A_{ij} = \beta_{ij}$$

F_b = the vector of unknown reactions

$$B_i = -\Delta_{c,i} - \Delta_{oi} \qquad \text{(I 3.7)}$$

The reactions are obtained by solving this system of equations.

Step 5. Calculate the reactions at the initial supports again, this time with both the external loads and the calculated reactions acting on the shaft.

Step 6. The deflections and slopes are calculated again as in Step 2, this time with external loads and all reactions acting on the shaft.

Step 7. The deflections are expressed in the original coordinate system by addition of δ_{y0} to the lateral deflection and Θ_{z0} to the slopes.

APPENDIX I 4

CONCENTRATED CONTACT CALCULATIONS

APPENDIX I 4

CONCENTRATED CONTACT CALCULATIONS *

I 4.1 INTRODUCTION

This section deals with the calculation of the forces which develop in rolling element-raceway contacts in ball and cylindrical roller bearings.

I 4.2 COORDINATE SYSTEMS

Consider a plane through the bearing axis and the center of a rolling element Fig. 2.4. The position of the center of the rolling element relative to the outer ring is described as a coordinate system fixed to the rolling element center, having its x-axis parallel to the bearing X-axis and y-axis radially outward from the bearing axis.

I 4.3 BALL RACEWAY FORCES

In a ball bearing, the outer and inner ring groove curvature centers EC and IC, are defined by the vectors $\mathcal{G}_1$ and $\mathcal{G}_2$, respectively, Fig. 4.1 and 4.2.

The normal force Q is obtained from the Hertz theory for bodies in contact under load.

$$Q = K_1 \delta_{el}^{3/2} \qquad \text{(I 4.1)}$$

where K_1 = a function of the initial geometry and of the material properties.

δ_{el} = the elastic deflection

*This Appendix is based upon the original work {1}

The elastic deflection at one ring is obtained from the distance between the ball center and the groove curvature center, that is $|\mathcal{G}_1|$ or $|\mathcal{G}_2|$. When the elastic deflection is zero, this distance is $r_g - 0.5D$ where r_g is the groove curvature radius. When there is elastic deflection, this distance is greater by the amount δ_{el} of the elastic deflection. Thus,

$$\delta_{el,m} = |\mathcal{G}_m| - (r_{gm} - 0.5D), \quad m = 1,2 \tag{I 4.2}$$

The dimensions of the contact ellipse are obtained from the same theory,

$$a = K_2 \, Q^{1/3} \tag{I 4.3}$$

$$b = K_3 \, Q^{1/3} \tag{I 4.4}$$

where a = the major half-axis

b = the minor half-axis

K_2 and K_3 = functions of the initial geometry and of the material properties

$$\mathcal{G}_1 = \begin{pmatrix} -X_1 \\ -Y_1 \\ 0 \end{pmatrix} \tag{I 4.5}$$

$$\mathcal{G}_2 = \mathcal{G}_1 + \mathcal{G}_0 + \mathcal{G}_\Delta$$

FIGURE I 4.1

Ball Bearing Geometry

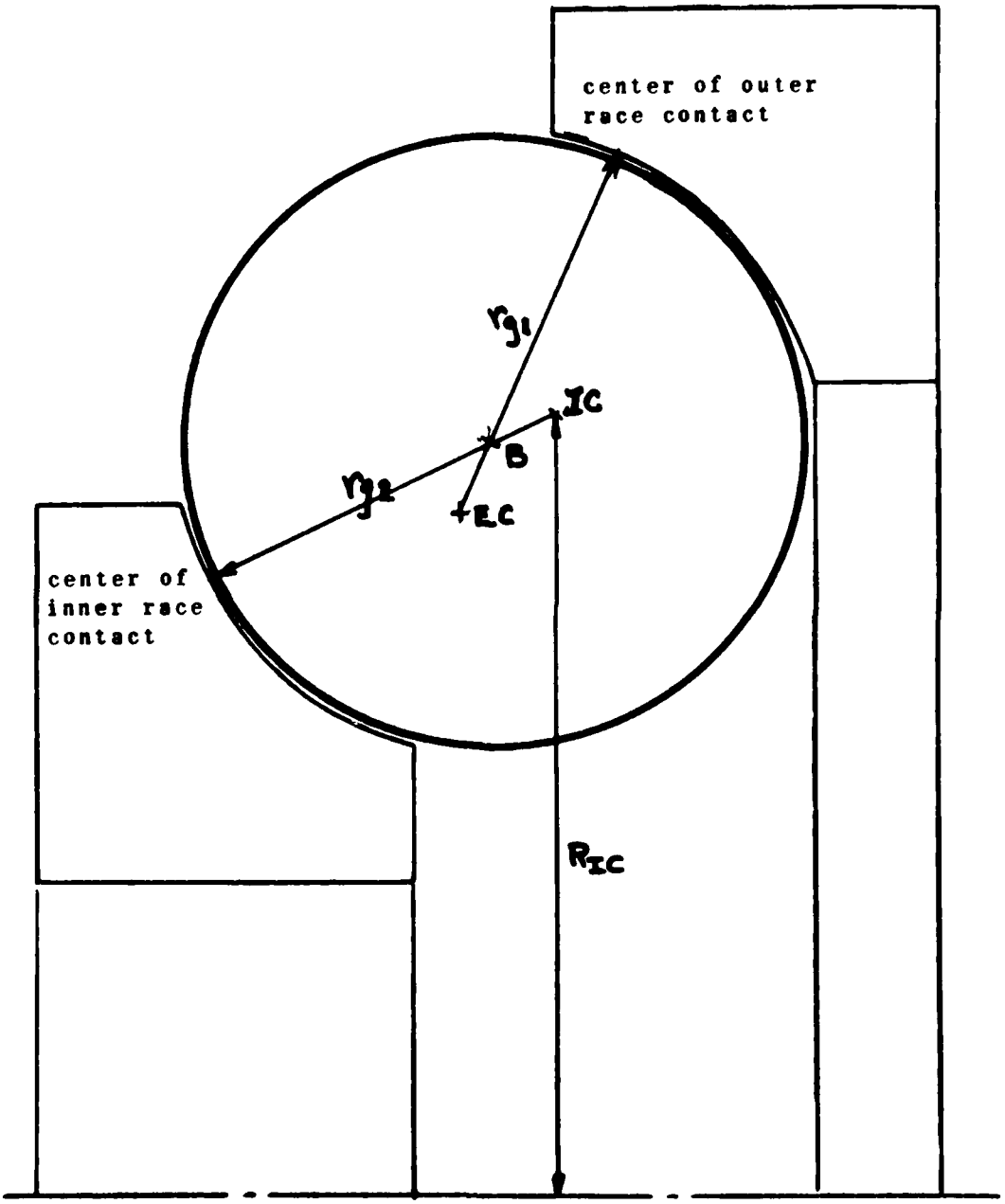

FIGURE I 4.2

Ball Coordinate System Showing Ball Center Position Vectors

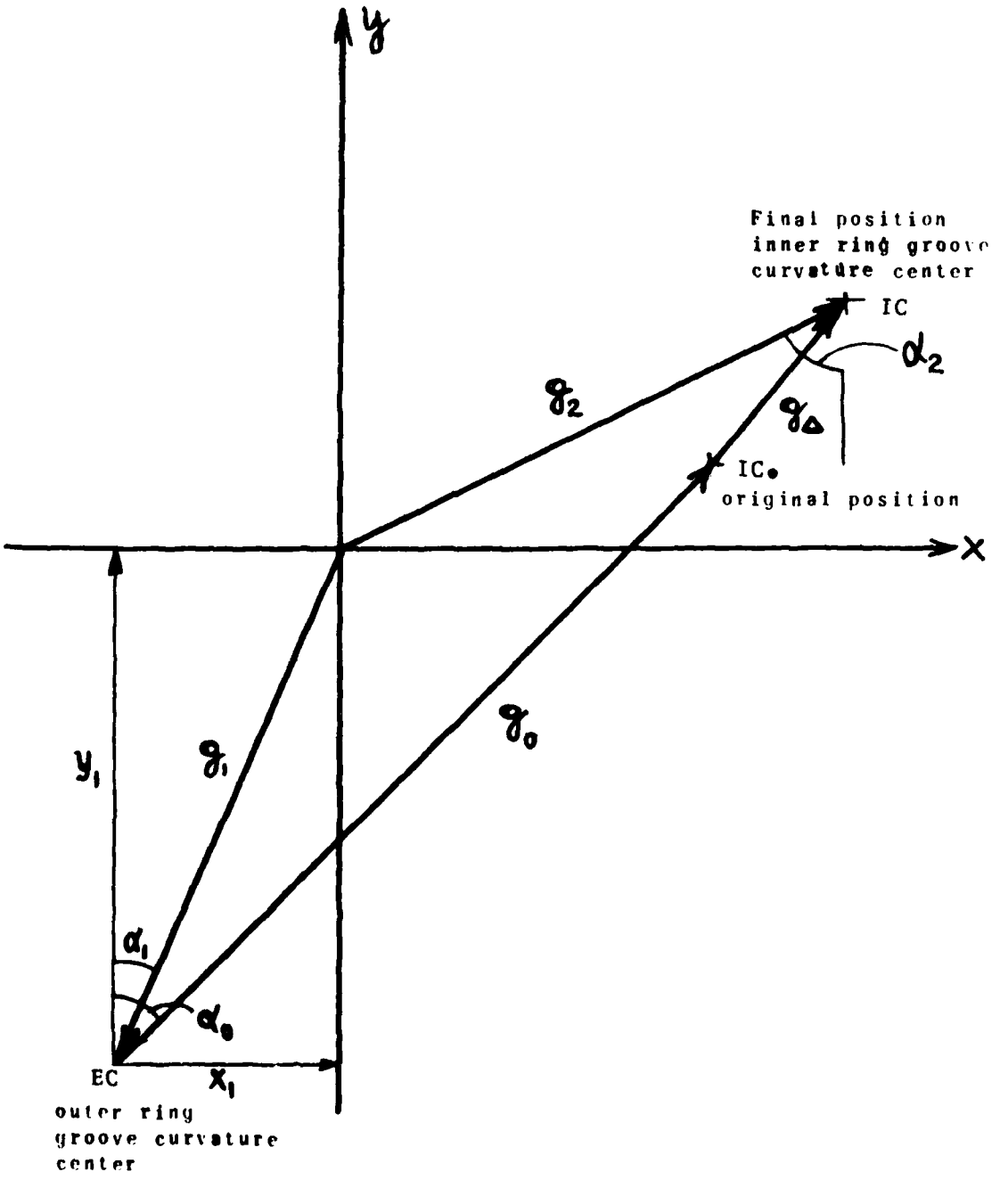

where $\mathfrak{g}_0$ = a vector from ED to the original position of IC_0.
$\mathfrak{g}_\Delta$ = a vector between IC_0 and IC

$$\mathfrak{g}_0 = \begin{pmatrix} g_0 \sin\alpha_0 \\ g_0 \cos\alpha_0 \\ 0 \end{pmatrix}$$

where (I 4.6)

$$g_0 = r_{g1} + r_{g2} - D - \delta_0$$

δ_0 = the total clearance at one ball in the direction of $\mathfrak{g}_2$

$\mathfrak{G}$ is the displacement of the inner ring groove curvature center at a ball from original position to loaded position in the bearing coordinate system. $\mathfrak{g}'_\Delta$ is the vector $\mathfrak{G}$ in the rolling element coordinate system.

$$\mathfrak{g}'_\Delta = \mathbb{T} \cdot \mathfrak{G} \qquad \text{(I 4.7)}$$

The vector $\mathfrak{g}_\Delta$ is the projection of $\mathfrak{g}'_\Delta$ on the x-y plane, i.e. $\mathfrak{g}'_\Delta$ with the z-component equal to zero.

$\mathbb{T}$ is the rotational transformation matrix which transforms forces and moments described in the bearing coordinate system to their equivalents in the rolling element coordinate system.

$$\mathbb{T} = \begin{bmatrix} 1 & 0 & 0 \\ 0 & \cos\phi & -\sin\phi \\ 0 & \sin\phi & \cos\phi \end{bmatrix} \qquad \text{(I 4.8)}$$

where ϕ is the rolling element aximuth angle described in Fig. 2.4.

The vector $\mathbb{G}$ is obtained from the bearing linear deflection vector $\mathbb{D}$ and angular deflection vector Θ

$$\mathbb{G} = \mathbb{D} + \Theta \times \mathbb{R}_{IC} \qquad \text{(I 4.9)}$$

where

$$\mathbb{D} = \begin{pmatrix} \delta_x \\ \delta_y \\ \delta_z \end{pmatrix}, \quad \Theta = \begin{pmatrix} 0 \\ \Theta_y \\ \Theta_z \end{pmatrix}, \quad \mathbb{R}_{IC} = \begin{pmatrix} 0 \\ R_{IC}\cos\phi \\ R_{IC}\sin\phi \end{pmatrix}$$

I 4.4 ROLLER RACEWAY FORCES

In a roller bearing the position $x_1 = 0$ and $y_1 = 0$ for the roller center is defined as the position of the roller center when it is centrally located in relation to the raceway in the x-direction, and when the roller under no load and no misalignment touches the outer raceway, Fig. I 4.3.

FIGURE I 4.3
Roller Bearing Geometry and Roller Coordinate System

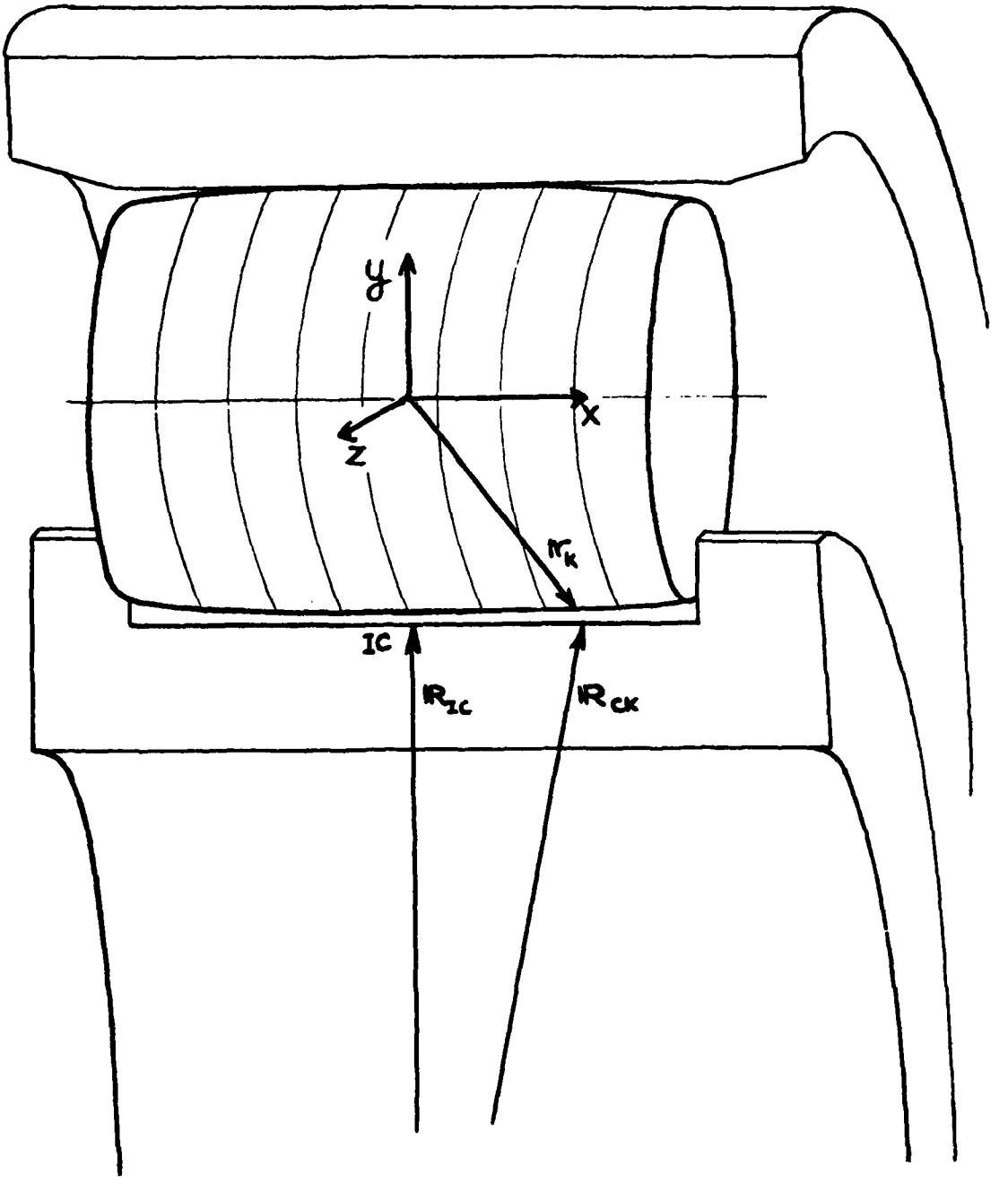

To obtain the normal forces on the roller, it is thought of as divided into n_k slices. The force on each individual slice is calculated separately, as though the entire length of the roller was deflected to the amount which obtains at the actual slice. Shear forces between slices are neglected. The relation between deflection and force is given by the following formula, {25}

$$Q = K_4 \cdot l_{re}^{8/9} \cdot \delta_{el}^{10/9} \qquad \text{(I 4.10)}$$

where Q = roller load

l_{re} = roller length

δ_{el} = elastic deflection

The load per unit length of the contact is q.

$$q = \frac{Q}{l_{re}} \qquad \text{(I 4.11)}$$

The slice load, Q_k is obtained from:

$$Q_k = q \cdot \Delta l_{re} = \frac{Q}{l_{re}} \cdot \Delta l_{re} = \frac{K_4 l_{re}^{8/9} \cdot \delta_{el,k}}{l_{re}} \Delta l_{re} \qquad \text{(I 4.12)}$$

$$= \frac{K_4 l_{re}^{8/9} \delta_{el,k}^{10/9}}{n_k}$$

At the outer race, the deflection δ_{el} at slice k is the difference between the normal approach δ_n and the crown drop δ_{ck}. See Fig. 3.3.

$$\delta_{el\,k} = \delta_{nk} - \delta_{ck} \qquad \text{(I 4.13)}$$

where δ_{c1k} = sum of roller and race crown drops

$$\delta_{nk} = (-\mathbb{g}_1 + \boldsymbol{\theta} \times \mathbb{r}_k) \cdot \hat{y} \qquad \text{(I 4.14)}$$

$\hat{y}$ = a unit vector in the y-direction

$$\mathbb{g}_1 = \begin{pmatrix} -x_e \\ -y_e \\ 0 \end{pmatrix} \qquad \boldsymbol{\theta} = \begin{pmatrix} 0 \\ \theta_y \\ \theta_z \end{pmatrix}$$

The vector $\mathbb{r}_k$ from the rolling element center to the center of slice k in the roller raceway contact is defined as follows:

$$\mathbb{r}_k = \begin{pmatrix} x_k \\ D/2 \\ 0 \end{pmatrix} \qquad \text{(I 4.15)}$$

$$x_k = -\ell_{re}/2 + (k - 0.5) \cdot \ell_{re}/n_k$$

At the inner race, the deflection at slice k is:

$$\delta_{el2k} = -\delta_{nk} + (\mathbb{D} + \boldsymbol{\theta} \times \mathbb{R}_{ck}) \cdot \hat{y} - \delta_0 - \delta_{c2k} \qquad \text{(I 4.16)}$$

where the vector from the inner ring center to the contact at the inner race, $\mathbb{R}_{ck}$ is

$$\mathbb{R}_{ck} = \begin{pmatrix} x_k \\ R_{IC} \cos \phi \\ R_{IC} \sin \phi \end{pmatrix}$$

Since the roller rotates only about its geometric axis, the angular alignment of the roller may be described in terms of the orthogonal components of the roller rotational speed (ω) as follows:

$$\theta_y = \tan^{-1}(-\omega_z/\omega_x) \approx -\omega_z/\omega_x \qquad \text{(I 4.17)}$$

$$\theta_z = \tan^{-1}(\omega_y/\omega_x) \approx \omega_y/\omega_x \qquad \text{(I 4.18)}$$

I 4.5 SUMMATION OF CONTACT TRACTION FORCES

Of all the forces which develop within various concentrated contacts, only the elastic Hertz force in a ball raceway contact may be treated as a point force. The elastic forces which develop in a roller raceway contact and both ball and roller traction forces cannot be treated as point forces since they are not necessarily symmetric. Within the extremely small areas which develop in concentrated contacts, the variation in surface pressure is extreme. Despite the small area, significant variation in rolling element-raceway, relative surface velocities may occur within the contact. The acute pressure variations plus the changes in surface velocities necessitate that concentrated contact areas be subdivided into smaller elemental areas. Over the latter the assumptions of a circular pressure distribution and constant relative sliding velocity closely approach the physical situation.

For the roller raceway contact, the same contact sub-areas used to calculate the elastic force distribution are subsequently used to evaluate the traction force distribution. For the ball raceway contact, the sub-areas consist of slices perpendicular to the contact major axis.

I 4.5.1 VECTOR TO THE CONTACT CENTER FROM THE ROLLING ELEMENT CENTER

For roller bearings the vector $\mathbf{r}$ has been given previously.

In a ball bearing the vector $\mathbf{r}$ is required to calculate the ball raceway friction forces and is given by its components n and t. See Fig. I 4.4.

$$\mathbf{r} = n \cdot \hat{\mathbf{n}} + t \cdot \hat{\mathbf{t}} \qquad \text{(I 4.19)}$$

$$\hat{\mathbf{n}} = \begin{pmatrix} \pm \sin\alpha \\ \pm \cos\alpha \\ 0 \end{pmatrix}$$

$$\hat{\mathbf{t}} = \begin{pmatrix} \mp \cos\alpha \\ \pm \sin\alpha \\ 0 \end{pmatrix}$$

The upper and lower signs apply for outer and inner ring contacts respectively.

The radius of the deformed surface, Fig. I 4.5, is given by Eq. I 4.20.

$$r_{def} = \frac{D}{2} \cdot \frac{2 r_g}{r_g + D/2} \qquad \text{(I 4.20)}$$

$$n = \left(r_{def}^2 - t^2\right)^{1/2} - n_0 \qquad \text{(I 4.21)}$$

$$n_0 = \left(r_{def}^2 - a^2\right)^{1/2} - \left((D/2)^2 - a^2\right)^{1/2} \qquad \text{(I 4.22)}$$

The coordinates t and n are used with the other components of the ball rotational speed to calculate the ball surface velocity components.

I 4.5.2 SUMMING THE TRACTION FORCE OVER A CONCENTRATED CONTACT AREA

In computing the traction force acting in a contact, the high pressure contact region is divided into a number of slices parallel to the minor axis. In a roller raceway contact, these slices are the same as those used to calculate the normal force. In a ball raceway contact the total contact length as determined by the Hertz analysis is divided into approximately 21 slices. The tractive force is computed for each slice and then summed to give the total.

FIGURE I 4.4

Ball Coordinate System Showing Ball-Race Contact Position Vectors

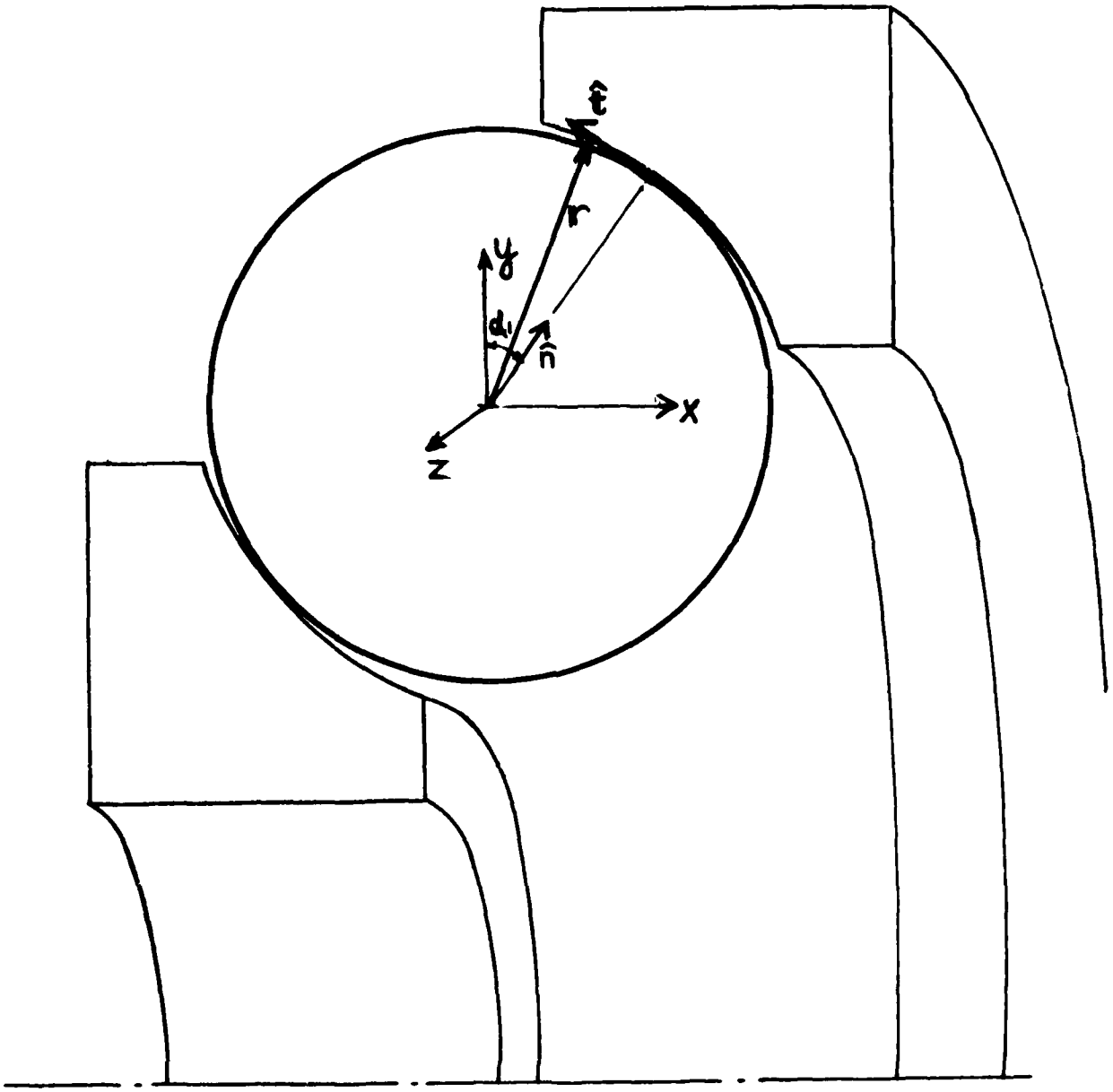

FIGURE I 4-5

Ball Race Deformed Contact and Deformed Surface Radius

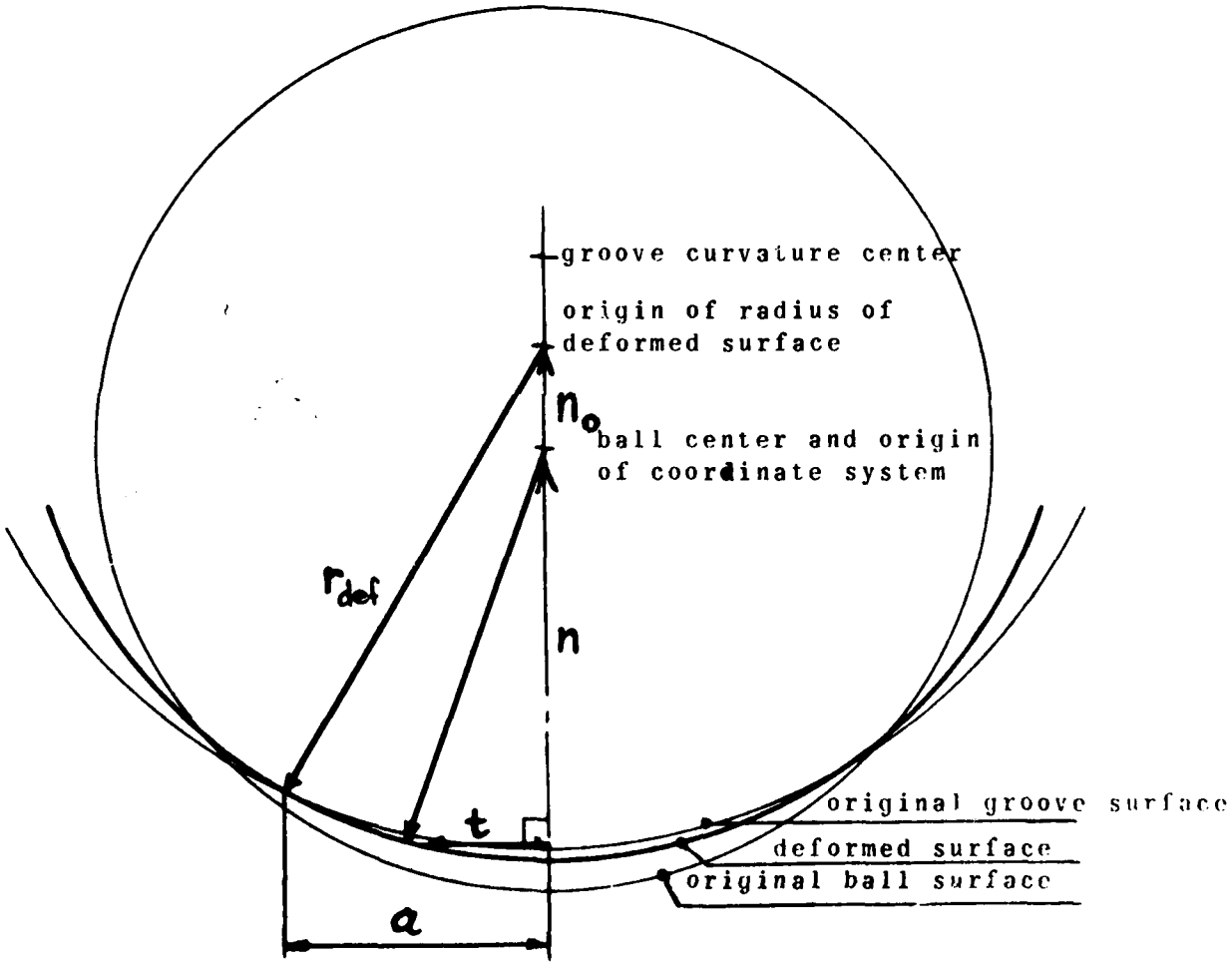

Figure I 4.6a shows a Hertzian contact area with the semi-elliptical distribution of pressure due to elastic deformation (effects of the lubricant on the pressure distribution are neglected) and a local coordinate system established at the contact center ($t = 0$).

By considering a sufficient number of slices the variation of pressure in the x-direction over a slice width may be neglected, i.e. each slice is regarded as the contact zone due to a cylindrical disk (without edge effects).

Sliding velocities at a typical race slice are shown in Fig. I 4.6b. A sliding velocity in the x-direction results if the ball rotational vector has a component ω_z. The sliding velocity u_{sx} is always equal for all slices.

Because of groove curvature the sliding velocity component u_{sz} will vary from slice to slice across the contact ellipse.

Figure I 4.6c shows the traction components T_x and T_z on the slice. T indicates the resultant for the given slice. The forces T_x and T_z are computed for each slice and summed to give the components of the total traction force acting at the contact.

Additionally, during the integrations, friction moments of the tractions about the rolling element center are obtained, using the radius vector coordinates n and t.

FIGURE I 4.6

Calculation of Traction Force Components

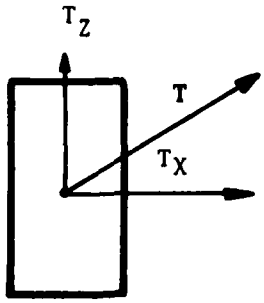

c. TRACTION COMPONENTS AND THEIR RESULTANTS AT A TYPICAL SLICE

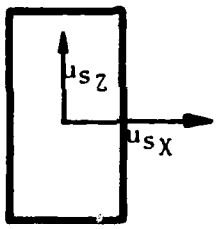

b. SLIDING VELOCITIES ON TYPICAL SLICE

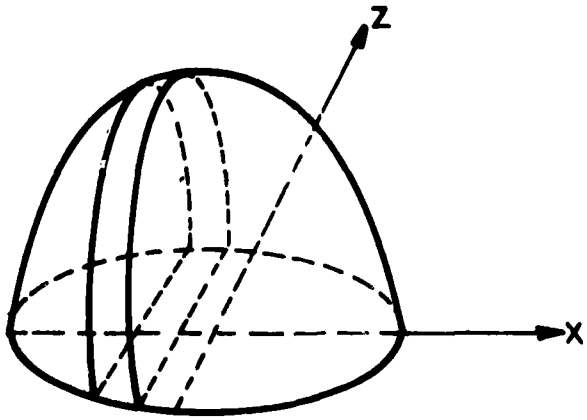

a. CONTACT ELLIPSE AND PRESSURE DISTRIBUTION

APPENDIX I 5

LUBRICANT PROPERTY AND EHD FILM THICKNESS MODELS

APPENDIX I 5

LUBRICANT PROPERTY AND EHD FILM THICKNESS MODELS *

I 5.1 LUBRICANT PROPERTY MODELS

Many of the calculations performed by computer program SHABERTH require that the viscosity η and the pressure-viscosity coefficient α be known at a given temperature.

Accordingly, the program employs subroutines which, when given lubricant kinematic viscosity ν at 100°F (37.78°C) and 210°F (98.89°C), density ρ at 60°F (15.56°C) and the thermal coefficient of expansion, determine the lubricant density, viscosity, and the pressure-viscosity coefficient at any temperature required.

The kinematic viscosity ν (cs) at atmospheric pressure is calculated at a given temperature t (°F) from Walther's relation {13}

$$\log_{10} \log_{10} (\nu + 0.6) = A - B \log_{10} (t + 460) \qquad \text{(I 5-1)}$$

where A and B are constants determined by substituting the known values of ν at t = 100°F and t = 210°F into Eq. (I 5-1) and solving the two equations which result for A and B.

Having calculated ν at a specific t, η is computed as

$$\eta = \nu \rho \qquad \text{(I 5-2)}$$

* This Appendix is basedupon the original work {9} .

TABLE I 5-1

LUBRICANT PROPERTIES OF FOUR OILS USED IN PROGRAM SHABERTH

Oil No.	Oil Type	Kinematic Viscosity, (cs) 100°F.	210°F.	Walther Equation Constants A	B	Density @ 60°F. gm/cm³	Thermal Conductivity Kf Btu/Hr/Ft/°R.	Thermal Coeff. of Expansion G	Temp. Viscosity Coeff. (°R⁻¹)
1	Mineral Oil	64	8.0	10.349	3.673	0.8800	0.0671	3.52×10^{-4}	0.0193
2	MIL-L-7808G	12.8	3.2	10.215	3.698	0.9526	0.0879	3.94×10^{-4}	0.0132
3	C-Ether	25.4	4.13	11.452	4.113	1.201	0.0690	4.15×10^{-4}	0.0168
4	MIL-L-23699	28.0	5.1	10.207	3.655	1.010	0.0879	4.14×10^{-4}	0.0161

where ρ the lubricant density at temperature t is given by,

$$\rho(t) = \rho(60°F) - G\{t - 60°F\} \qquad \text{(I 5-3)}$$

where G is the lubricant coefficient of thermal expansion.

The pressure-viscosity index α is defined implicitly by the relation

$$\eta(p) = \eta(p = 0) \cdot e^{\alpha p} \qquad \text{(I 5-4)}$$

where η (p) denotes the viscosity at pressure p at an arbitrary temperature.

The value of α itself varies with pressure. The appropriate value of α to use in the film thickness prediction equations wherein it appears, is the value applicable at the inlet, i.e., at atmospheric pressure.

The value of α at a given temperature and at atmospheric pressure is calculated by the relation developed by Fresco, {14}

$$\alpha = (2.303)\ 10^{-4}\ [C + D\log_{10} + E(\log_{10})^2]^{\frac{(560)}{(t + 460)}} (\text{in.}^2/\text{lb}) \qquad \text{(I 5-5)}$$

wherein ν is evaluated at temperature t (^{o}F) and C, D, and E are constants tabulated by Fresco as a function of S $\cong$ 0.2B where B is the coefficient in Walther's equation.

Another lubricant property that appears in the model for film thickness reduction due to inlet heating is the temperature viscosity coefficient β, that appears in Reynolds' exponential temperature - viscosity relationship.

β is computed from the viscosity values at t = 100°F and 210°F as follows,

$$\beta = 0.00909 \ln \frac{\eta\ (t = 100^{o}F)}{\eta\ (t = 210^{o}F)} \qquad \text{(I 5-6)}$$

Relevant lubricant properties for the oils whose properties have been preprogrammed in SHABERTH are listed in Table I 5-1. These property values have been supplied by the manufacturers.

I 5.2 LUBRICANT FILM THICKNESS

The elastohydrodynamic (EHD) film thickness,h, at each contact is computed as the product of the film thickness predicted by the Archard-Cowking 20 (point contact) or by the Dowson-Higginson {21} (line contact) formulas and two reduction factors ϕ_t and ϕ_s. The factors ϕ_t and ϕ_s account respectively for the reduction in film thickness due to heating in the contact inlet and the decrease in film due to lubricant starvation, i.e.,due to the finiteness of the distance between the contact zone and the inlet oil meniscus. In equation form,

$$h = \phi_t \cdot \phi_s \cdot \left\{ h_{\substack{A.C.\\D.H.}} \right\} \qquad \text{(I 5-7)}$$

The Archard-Cowking and Dowson Higginson film thickness formulas take the following forms respectively.

$$h_{A.C.} = 2.04 \left[1 + \frac{2R_x}{3R_y}\right]^{-0.93} (\alpha \eta V)^{0.740} R^{0.407} (Q/E')^{-0.074} \qquad \text{(I 5-8)}$$

$$h_{D.H.} = 1.6 . R_x \cdot (\alpha E')^{0.6} \cdot \left(\frac{\eta V}{zE'R_x}\right)^{0.7} \Big/ \left(\frac{q}{E'R_x}\right)^{0.13} \qquad \text{(I 5-9)}$$

R_x, R_y - effective radii of curvature parallel and transverse to the rolling direction respectively

α - pressure viscosity coefficient

V - lubricant entrainment velocity

R = $\left[R_x^{-1} + R_y^{-1}\right]^{-1}$

q = maximum load per unit length

Q = load

E' = $2\left[\frac{1-\nu_1^2}{E_1} + \frac{1-\nu_2^2}{E_2}\right]^{-1}$

η = absolute viscosity

E_1, E_2 = Young's modulus for the contacting bodies

ν_1, ν_2 = Piosson's ratio for the contacting bodies

I 5.2.1 Inlet Heating Factor ϕ_t

A Grubin type inlet film thickness analysis considering full thermal effects was developed for line contact by Cheng {10}. Results presented in {10} covering wide ranges of loads, speeds, and lubricant parameters were used to develop regression formulas for the thermal reduction factor ϕ_t. Based on 28 sets of data, each containing 15 data points, the regression formulas obtained take the following form:

$$\phi_t = e^{x_o} \qquad \text{(I 5-10)}$$

where

(1) $x_o = -0.3011 - 0.00432 \ln (p_o/E') - 0.03469 \ln (1 + S)$
$-0.16423 \ln Q_m - 0.01728 (\ln Q_m)^2 + 0.00389 \ln \alpha'$
$- 0.06316 \ln \beta'$

for $0 < Q_m < 0.1$, $\beta' > 11.5$ and $0 < Q_m < 0.4$, $\beta' < 11.5$

(2) $x_o = -1.119304 - 0.16192 \ln (p_o/E') - 0.0895 \ln (1+S)$
$- 0.29 \ln Q_m - 0.04572 (\ln Q_m)^2 + 0.13615 \ln \alpha'$
$- 0.31615 \ln \beta'$

for $0.1 < Q_m < .1$, $\beta' > 11.5$ and $0.4 < Q_m \leq 1$, $\beta' < 11.5$

(3) and $x_o = -3.66426 - 0.48511 \ln (p_o/E') + 0.00568 \alpha'$
$- 0.05491 \beta' - 0.1678 \ln (1+S) - 0.19573 \ln Q_m$
$- 0.09392 (\ln Q_m)^2 + 0.20908 \ln \alpha'$

for $Q_m > 1$

where, $\alpha' = \frac{\pi}{2} \alpha p_o$

$\beta' \approx \beta t$

$S = (u_2 - u_1)/2V$

$Q_m = 2\ V^2/K_f\ t_o$

α - pressure viscosity coefficient, in ^{2}/lb.

b - half of Hertzian width in the rolling direction, in

p_o - maximum Hertz pressure, lb/in^2

β - temperature viscosity coefficient, $^oR^{-1}$ computed via Eq. (4-6)

t - ambient temperature, ^oR

η - ambient viscosity, (lb.sec/in^2)

U_1, U_2 - surface velocity of bodies No. 1 and 2, (relative to the contact) in/sec

K_f - conductivity of the film (lb/^{o}F.sec)

V - $(u_1 + u_2)/2$, lubricant entrainment velocity (in/sec)

It is noted that for small values of Q_m, ϕ_t computed from Eq. (I 5-10) may be larger than unity. $\phi_t = 1.0$ is used whenever the value computed using Eq. (I 5-10) is larger than 1.0.

In evaluating ϕ_t for the elliptical point contacts in a ball bearing, p_o is taken to be the maximum of the Hertzian pressure ellipse.

The point contact is thus treated as if it were a line contact having a maximum contact pressure p_o along its entire length of contact. This is a conservative approximation inasmuch as it will tend to underestimate ϕ_t and hence underestimate film thickness.

The magnitude of the error resulting from this approximation is small as p_o is not a highly influential variable in the expression for ϕ_t.

I. 5.2.2 Starvation Reduction Factor ϕ_s

A hydrodynamic analysis of an elliptical point contact having two equivalent principal radii of curvature R_x and R_y (parallel and transverse to the rolling direction, respectively) is used for calculating ϕ_s. Finite thickness of the half films ($h_{1,1}$ and $h_{1,2}$) upstream from the inlet are set. The flow rate in the center plane at the meniscus line is set equal to the incoming flow rate at the contact centerline. The complete analysis is given in {11} and {23}.

Figure I 5-1 shows the geometry considered. The starved plateau film thickness is h_s and the meniscus distance from the contact center along the direction of rolling is r^*. The ambient film layers move toward the contact zone with velocities u_1 and u_2.

The analysis shows h_s and r^* to be related to h_1, the sum of the upstream ambient film layer thicknesses, ($h_1 = h_{1,1} + h_{1,2}$) through the following two equations:

$$\frac{5.5V\eta\alpha R_x^{1/2}}{h_s^{3/2}(3+2k)} - \frac{12V\eta\alpha r^*}{(3+2k)\,(h_s + r^{*2}/2R_x)^2} = 1.0 \qquad \text{(I 5-11)}$$

and

$$h_1 = \frac{2(2+k)}{3+2k}(h_s) + \frac{kr^{*2}}{(3+2k)R_x} \qquad \text{(I 5-12)}$$

FIGURE I 5-1

Film Geometry

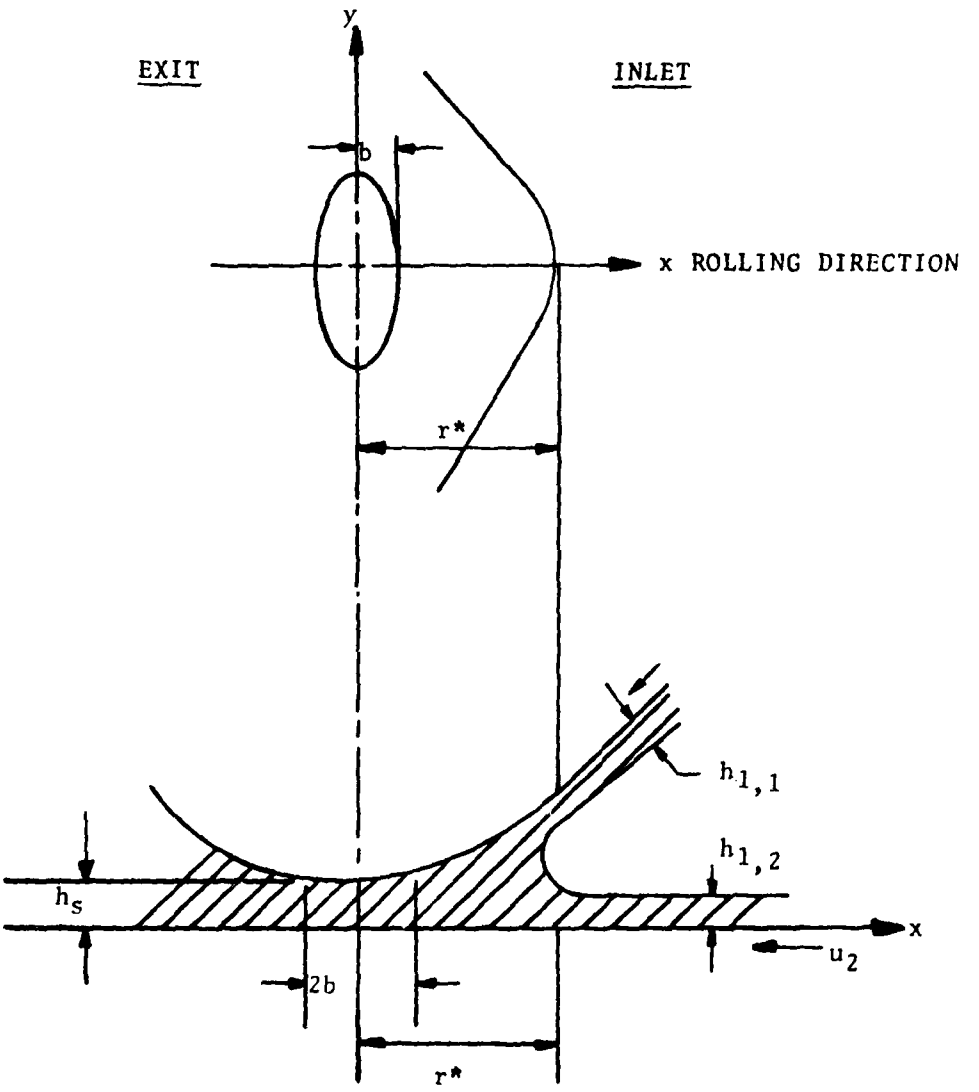

$$h_1 \equiv h_{1,1} + h_{1,2}$$

where $k \equiv R_x/R_y$, η is the viscosity of oil at the contact inlet, α the pressure-viscosity coefficient and $V \equiv \frac{(u_1 + u_2)}{2}$ is the entrainment velocity in the x-direction.

The simultaneous solution of Eqs. (I 5-11) and (I 5-12) for given values of R_x, R_y, V, η, α and h_1 yields the associated values h_s and r^*. Subroutine STARFC performs this calculation.

As the meniscus distance r^* increases, the film thickness h_s increases, asymptotically approaching a value h_f as $r^* \rightarrow \infty$. Therefore, h_f is the film thickness under fully flooded conditions.

On letting $r^* \rightarrow \infty$ and $h_s \rightarrow h_f$ in Eq. (I 5-11), the second term on the left hand side vanishes and one may solve for h_f as

$$h_f = \left[\frac{5.5V\eta\alpha(R_x)^{1/2}}{(3+2k)} \right]^{2/3} \qquad \text{(I 5-12)}$$

Note that for line contacts, the contact curvature ratio k is set equal to a small value.

$$K = R_{x/R_y} = 0.01.$$

This k value results in a contact length to width ratio of 18 : 1.

The lubricant meniscus distance in the rolling element-cage contact is assumed to be proportional to the rolling element radius.

$$r^* = 0.25 \cdot r$$

Subroutine STARFC evaluates h_f from Eq. (I 5-13) and then calculates the ratio $\phi_s = h_s/h_f$. As given by Eq. (I 5-13), it does not indicate a dependence upon load. This is characteristic of film thickness formulas derived from a Grubin type assumption applied to rigid bodies. It is considered preferable to use the Archard-Cowking and Dowson Higginson formulas for the unstarved cases rather than h_f since these formulas better describe the dependence of film thickness upon the influential physical variables. The only role played by h_f is to scale h_s to yield the ratio ϕ_s, which is applied as a multiplicative factor on the Archard-Cowking and Dowson Higginson predictions of unstarved film thickness.

I 5.3 Film Replenishment

As noted above, it is necessary to know the combined oil layer thickness h_1 to calculate ϕ_s and r^*.

As a rolling element passes a point on the inner or outer raceway of a bearing, a very thin lubricant film remains on each of the components and is of the same order of magnitude as half the plateau film thickness in the EHD contact. Replenishment of the lubricant layer on the raceway is required in order to assure sufficient lubricant in the inlet region of the succeeding contact, so that the EHD film thickness will be the same as in the preceding contact. If replenishment fails to occur, each successive rolling element pass would have a thinner EHD film and steady state operation with EHD lubrication would not be possible.

Many mechanisms serve to replenish the lubricant in the track of a high speed bearing. Of prime concern is replenishment at the inner race in high speed ball bearings since centrifugal force tends to direct free fluid away from that surface. Seven replenishment mechanisms have been identified:

(1) Centrifugal flinging of the lubricant from the ball.

(2) Centrifugal travel of oil along the surface.

(3) Random splashing of lubricant in the bearing cavity.

(4) Direct deposition from a jet.

(5) Back flow along the surface into the track, from its edges resulting from lubricant surface tension.

(6) Carrying into the contact, of lubricant adhering to the ball.

(7) Back flow into the gap behind the contact exit due to vacuum in the cavitated area.

A model exists for item (5) above. In view of the other, possibly more influential sources of replenishment enumerated above, this model has not been adopted in this program. Instead, it is assumed that an externally supplied replenishment, amount $\Delta\zeta$, adds to the plateau film thickness to yield h_1.

As a simplification, since $\Delta\zeta$ is usually much larger than h, the approximation $h \sim h_s$ is used so that,

$$h_1 = h_s + \Delta\zeta \qquad (I\ 5\text{-}13)$$

Subroutine STARFC uses Eq. (I 5-13) in solving Eqs. (I 5-10) and (I 5-11), with a user specifified $\Delta\zeta$ value.

Criteria for estimation of $\Delta\zeta$ are presented in Sect. 3.3.15.

APPENDIX I 6

TRACTION AND INLET FRICTION CALCULATIONS

APPENDIX I 6

TRACTION AND INLET FRICTION CALCULATIONS

I 6.1 INTRODUCTION

The traction model developed for use in program SHABERTH is applicable to the partial EHD regime in which the lubricant film separating the contacting surfaces may be small enough to permit some degree of asperity contact. The model computes the traction coefficient as a function of the ratio (h/σ), film thickness h to composite surface roughness σ. For small values of h/σ ($h/\sigma < 0.4$) the model represents dry friction. For large values of h/σ ($h/\sigma > 3$) the model becomes a non-Newtonian semi-empirical fluid film model in which the traction coefficient, μ_{EHD}, depends upon sliding rate, as well as the load, rolling speed and lubricant properties at operating temperture. For intermediate values of h/σ the model is a combination dry and fluid film friction. Essential features of the model are described below.

A single, two dimensional, functional relationship is used to model aspects of both wet and dry friction. The function is plotted in Fig. I 6-1 and is valid over the range.

$$0 \leq X^* < \infty$$

and has the following characteristics.

$$y^* = \frac{Y_B}{X_B} X^* \qquad 0 \leq X^* \leq X_B \qquad \text{(I 6-1)}$$

$$y^* = Y_B (1 + Y_D * X_D / (Y_D * X_B + Y_B * X_D)) \qquad \text{(I 6-2)}$$

where:

$$Y_D = 1 - Y_B$$

$$X_D = X^* - X_B$$

$0 < Y_B < 1$, Y_B defines the value of y^* below which y^* is a linear function of X^*.

$0 < X_B < \infty$, X_B defines the value of X^* below which y^* is a linear function of X^*.

FIGURE I 6-1 Auxiliary Function y* vs x*

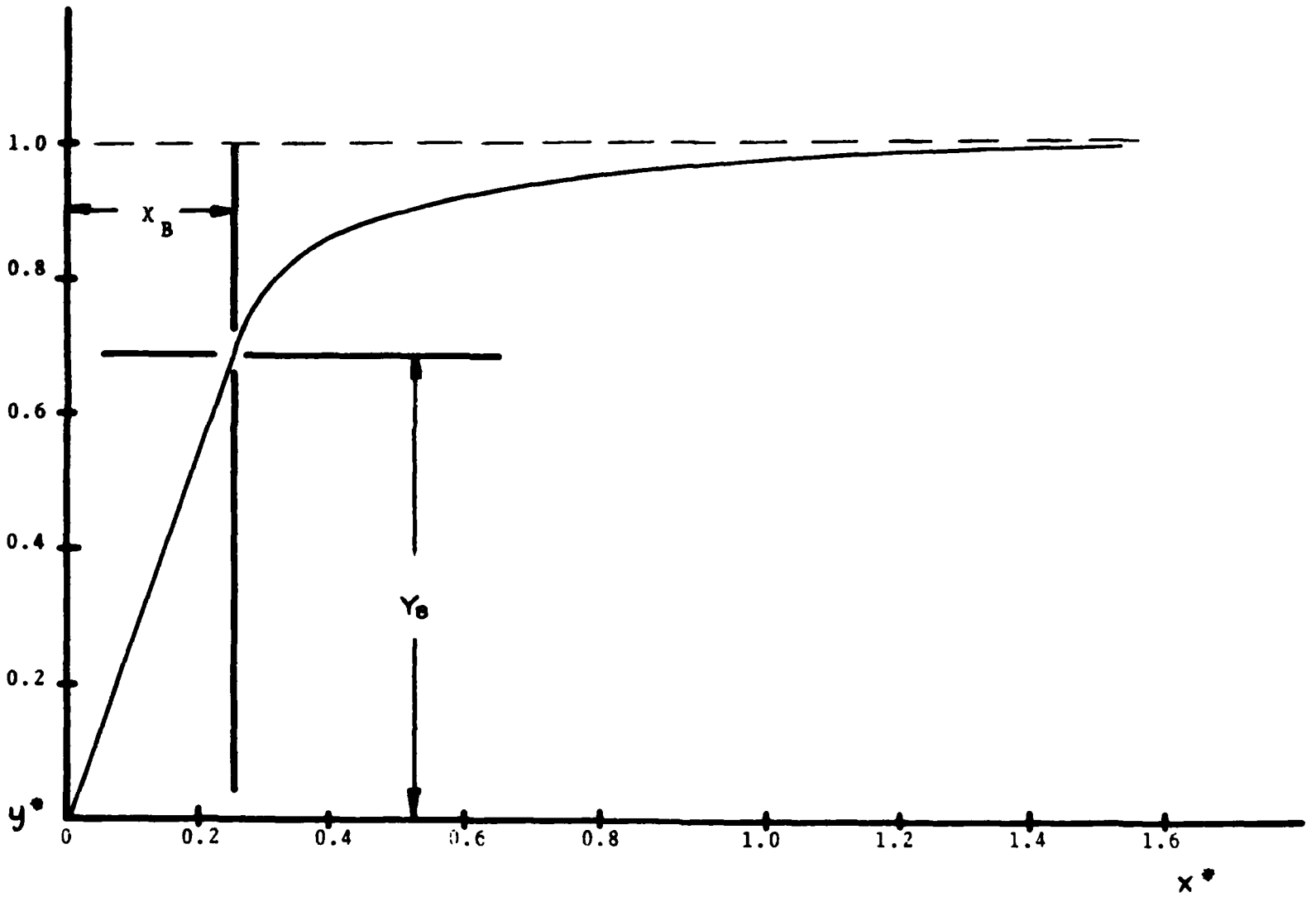

Note that y^* increases monotonically with x^* and that $\frac{dy^*}{dx^*}$ is continuous at $x^* = x_B$.

Both wet and dry friction coefficients will be defined in terms of Eqs. (I 6.1 and I 6.2).

I 6.2 ASPERITY TRACTION MODEL

If Q is the total load applied to a concentrated contact (or to a suitable sub-element of a contact), a portion of this load, designated Q_a will be carried by elastically deformed asperities and the remaining, $Q-Q_a$, will be carried by the EHD film. The traction force T_s then is,

$$T_s = \mu_a Q_a + \mu_{EHD} (Q - Q_a) \qquad \text{(I 6.3)}$$

Under the assumption that the rough surface consists of two-dimensional ridges of random height and slope angle, the average asperity borne load Q_a is the following function of the ratio h/σ.

$$Q_a = \frac{E'}{4\pi^2} A \sigma_\theta I\ (h/\sigma, \alpha) \qquad \text{(I 6.4)}$$

where

$E' = 2\left[\frac{1-\nu_1^2}{E_1} + \frac{1-\nu_2^2}{E_2}\right]$

E_1, E_2 = Young's moduli of the contacting bodies

A = contact area

σ_θ = RMS value of the distribution of asperity slope angles (radians)

$I(h/\sigma, \alpha)$ = function defined in {12} of the film parameter h/σ and a statistical micro-geometry parameter σ defined in Nayak {26}.

It is shown in {27} that $\alpha = 2$ is a reasonable value to use for rolling bearing surfaces. The following polynomial fit to the function $I(h/\sigma, \alpha = 2.0)$ is used in computation:

$$I(h/\sigma, 2) = 2.31e^{-1.84h/\sigma} + 0.1175(h/\sigma - 0.4)^{0.6}(2 - h/\sigma)^2 \qquad \text{(I 6.5)}$$

$0.4 \leq h/\sigma \leq 2$

$$I(h/\sigma, 2) = 17e^{-2.84h/\sigma} + 1.44 \times 10^{-4}\ (h/\sigma - 2)^{1.1}(4 - h/\sigma)^{7.8}$$

$2 < h/\sigma$

When $h/\sigma < 0.4$ the asperities are assumed to carry the entire contact load.

The asperity friction coefficient (μ_a) is calculated as follows:

$$\mu_a = \mu^* y^* \qquad \text{(I 6.6)}$$

μ^* is supplied by the user, 0.1 to 0.2 is the recommended range of values.

where y^* is calculated from Eq. (I 6.1 or I 6.2) in which:

Y_B is 0.66
X_B is 0.005
$x^* = \left\{ \frac{2(U_2 - U_1)}{U_2 + U_1} \right\}$ calculated, local slide to roll ratio

U_2 and U_1 are defined in Fig. I 6.4

This relationship is believed to better approximate the asperity friction phenomena than the coulomb friction model.

This relationship causes the friction coefficient to be a function of the small tangential displacement of the surface of one body with respect to the other. The slide to roll ratio provides a measure of the displacement.

In the numerical solutions being employed, it is important that the functional relationships produce a unique set of forces for a given set of rolling element rotational speeds. The use of the above asperity friction model helps guarantee this uniqueness.

The value $\mu^* = 0.1$ was recommended in {27} as being consistent with values deduced in traction measurements in the partial EHD regime.

I 6.3 FLUID TRACTION COEFFICIENT $_{EHD}$

The general behavior of the fluid traction coefficient μ_{EHD} as a function of sliding rate is illustrated by the curves in Fig. (I 6.2). (Throughout this section the subscript on μ_{EHD} will be omitted.)

In the curve in Fig. (I 6.2a) the traction coefficient increases linearly, at low sliding speeds, reaches a maximum $\mu = \mu^*$ at speed $u_s = u_s^*$, and decreases thereafater.

In the curve in Fig. (I 6.2b) the traction coefficient increases linearly at low sliding speeds and then approaches an asymptotic value μ^*.

Both types of traction curves have been experimentally observed. Both signify a departure from isothermal Newtonian fluid behavior since for this situation the traction coefficient increases linearly with sliding speed.

For the curve of Fig. (I 6.2b), μ^* denotes the asymptotic traction coefficient. Define $u_s^* = 3 \times u_{sc}$, where u_{sc} is the sliding speed at which the line $\mu = \mu^*$ intersects the extended linear portion of the curve μ vs. u_s.

It has been found that μ^* for either type of curve increases with the contact pressure and decreases with rolling velocity and lubricant viscosity (and hence ambient temperature); μ_s^* on the other hand decreases with pressure and increases with rolling velocity and viscosity. This joint variation has been found to result in a scale change in the two axes but not in a substantial change in the character of the traction curve.

This means that traction curves obtained under widely different conditions of pressure, rolling velocity and temperature when plotted on a grid with coordinates $\mu_r = \mu/\mu^*$ and $x = u_s/u_s^*$, yield substantially the same curve {23,27}.

A characteristic of the curves of the type of Fig. (I 6.2a) is that μ_r decreases indefinitely with large x. Curves of this type can cause convergence difficulties in a bearing computer program because there are two sliding speeds associated with each value of the traction coefficient. The solution may cycle

FIGURE I 6.2

Typical Traction Curves

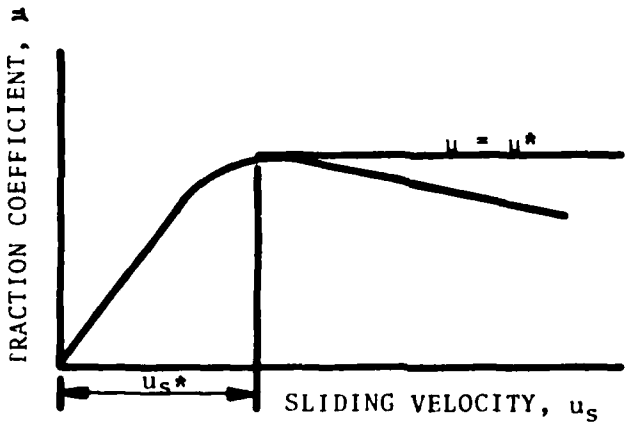

a) A CURVE EXHIBITING A PEAK

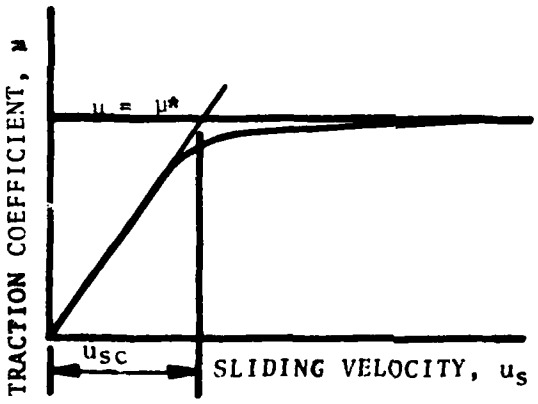

b) A CURVE EXHIBITING ASYMPTOTIC BEHAVIOR

between two values in seeking an equilibrium condition.

An approach to avoiding this difficulty is to use the previously mentioned monotonically increasing curve Eq. (I 6.1 and I 6.2) that is a good match to the actual curve over the increasing portion of that curve. If the program then converges at a sliding speed that is within the range where the curves match, the solution is valid.

In the present context, let y^* and x^* from Eq. (I 6.1 and I 6.2) correspond to the relative traction coefficient (μ_R) and the sliding speed u_s, respectively.

If we now define μ^* as the asymtotic EHD traction coefficient the acatual coefficient μ_{EHD} is:

$$\mu_{EHD} = \mu^* + \mu_R \qquad \text{(I 6.8)}$$

For a given oil, the maximum traction coefficient μ^* has been found {27} to vary with pressure, viscosity, rolling velocity, and film thickness in the following manner:

$$\mu^* \sim f(p_o)^{0.61} p_o^{(-1.14)} \eta^{(0.59)} V^{(0.48-0.61\lambda)} h^{(-0.45)} \qquad \text{(I 6.9)}$$

where

p_o = the maximum contact pressure (lb/in^2)

h = plateau EHD film thickness (in)

$f(p_o)$ = a function governing the dependence of viscosity on pressure p_o (oil parameter)

λ = a visco-elastic constant (oil parameter)

Similarly, u_s^* exhibits the following dependence on p_o, η_o, V and H.

$$u_s^* \sim p_o^{(-0.14)} f(p_o)^{(-0.40)} \eta^{(-1.1)} V^{(0.40\lambda-0.09)} h^{(0.55)} \qquad \text{(I 6.10)}$$

The quantities μ^*, μ_s^* and h can be measured experimentally for a set of given values of p_o, η, and V. For the oils thusfar examined, the function $f(p_o)$ has been found to follow a law of the form,

$$f(p_o) \sim (p_o/p_1)^{A_1} \qquad p_o < p_1$$
$$\sim (p_o/p_1)^{A_2} \qquad p_o > p_1 \qquad \text{(I 6.11)}$$

where A_1, A_2 and p_1 are lubricant dependent constants. Values of A_1, A_2 and p_1 for four oils are listed in Table (I 6.1). The procedure for determining these values for other oils is given in {23,27}.

Making use of Eq. (I 6.11), Eqs. (I 6.9) and (I 6.10) can be expressed in the following form on introducing C_1 and C_2 as proportionality constants.

$$\mu^* = C_1 p_o^{-1.14} \cdot (p_o/p_1)^{0.61 A_i} \eta^{(0.59)} \cdot V^{(0.48-0.61\lambda)} h^{-0.45} \quad \text{(I 6.12)}$$

$$u_s^* = C_2 p_o^{-0.14} \cdot (p_1/p_o)^{0.4 A_i} \cdot \eta^{(-1.1)} \cdot V^{(0.40\lambda - 0.09)} \cdot h^{0.55} \quad \text{(I 6.13)}$$

$$i = 1, 2$$

The values of C_1 and C_2 are evaluated by substituting measured μ^*, u_s^* and h values for a specific test condition. Then knowing values of C_1, C_2, p_1, A_i and h (starved), it is possible to predict values of μ^* and u_s^* as functions of the operating parameters p_o, V, and η by Eqs. (I 6.12) and (I 6.13). Values for C_1 and C_2 thus calculated for four oils are tabulated in Table (I 6.1). The units in Eqs. (I 6.12) and (I 6.13) are V (in/sec), η (cp), P_o (ksi) and h (microinches). Also shown in Table (I 6.1) are the values of $(\mu_r)_B$ and $(u_s)_B$ used for the four oils. These data have been preprogrammed into SHABERTH.

In summary, the calculation of μ_{EHD} at a given sliding velocity u_s and for a given pressure p_o, film thickness h, rolling velocity V and temperature t, proceeds as follows:

1. Calculate viscosity η at temperture t.
2. Using appropriate constants from Table (I 6.1), calculate μ_s^* and μ^* for given p_o, h, V and $\eta(t)$.
3. Calculate $x = u_s / u_s^*$

TABLE I 6.1

TABULATION OF CONSTANT FOR FOUR OILS

Oil No.	Oil Type	λ	A_1	A_2	$p_1 \times 10^5$	C_1	C_2	$(\mu_r)B$	$(V_s)B$
1	Mineral (1) Oil	0.3	3.42	2.14	1.5	1.8	115.9	0.65	0.10
2	MIL-L-7808 (2)	0.94	4.08	1.48	1.7	17.6	39.0	0.68	0.25
3	C-Ether	0.70	3.29	1.50	1.7	26.2	6.6	0.65	0.15
4	MIL-L-23699 (2)	0.93	6.88	3.44	2.2	10.4	47.3	0.68	0.25

NOTES:

(1) obtained from Traction Data reported by Johnson and Cameron (28)

(2) S K F tests

(3) obtained from Traction Data reported by Smith et al (29)

4. Use Eq. (I 6.1 and I 6.2) with values of $(\mu_r)_B$ and $(u_s)_B$ from Table I 6.1 to calculate μ_r associated with the value of x calculated in Step 3.

5. Compute $\mu_{EHD} = \mu_r \cdot \mu^*$

I 6.4 INLET REGION HYDRODYNAMIC FRICTION FORCES

I 6.4.1 ELLIPSOIDAL CONTACT

The contacts between ball and race and between ball and cage pockets are "point" contacts. Under lubricated conditions, the surfaces are separated by a fluid film and there is a pressure build-up around the contact caused by the sweeping-in motion of the surfaces. This pressure build-up contributes to the friction in rolling. Tangential surface forces are required to pump the oil into the high pressure zone.

The pumping forces are due to rolling, (F_R), and sliding (F_S).

Expressions as a function of a finite meniscus distance r* have been found for these forces. The complete analytical development is contained in {11} and {27}.

Since these forces arise in the contact inlet region, elastic deformation is not considered to have a significnat effect and the analysis invokes a rigid body assumption.

Figure (I 6-3) shows the relevant geometry. Two rigid bodies are shown in nominal point contact separated by an oil film and undergoing relative rolling and sliding. A local cartesian coordinate system is established with the x-y plane parallel to the tangent plane of the two bodies and with the origin coincident with the surface of body 2. The coordinate system remains fixed in the contact as the surfaces of the two bodies move. The principal radii of curvature of the two bodies are $(R_x)_i$ and $(R_y)_i$, i = 1,2. The equivalent radii are

$$R_x = \left(1/R_{x1} + 1/R_{x2}\right)^{-1} ; R_y = \left(1/R_{y1} + 1/R_{y2}\right)^{-1} \qquad \text{(I 6.14)}$$

FIGURE I 6.3

Notation for Rolling Sliding Point Contact

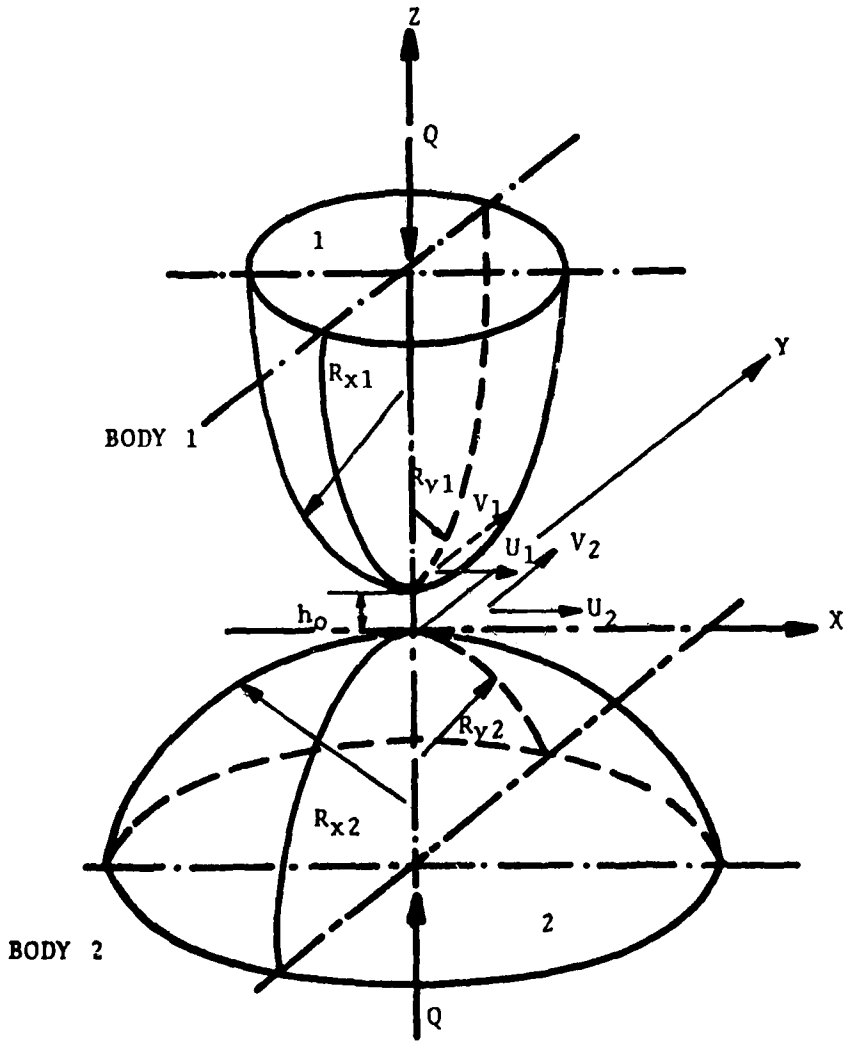

FIGURE I 6.4

Friction Forces on Sliding and/or Rolling Disks

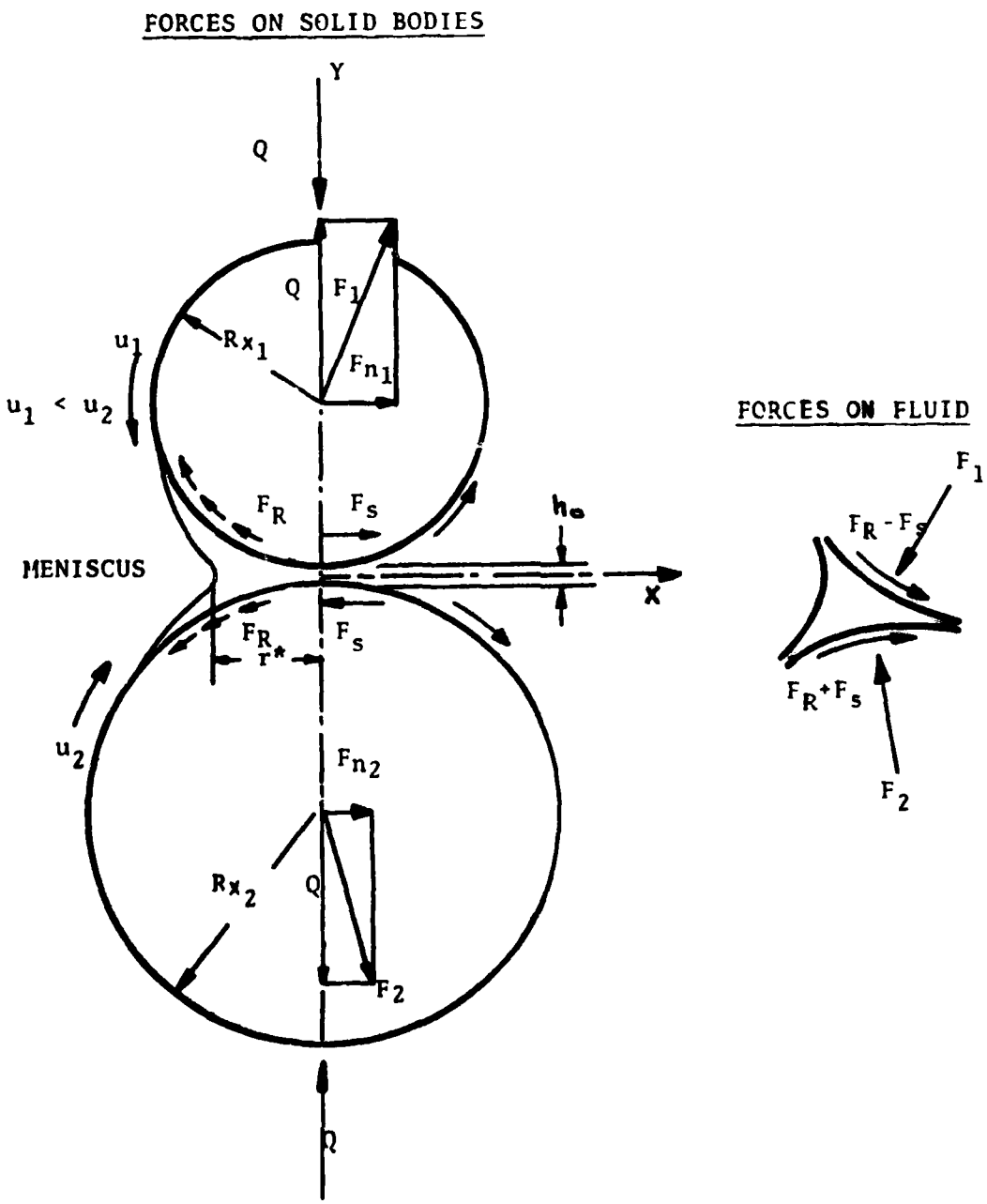

The normal separation of points on the two bodies near the origin is given by

$$h = h_o + \frac{x^2}{2R_x} + \frac{y^2}{2R_y} \qquad \text{(I 6.15)}$$

where h_o is the minimum film thickness at the origin. This separation function is applicable if the width of the Hertzian flat region in the contact is negligible compared to the relevant x and y dimensions in the inlet and outlet.

The surfaces are assumed to be moving with velocities u_i and v_i (i = 1,2) relative to the origin in the x and y directins. The rolling velocities in the x and y directions are defined respectively as $V_x = (u_1 \text{ and } u_2)/2$ and $V_y = (v_1 \text{ and } v_2)/2$ and sliding velocities in the respective directions are $u_{sx} = u_1 - u_2$ and $u_{sy} = v_1 - v_2$.

Q is the portion of the normal load that is being supported by hydrodynamic forces in the inlet. For elastic ball race contact Q is considered negligible when compared to the load supported over the Hertzian contact zone.

The forces F_R, F_s and F_n are displayed in Fig. (I 6.4). For clarity the special case of contact between two disks is illustrated. In this case, R_y is infinite and the forces are directed along the x axis. In the general point contact case the forces have both x and y components.

The force F_R acts in the same direction on both contacting bodies and opposite to the direction of motion. F_s acts in opposite directions on the two bodies in such a way as to tend to increase the speed of the slower body and to decrease the speed of the faster body.

The forces F_1 and F_2 are the resultants of the hydrodynamic pressure distribution in the inlet and act through the centers of the two bodies. The component of these forces in the y direction

represents the (small) portion of the total load supported hydrodynamically. The components F_{n1} and F_{n2} acting in the x direction contribute to the force balance in the rolling direction.

The magnitudes of F_R, F_s and F_n depend upon the meniscus location r*. The calculation of r* for the rolling element race and rolling element cage contacts is discussed in Appendix I 5.

Expressions for the x and y components of the forces F_R, F_s and F_n are given below in terms of the dimensionless quantities F_R and F_s.

<u>Pumping Forces</u>
<u>Rolling Component</u>

$$F_{Ry} = \tfrac{1}{2} C_o \bar{F}_R \cos\gamma \qquad \text{(I 6.16)}$$

$$F_{Rx} = \tfrac{1}{2} C_o \bar{F}_R (\sin\gamma)\ (R_y/R_x)^{\frac{1}{2}} \qquad \text{(I 6.17)}$$

<u>Sliding component</u>

$$F_{sy} = \bar{F}_s\ \eta\ u_{sx}\ (R_x R_y)^{\frac{1}{2}} \qquad \text{(I 6.18)}$$

$$F_{sx} = \bar{F}_s\ \eta\ u_{sy}\ (R_x R_y)^{\frac{1}{2}} \qquad \text{(I 6.19)}$$

<u>Normal Forces (on ball)</u>

$$F_{ny} = C_o \bar{F}_R \frac{R_x}{r} \cdot \cos\gamma \qquad \text{(I 6.20)}$$

$$F_{nx} = C_o \bar{F}_R \frac{R_y}{r} \cdot (\sin\gamma)\ (R_y/R_x)^{\frac{1}{2}} \qquad \text{(I 6.21)}$$

(For a ring, r is replaced by the raceway radius) where

$$C_o = \eta\ V_x (R_x R_y)^{\frac{1}{2}} \left[(3+2k)^{-2} + (V_x/V_y)^2\ (3+2k^{-1})^{-2} k^{-1} \right]^{\frac{1}{2}} \qquad \text{(I 6.22)}$$

$$\gamma = \tan^{-1} \left[\frac{3+2k}{k^{\frac{1}{2}}\ (3+2k^{-1})} \cdot \frac{V_x}{V_y} \right] \qquad \text{(I 6.23)}$$

$k \doteq R_y/R_x$

η = absolute ambient viscosity

The quantities $\bar{F}_R$ and $\bar{F}_s$ are dimensionless and depend upon two further dimensionless parameters $\bar{\alpha}$ and ρ_1 . ρ_1 is a dimensionless meniscus distance defined as

$$\rho_1 = \left[r^*/(2h_oR_x)^{\frac{1}{2}}\right]\left[(\cos^2\gamma + (1/k)\sin^2\gamma)^{\frac{1}{2}}\right] \quad \text{(I 6.24)}$$

h_o for ball-race contact is taken as the plateau EHD film thickness.

For ball-cage contact h_o is as calculated in Appendix I 8.

r^* is the distance of the oil meniscus from the contact center along the rolling direction.

$\bar{\alpha}$ is the product of the pressure viscosity coefficient of the lubricant and the maximum fluid pressure q_{max} that prevails if the lubricant is isoviscous.

$\bar{\alpha}$ assumes values between 0 and 1 with $\bar{\alpha} = 0$ indicative of purely hydrodynamic and $\bar{\alpha} = 1$ of purely elasto-hydrodynamic conditions. $\bar{\alpha} = 1$ is taken for ball-race and $\bar{\alpha} = 0$ for ball-cage pocket calculations.

Plots of $\bar{F}_s$ and $\bar{F}_R$ as a function of ρ_1 for various values of $\bar{\alpha}$ are given as Figs. (I 6.5) and (I 6.6) taken from {23}

For the EHD ball race contacts the following expressions have been fit to the $\bar{F}_R$ vs. ρ_1 curve in Fig. (I 6.6) for $\bar{\alpha} = 1$.

$$F_R = 28.59 \text{ in } \rho_1 - 10.1; \quad \rho_1 \leq 5 \qquad \text{(I 6.25)}$$

$$F_R = 36.57 \text{ in } \rho_1 - 22.85; \quad \rho_1 > 5$$

F_s is not considered for a ball-race contact because the amount of sliding is so small.

For the predominantly hydrodynamic contacts, ($\bar{\alpha} = 0$) which arise between the ball and the cage web, both pumping and sliding friction are considered. The following equations were fit to the $\bar{\alpha} = 0$ curves in Fig. (I 6.5) and (I 6.6).

FIGURE I 6.5

Variation of $\bar{F}_s$ with ρ_1

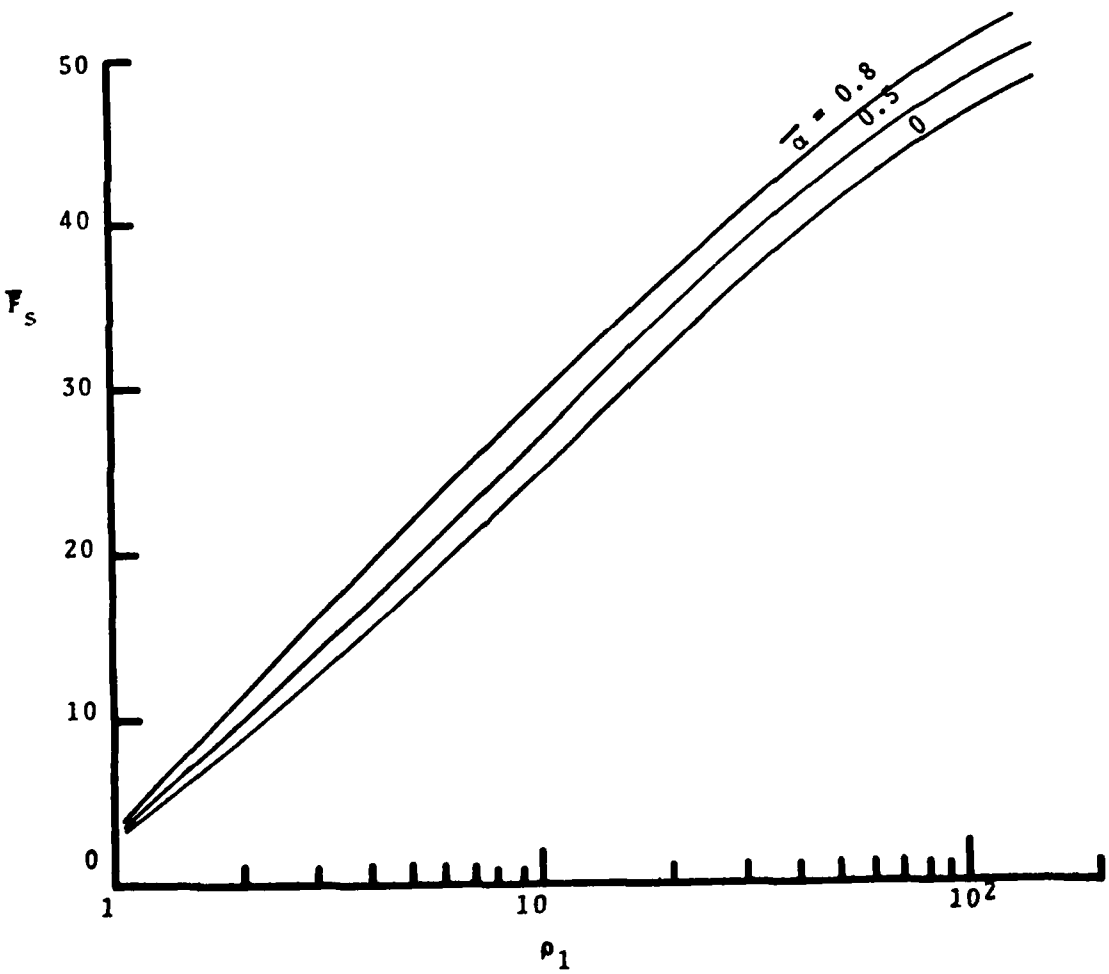

FIGURE I 6.6

Variation of $\bar{F}_R$ With the Dimensionless Meniscus Distance ρ_1

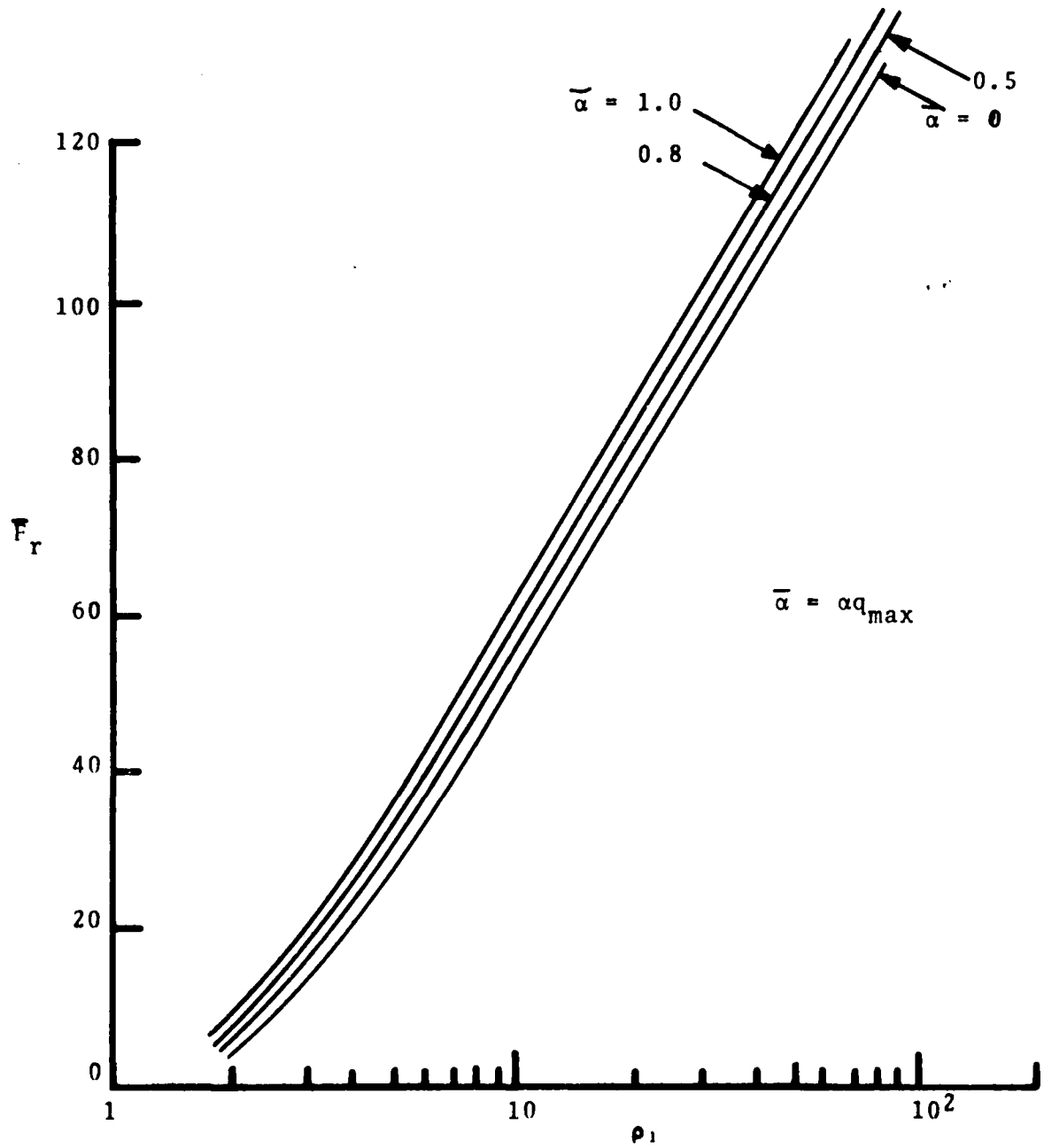

$$\bar{F}_R = 8.53 \times 10^{-14} \left[\ln(1000\ \rho_1)\right]^{15.570};\ \rho_1 < 5.4 \qquad \text{(I 6.26)}$$
$$\bar{F}_R = 36.576 \ln \rho_1 - 29.32;\ \rho_1 \geq 5.4$$

$$\bar{F}_s = 1.71 \times 10^{-9} \left[\ln(1000\ \rho_1)\right]^{11.01};\ \rho_1 < 2$$
$$\bar{F}_s = 10.115\ (\ln \rho_1)^{.965} + 1.5;\ \rho_1 \geq 2 \qquad \text{(I 6.27)}$$

In applying the above results to ball-cage web and ball-race contacts, it is necessary to interpret the geometrical parameters of the general configuration of Fig. (I 6.7) in terms of the appropriate bearing dimensions.

Figure I 6.7 shows the relevant geometry for the two contact types as well as the direction of the various force components.

In this figure r denotes the ball radius, r' the cage pocket radius, r_g the outer ring groove radius, R the radius to the center of the contact ellipse and α the outer ring contact angle.

I 6.4.2 INLET REGION HYDRODYNAMIC FRICTION FORCES LINE CONTACTS

A model has been developed for calculating hydrodynamic pumping and sliding friction forces in the inlet regions of roller bearing race contacts wherein film variable viscosity and starvation effects are included. The contacting bodies are assumed to be rigid. The model was developed by Dr. Y. P. Chiu of S K F Industries.

Consider two rigid cylinders of radius R_{y1} and R_{y2} moving at surface velocity u_1 and u_2 as shown in Figure I 6-4. Floberg in {30} has obtained expressions for the fluid pressure distribution p, normal rolling friction forces F_{n1} and F_{n2} and tangential friction forces F_R as functions of a dimensionless meniscus distance $X_{01} = r^*/(R-h_0)^{1/2}$. Isoviscosity is assumed. h_o is the minimum film thickness and $R = (1/R_{y1} + 1/R_{y2})^{-1}$.

FIGURE I 6-7 Configuration of Contacts
(a) Ball-Cage Contact
(b) Ball-Race Contact (Outer Ring)

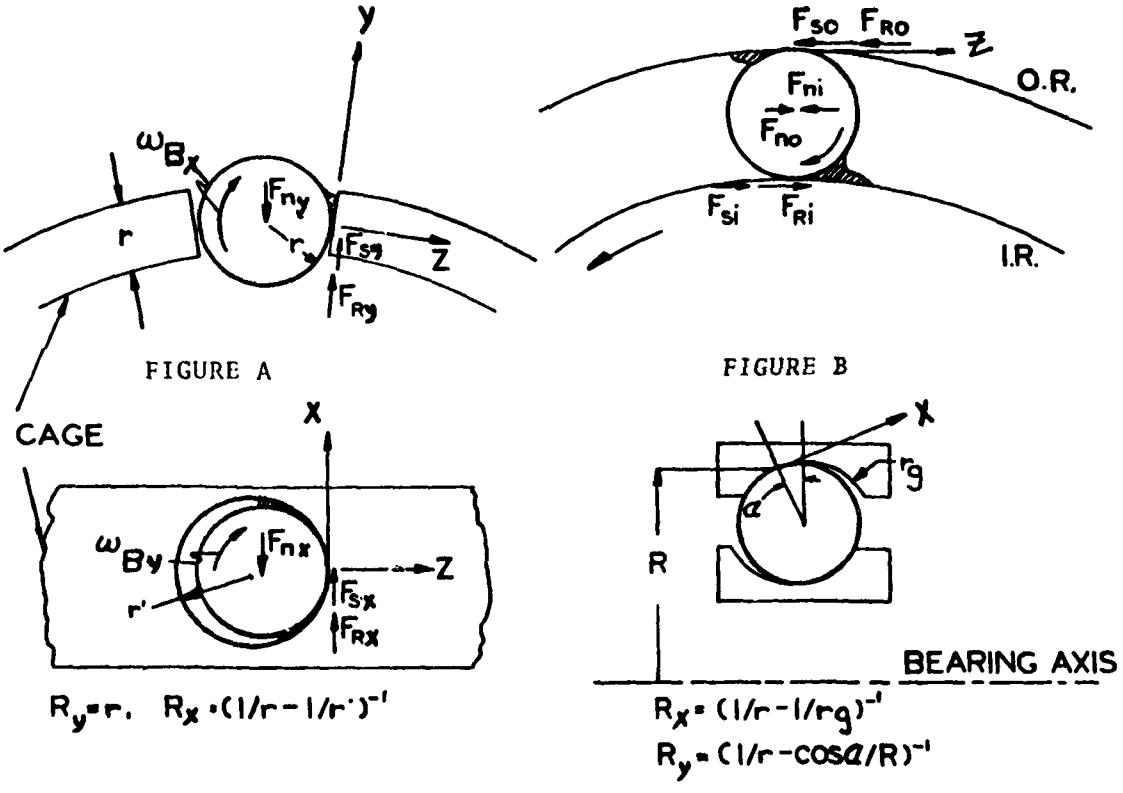

Specifically, the maximum fluid pressure P_{max} is given by

$$P_{max} = P_o^* \, (2\eta \cdot uR^{1/2}) h_o^{-3/2} \qquad \text{(I 6.29)}$$

where P_o^* is a function of X_{01} as shown in Table I 6.2. The normal friction forces acting through the centers of the two cylinders of length ℓ are

$$\begin{pmatrix} F_{n1} \\ F_{n2} \end{pmatrix} = \begin{pmatrix} R_{y2} \\ R_{y1} \end{pmatrix} \ell \, \bar{P}_{xo} \left(2\eta u R^{1/2}\right) \left[h^{1/2}(R_{y1} + R_{y2})\right]^{-1} \qquad \text{(I 6.30)}$$

The pumping forces are

$$F_R = 0.5 \, (F_{n1} + F_{n2}) \qquad \text{(I 6.31)}$$

where $u = (u_2 + u_1)/2$

The dimensionless coefficients $\bar{P}_{xo}$, A, B and C, given in Table I 6.2 below, are functions of X_{01} and were calculated by Floberg

Table I 6.2

Dimensionless Coefficients for the Calculation of Line Contact Inlet Friction

X_{01}	$\bar{P}_{xo}$	A	C	B
$-\infty$	4.6	3.5	4.485	3.41
-2.245	0.81	2.72	0.877	2.94
-1.380	0.25	2.27	0.322	2.92
-0.954	0.11	2.02	0.176	3.22

For the case that the fluid viscosity increases exponentially with pressure, i.e. $\eta = \eta_o e^{\alpha P}$ it is desireable to use the Archard-Snidle approximation {31} that the minimum film thickness h_o in an EHD contact is determiend from Eq. (I 6-25) by setting P_{max} equal to the reciprocal of the pressure viscosity coefficient (α^{-1}). Using $P_{max}\alpha = 1$, one then has,

$$P_o^* = h^{3/2} / (2\eta u \alpha R^{1/2}) \qquad \text{(I 6.32)}$$

and

$$\begin{pmatrix} F_{n1} \\ F_{n2} \end{pmatrix} = \begin{pmatrix} r_2 \\ r_1 \end{pmatrix} C \left(\frac{2\eta u \alpha}{R}\right)^{2/3} R/\alpha \, (r_1 + r_2) \qquad \text{(I 6.33)}$$

$$F_R = \left(\frac{2\eta u \alpha}{R}\right)^{2/3} \ell \, R/2\alpha \left[C \pm \frac{2(1-k)}{1+k} B\right] \qquad \text{(I 6.34)}$$

$$k = u_1/u_2$$

where

$$C = (P_{1xo} + P_{2xo}) / (P_o^*)^{1/3} \qquad \text{(I 6.35)}$$

The values of C and B, as functions of X_{01}, are tabulated in the last two columns of the above table.

For the case where one has pure rolling suach that k = 1.0, Eq. (I 6.30) yields,

$$F_e = c\left(\frac{2\eta u \alpha}{R}\right)^{2/3} R\ell/(2\alpha) \qquad \text{(I 6.36)}$$

The forces F_n exerted on the roller race contacts are,

$$\begin{pmatrix} F_n(\text{outer ring}) \\ F_n(\text{inner ring}) \end{pmatrix} = \begin{pmatrix} R_o \\ R_i \end{pmatrix} C\left(\frac{2\eta u \alpha}{R}\right)^{2/3}\left(\frac{R}{\alpha R_m}\right) \qquad \text{(I 6.37)}$$

where $R_m = R_o - r = R_i + r$ = roller pitch radius.

Chiu {15} has determined in his analysis that contact load has a negligible effect on the above pumping forces, and has obtained good agreement with experiment for his rigid body assumption.

Sliding friction has been determined to be {23},

$$\begin{pmatrix} F_s(\text{outer ring}) \\ F_s(\text{inner ring}) \end{pmatrix} = B \cdot \frac{V\begin{pmatrix}\text{outer}\\ \text{inner}\end{pmatrix}}{\left|u\begin{pmatrix}\text{outer}\\ \text{inner}\end{pmatrix}\right|} \cdot \frac{R}{2\alpha}\left[\frac{2\eta u\begin{pmatrix}\text{outer}\\ \text{inner}\end{pmatrix}\alpha}{R_x}\right]^{2/3} \qquad \text{(I 6.38)}$$

where u = entrainment velocity = $(u_2 + u_1)/2$ and V = sliding velocity = $u_2 - u_1$

I 6.4.3 HEAT GENERATION RATES

In the ball-race and ball-cage inlet regions, the heat generated due to the sliding force F_s and sliding force F_R is calculated as,

$$q_I = 2F_R V + F_s u \qquad \text{(I 6.28)}$$

where V = fluid entrainment velocity at the contact center

u = sliding velocity at the contact center

I 6.5 BALL DRAG FORCE IN BULK LUBRICANT

In {3} the following form of "churning friction force" is cited, to account for all friction losses on the ball other than EHD sliding traction in the ball/race contacts:

$$F_w = \frac{\rho A_v C_v (d_m \omega_o)^2}{8 g} \qquad \text{(I 6.39}$$

where F_w is the drag force

A_v: the ball frontal area

C_v: a drag coefficient given in {35} as a function of the Reynolds number

d_m: the bearing pitch diameter

ω_o: the ball orbital angular velocity

g: the gravitational constant

ρ : the density of the air-oil mixture in the bearing cavity

$$\rho = XCAV \cdot \rho_o \qquad \text{(I 6.40)}$$

XCAV: the fractional amount of lubricant assumed to be in the bearing cavity

ρ_o: the density of the oil

In the present model, three hydrodynamic force components at each point contact on a ball have been defined.

These components tend to retard ball motion as would F_w. Since two race contacts and a cage contact exist for each ball, 15 force components have been made explicit. After accounting for all contact friction forces, there is left a residual loss due to "windage" or "drag" acting on a ball as it moves through the air-oil mixture in the bearing cavity. Eq. (I 6.37) has been used to model this windage force. Although the effect of the drag force is less significant than calculated in {3} , it remains important.

XCAV values of one percent or less are recommended. In actuality, XCAV is a function of lubricant supply rate, method of supply, speed and bearing and bearing cavity geometry.

APPENDIX I 7

ROLLING ELEMENT INERTIA FORCES AND MOMENTS

APPENDIX I 7

ROLLING ELEMENT INERTIA FORCES AND MOMENTS

A rolling element, Fig 2-4, traveling between azimuth locations, is forced to undergo changes in its rotational velocity components ω_x, ω_y, and ω_z, as well as in its orbital velocity ω_o. The forces which must act on an element to produce time variations in its rotational and orbital velocities may be deduced from Newton's Laws of Motion as follows:

$$\vec{F} = \begin{Bmatrix} F_x \\ F_y \\ F_z \end{Bmatrix} = m \begin{bmatrix} 0 & \ddot{x} & 0 \\ \ddot{y} - \omega_o^2 (R+y) \\ 2\,\omega_o \dot{y} + \dot{\omega}_o (R+y) \end{bmatrix} \qquad \text{(I 7.1)}$$

where F_x, F_y and F_z are the components of the forces in the rotating coordinate system attached to the element, m is the ball mass, x and y are the element center displacements shown in Fig. 2-4, and R is the radius of outer ring groove centers.

A rough estimation assuming stable operation yields that the term x is smaller than $\omega_o^2 \cdot (R+y)$ by a factor of the order of x_m/R, where x_m is the maximum variation of x. Similarly, the terms y and $2\,\dot{\omega}_o y$ are smaller than $\omega_o^2 R$ by a factor in the order of y_m/R where y_m is the maximum variation of y. Note that both x_m/R and y_m/R are very small in magnitude. The second derivatives with respect to time of x and y are thus neglected as is the Coriolis term $2\,\omega_o \dot{y}$. The term $\dot{\omega}_o$ is expressible as follows:

$$\dot{\omega}_o = \frac{d\omega_o}{dT} \cdot \frac{d\omega_o}{d\phi} \quad \frac{d\phi}{dT} = \omega_o \quad \frac{d\omega_o}{d\phi} \tag{I 7.2}$$

The term $\frac{d\omega_o}{d\phi}$ is approximated for ball i as follows:

$$\left[\frac{d\omega_o}{d\phi}\right]_i = \frac{(\omega_o)\ i+1 - (\omega_o)i-1}{2\Delta\phi} \tag{I 7.3}$$

where $\Delta\phi$ is the angular distance between rolling elements.

The moments necessary to cause the element velocity to change are as follows:

$$\vec{M} = \begin{Bmatrix} M_x \\ M_y \\ M_z \end{Bmatrix} = [J] \begin{bmatrix} 0 & \dot{\omega}_x & 0 \\ \dot{\omega}_y - \omega_o & & \omega_z \\ \dot{\omega}_z + \omega_o & & \omega_y \end{bmatrix} \tag{I 7.4}$$

$$[J] = \begin{bmatrix} J_x & 0 & 0 \\ 0 & J_y & 0 \\ 0 & 0 & J_z \end{bmatrix} \tag{I 7.5}$$

For a ball:

$$J_x = J_y = J_z = mD^2/10 \tag{I 7.6}$$

for a roller:

$$J_x = mD^2/8$$

$$J_y = J_z = m/12\ (3/4\ D^2 + \ell re^2) \qquad \text{(I 7.7)}$$

m is the element mass

D is the element diameter

ℓre is the element length

The time variation of the rotational velocity components ω_x, ω_y and ω_z are approximated in the same manner as ω_o, e.g.,

$$\dot{\omega}_x \approx \left[\frac{(\omega_x)_{i+1} - (\omega_x)_{i=1}}{2\Delta\phi} \right] \omega_o \qquad \text{(I 7.8)}$$

Using D'Alembert's principle, forces $-\vec{F}$ and moments $-\vec{M}$ calculated as described above are imposed on the element along with the other forces and moments due to friction and elastic contact. The combined system of forces is then regarded as being in static equilibrium.

Because the time rates of change of ω_o, ω_x, ω_y, and ω_z are included by approximation as described above, the analytical treatment is considered to be quasi-dynamic as distinct from analyses wherein these terms are neglected and only the centrigufal force $m\omega_o^2(R+y)$ and gyratory moments $J\omega_o \cdot \omega_Z$ and $-J\omega_o\omega_y$ are considered. The description "quasi-static" has been applied to slutions of this type.

APPENDIX I 8

ROLLING ELEMENT BEARING CAGE MODEL

APPENDIX I 8

ROLLING ELEMENT BEARING CAGE MODEL*

I 8.1 INTRODUCTION

The cage is driven by normal and friction forces which act at the interfaces between balls or rollers and cage pockets, and at the cage rail(s) and ring land(s). These forces are calculated as functions of the separation and speeds of the interfacing members. In this analysis it is assumed that:

- normal forces exerted by the rolling element on the cage pocket act in the plane of cage rotation which is coincident with the cage axial midplane.
- friction forces exerted by the rolling element on the cage pocket act orthogonal to a corresponding normal force and at the normal force point of application.
- the only friction force components considered in the cage equilibrium equations are those which lie in the plane of cage rotation. It is assumed that each rolling element is axially centered within its pocket.
- cage rail normal forces act at the cage midplane and pass through the axis of the cage. These forces are coplanar with the rolling element normal forces.
- cage-land friction forces act in the cage midplane such that any resulting torque tends to drive or retard the cage rotation.

*This Appendix is based upon the original work {15}

The analysis is used to determine the normal and traction forces at each rolling element and ring land on the basis of hydrodynamic, elastohydrodynamic and Hertzian concentrated contact theory.

I 8.2 GEOMETRY

Figure 2.4 shows a coordinate system (XYZ) with the origin on the outer ring axis in the plane of the outer raceway centers. A local coordinate system (x,y,z) is established at the center of each rolling element. The azimuth angle ϕ defined in the (X,Y,Z) coordinate frame locates the x axis penetration through the Y-Z plane. The x axis is parallel to X. The y direction is radially outward and the z direction is tangent to the direction of rolling.

A local coordinate z_c is also defined for each cage pocket, wherein the origin is located on the cage pitch circle. We wish to determine the position of each rolling element center with respect to the cage pocket center along z_c, in terms of the rolling element orbital speeds ω_o, the cage rotational speed ω_c and the cage rotational and translational displacement components.

I 8.3 CAGE MOTIONS

The equilibrium solution considers that the cage operates in one of three modes:

(1) The cage is <u>outer ring land riding</u> such that radial and small circumferential motions of the cage with respect to the rolling elements are resisted by hydronamic fluid film forces that develop between the cage rail land outside diametral surface and the bearing outer ring outside diametral surface. Three degrees of freedom

apply to the cage motion. These are the circumferential position of the cage relative to the rolling elements (ξ) and two components of radial displacement (ΔY and ΔZ in rectangular coordinates, or e and θ'_c in polar coordinates.) When the bearing is subjected to axial load only, or when the rolling element speed variation is inconsequential, the radial degrees of freedom are neglected.

(2) The cage is <u>inner ring land riding</u> when motions are resisted by hydrodynamic forces which develop at the cage inside surface and the bearing inner ring outside surface. Three or one degrees of freedom also apply.

(3) The cage is <u>ball or roller riding</u> in which case there are no net radial fluid film forces between the bearing rings and the cage, and consequently, no radial motion of the cage relative to the bearing axis of rotation. Angular motion of the cage relative to the rolling elements is the only applicable degree of freedom.

The circumferential displacement of rolling element No. 1 at azimuth location $\phi = \phi_1$, relative to its cage pocket center is designated ($-\xi$).

I 8.4 ROLLING ELEMENT MOTIONS

Returning to Fig. 2-4, the velocity with which the moving coordinate system rotates about the X axis is designated ω_o and is also assumed to be a function of azimuth angle, i.e. $\omega_o = \omega_o(\phi)$.

The rolling element is assumed to rotate relative to each of the axes in the moving system of coordinates. The angular velocities about each of the axes x, y, z are denoted ω_x, ω_y, and ω_z respectively and are shown as the orthogonal components of the rotational velocity vector ω in Fig. 2-4

The value of the ball center-cage pocket center offset z_c applicable at other ball positions is deduced relative to ball position No. 1, which remains fixed at its aximuth position. The cage is assigned a rotation ξ, so that the offset of cage pocket no. 1 relative to ball no. 1 is

$$\xi = \frac{d_m}{2} \Delta\theta_x \qquad \text{(I 8.1)}$$

In so doing, it is assumed that a rolling element orbital velocity remains constant as it traverses the distance corresponding to one half of the pitch spacing on either side of the nominal azimuth position. As a rolling element enters the azimuth location of the next adjacent rolling element the orbital speed undergoes a step change. This is illustrated in Fig. I 8.1 for ball Nos. 1 and 2. The top half of Fig. I 8.1 is a plot of the assumed variation of orbital velocity with respect to ball position.

The cage orbital velocity is denoted by ω_c and is assumed uniform and equal to the average of the ball orbital velocities, i.e.

$$\omega_c = \frac{1}{n} \sum_{i=1}^{n} (\omega_o)_i \qquad \text{(I 8.2)}$$

where n is the number of rolling elements.

Figure I 8-1

Cage and Rolling Element Speeds and Displacements

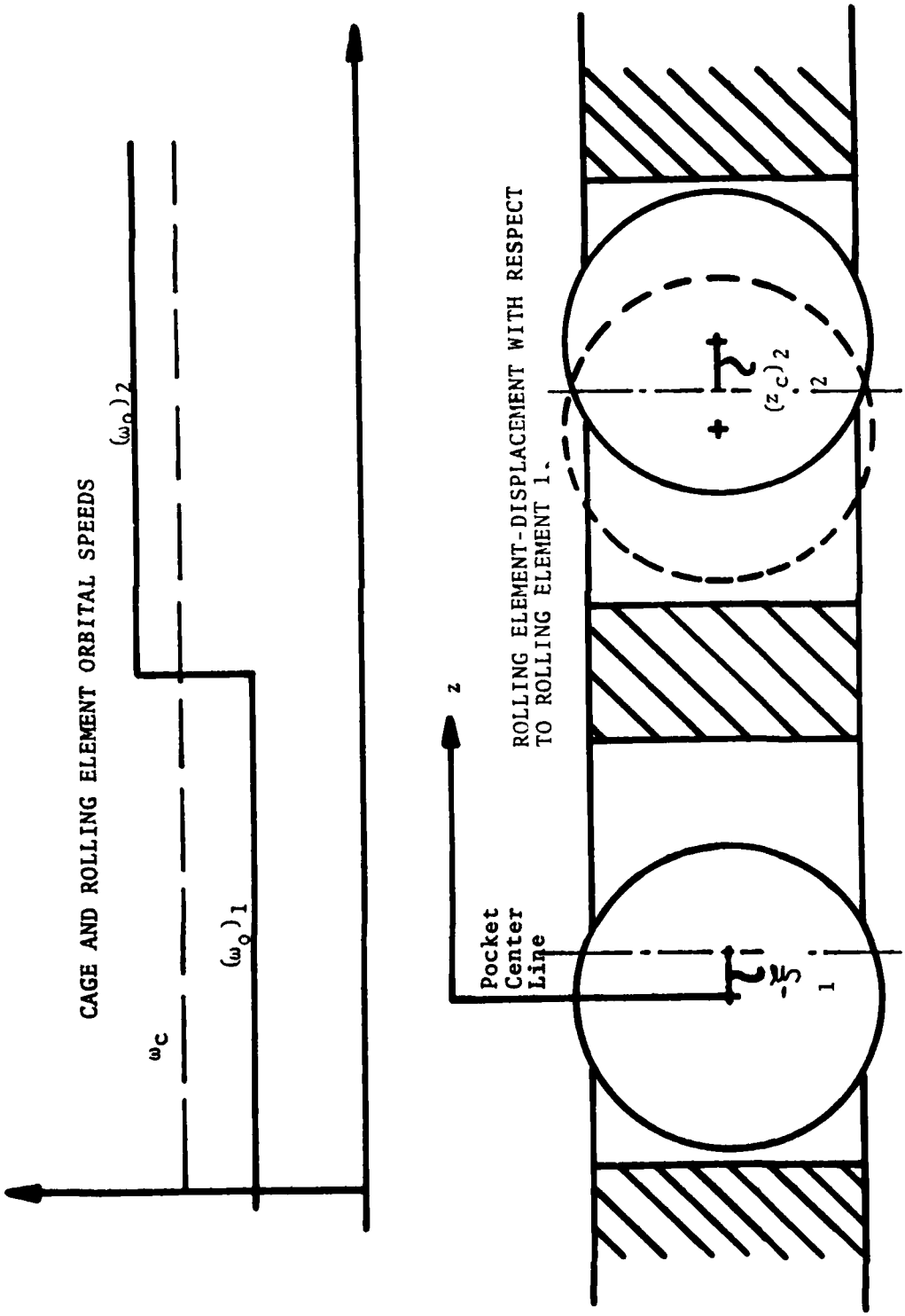

The distance between ball positions is the quotient of the circumference πd_m of the locus of rolling element centers (neglecting small excursions) and the number of rolling elements. The time ΔT for the cage to traverse this distance is then

$$\Delta T = \frac{\pi d_m}{n} \Big/ \left(\frac{d_m}{2} \cdot \omega_c \right) = \frac{2\pi}{n\omega_c} \qquad \text{(I 8.3)}$$

In this time period the center of rolling element No. 1 moves a circumferential distance of

$$\frac{d_m}{2}(\omega_o)_1 \cdot \frac{\Delta T}{2} + \frac{d_m}{2} \cdot (\omega_o)_2 \cdot \frac{\Delta T}{2} = \frac{d_m \Delta T}{4}\left[(\omega_o)_1 + (\omega_o)_2\right] \qquad \text{(I 8.4)}$$

The circumferential distance between the rolling element and cage pocket center at position No. 2 is obtained as the difference between the rolling element travel and cage travel in time ΔT, less the initial offset of the cage pocket center at rolling element position 1 with respect to the center of rolling element 1, (ξ), see Fig. I 8.1, plus the components of the radial eccentricity (ΔZ and ΔY) of the cage axis with respect to the bearing axis. Then

$$(Z_c)_2 = \frac{d_m \Delta T}{4}\left[(\omega_o)_1 + (\omega_o)_2 - \frac{\pi d_m}{n} - (\xi) - \Delta Y \sin\phi_2 + \Delta Z \cdot \cos\phi_2 \right. \qquad \text{(I 8.5)}$$

Letting $\Delta T = 2\pi / n\omega_c$ then Eq. (I 8.5) becomes for the general i-rolling element ;

FIGURE I 8-2

Cage Pocket Geometry

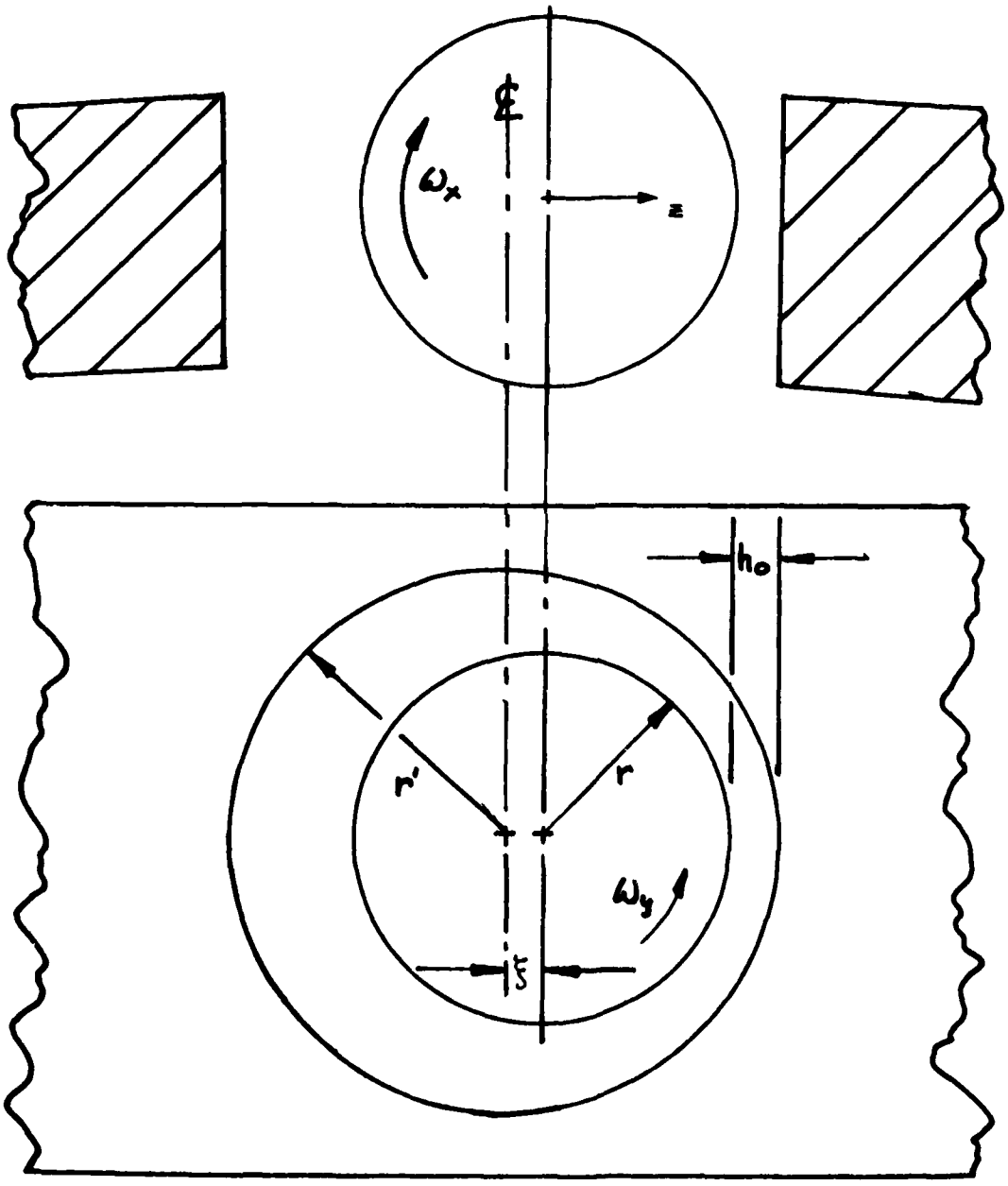

$$(z_c)_i = \frac{\pi d_m}{n} \sum_{j=2}^{i} \left[\frac{(\omega_o)_{j+1} + (\omega_o)_j}{2\omega_c} - 1 \right] - \left[\xi + \Delta Y \sin\phi_i - \Delta Z \cos\phi_i \right]$$

(I 8.6)

I 8.5 CALCULATION OF CAGE POCKET NORMAL FORCES

A means for calculating the cage driving forces due to the balls was developed in {23}. The analysis has been extended to include roller-cage pocket, line contacts, by approximating the line contact to be an elliptical contact that has a large curvature ratio (e.g.: $a^*/b^* = 18$).

The analysis is applied to determine the normal forces acting at two diametrically opposite points on a rolling element, i.e., the points of nearest and furthest approach of the ball or roller relative to the cage. The net normal force acting on the rolling element is the resultant of these two forces. The discussion below considers ball-cage, but it applies to roller contact.

The typical ball geometry is shown in Fig. I 8.2. z_c denotes the offset between the ball and cage pocket centers in the direction of rolling. ω_x and ω_y denote the components of the ball rotational velocity vector that result in relative surface speeds of the ball and cage pocket.

The closest approach h_o is the minimum film thickness when the cage is lubricated.

Given the ball cage pocket eccentricity the associated cage pocket load P can be calculated. When z_c is small the load is small and borne hydrodynamically by the lubricant film, which then has minimum thickness $h_o = r' - r - z_c$. In this regime, the load for a given value of the ball and the cage pocket clearance is that supported by a hydrodynamic contact of minimum thickness h_o. Elastic deformation is negligible in this regime. As z_c increases, h_o decreases until it reaches a critical value h_c, below which a further increase in z_c results in elastic deformation but no further decrease in film thickness. In this regime

$$h = h_c \qquad \text{(I 8.7)}$$

and the elastic deformation is calculated from,

$$\delta_e = z_c + h_c - C_r \qquad \text{(I 8.8)}$$

where C_r is the cage pocket radial clearance $(r' - r)$.

The load P in this case is assumed to be the sum of the load P_c hydrodynamically related to the film thickness h_c, and an additional load P_e associated with the elastic deformation through the Hertzian and flexural equations of contact elasticity.

An analysis was performed as described in {23} of the relationship between normal load P and minimum film thickness h_o in a lubricated point contact between two rigid bodies, each having two

principal radii of curvature, assuming that the lubricant viscosity increases exponentially with pressure. The analysis yielded a relationship between the nondimensional load parameter $\bar{Q}$ and the nondimensional film thickness parameter $\bar{H}$, as shown by the solid curve in Figure I 8.3. These nondimensional variables are defined as:

$$\bar{Q} = P \cdot (\alpha R_y/C_o^2)^{1/3} (R_x R_y)^{-1/2} = P \cdot D \qquad \text{(I 8.9)}$$

$$\bar{H} = h_o R_x (C_o R_x \alpha)^{-2/3} = \frac{h_o}{C_r} B \qquad \text{(I 8.10)}$$

where:

$$C_o = \eta_o V_y (R_x R_y)^{1/2} k_1 \qquad \text{(I 8.11)}$$

$$k_1 = \left[(3+2k)^{-2} + (3+2k^{-1})^{-2} k^{-1} \left(\frac{V_x}{V_y}\right)^2 \right]^{1/2} \qquad \text{(I 8.12)}$$

$$k \equiv R_y/R_x \qquad \text{(I 8.13)}$$

$$D \equiv (\alpha R_y/C_o^2)^{1/3} (R_x R_y)^{-1/2} \qquad \text{(I 8.14)}$$

$$B \equiv C_r R_x (C_o R_x \alpha)^{-2/3} \qquad \text{(I 8.15)}$$

$$R_x = \left(\frac{1}{r} - \frac{1}{r'}\right)^{-1} \frac{r^2}{C_r} \qquad \text{(I 8.16)}$$

$$R_y = r$$

$C_r = r' - r$, cage pocket radial clearance

FIGURE I 8-3

Load Capacity Vs. Film Thickness for Hydrodynamic and Elastohydrodynamic Operating Regimes

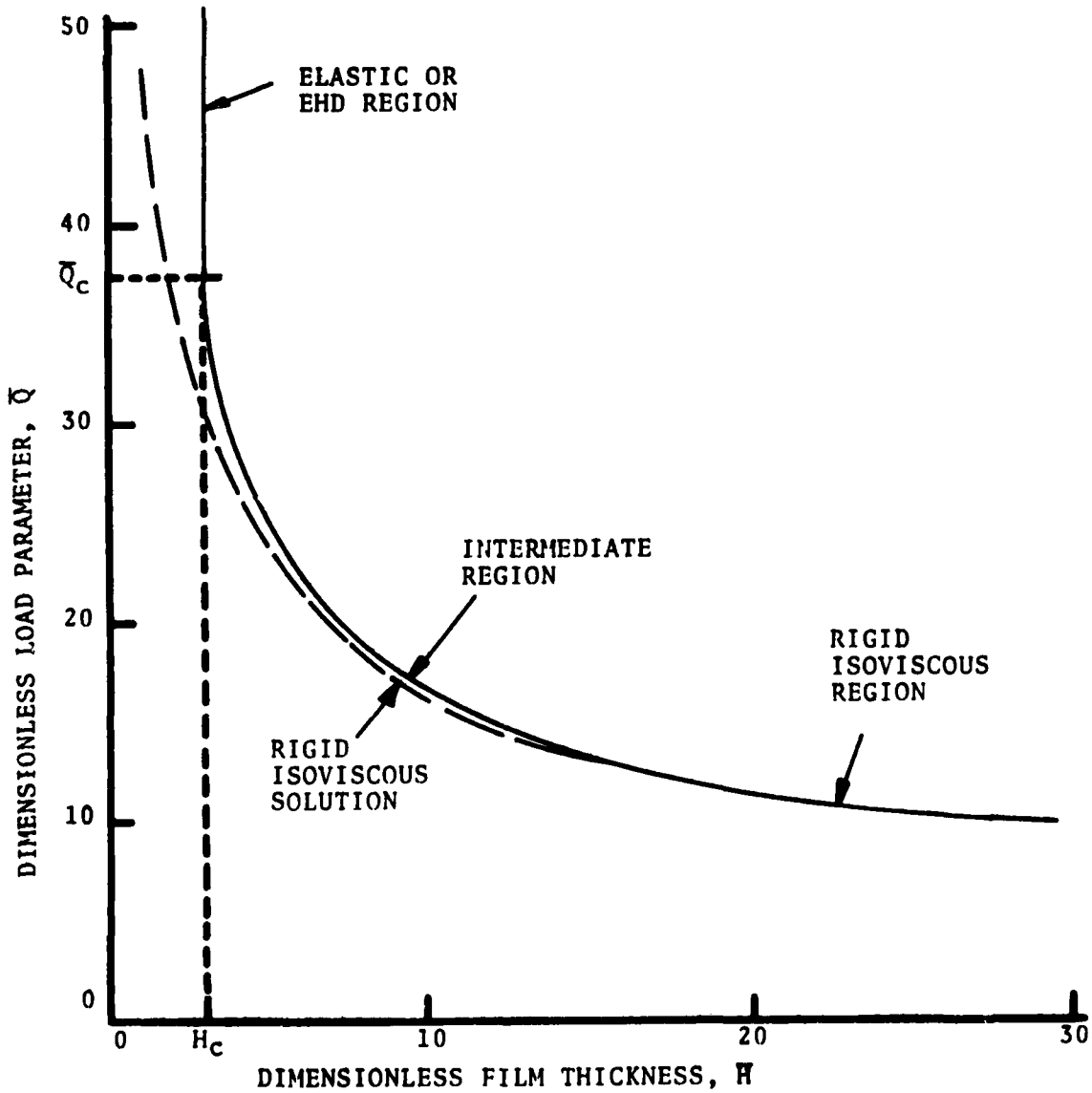

$V_x = 1/2\,\omega_y \cdot r$

η_o = bulk viscosity

$V_y = -1/2\,\omega_x \cdot r$

It has been found that the relationship between $\bar{Q}$ and $\bar{H}$ for an unstarved point contact can be approximated by the following formula:

$$\bar{Q} = 53.3\ (\bar{H})^{-1/2} + 163\ (\bar{H})^{-3} \qquad (\text{I } 8.17)$$

provided that:

$\bar{Q} < \bar{Q}_c = 37.6$

I 8.5.1 ELASTOHYDRODYNAMIC (EHD) CONTACT

For $\bar{Q} \geq 37.6$, the film thickness is independent of load and the nondimensional parameter $\bar{H}$ remains constant at $\bar{H}_c$. Operation in this case is in the EHD region.

$$\bar{H} = \bar{H}_c = 3.122 \qquad (\text{I } 8.18)$$

for EHD Contact

$$\bar{Q} \geq \bar{Q}_c = 37.6 \qquad (\text{I } 8.19)$$

Equations (I 8.18) and (I 8.19) result in the following for the EHD region of operation,

$$P_c = \bar{Q}_c/D = 37.6/D \qquad (\text{I } 8.20)$$

$$h_o = h_c = 3.122\ C_r/B \qquad (\text{I } 8.21)$$

The elastic deformation δ_e is given by,

$$\delta_e = z_c + h_c - C_r \qquad \text{(I 8.22)}$$

P_e (δe) was originally calculated according to Hertz Theory. This model has been changed, however, in an attempt to reduce the nonlinearity of rolling element-cage load displacement relationships. This was done through the assumption that the cage will respond to large rolling element loads through flexing as well as through the local contact displacements.

It was assumed that 95 percent of δe would be accommodated by cage flexing and the remainder would be accommodated by the Hertz deformation. The Hertz calculations are made based on the assumptions of a 9:1 major to minor contact axis ratios for a ball-cage contact and an 18.2:1 ratio for the roller-cage contact. The cage flexure deflection is calculated from

$$Pe(\text{flex}) = (0.95\,\delta e)\ R \cdot 13500 \qquad \text{(I 8.23)}$$

The spring constant 13500 R where R is the cage rail radius, was derived using circular ring theory, considering the cage material to be steel. The total ball-cage contact load P is thus

$$P = Pc + P_{HZ}\ (0.05\,\delta e) + P_{(flex)}\ (0.95\,\delta e) \qquad \text{(I 8.24)}$$

I 8.5.2 <u>HYDRODYNAMIC (HD) CONTACT</u>

If the contact film thickness h_o is greater than the critical value h_c, the contact is assumed to be hydrodynamic:

$$\bar{H} \geq H_c = 3.122 \text{ for HD contact}$$

The minimum film thickness for this case is given in terms of the ball-cage clearance and eccentricity z_c as:

$$h_o = C_r - z_c \qquad \text{(I 8.25)}$$

The calculation procedure is,

(a) Calculate h_o as above

(b) Evaluate $H = h_o R_x (C_o R_x)^{-2/3}$

(c) For H from (b) find $\bar{Q} = 53.3 (\bar{H})^{-1/2} + 163 (H)^{-3}$

(d) Calculate cage-ball load P as $\bar{Q}/D$

The procedure for determining the ball-cage normal load is performed for the points of nearest and further approach (h_o min and h_o max). The net normal load acting on the ball is given by:

$$\sum P = P\ (h_o \text{ minimum}) - P\ (h_o \text{ maximum}) \qquad \text{(I 8.26)}$$

I 8.5.3 DRY CONTACT

Normal cage-pocket rolling element contact forces for conditions of dry contact are calculated for the h_o (minimum) contact only. A continuous force displacement function is assumed for this calculation. A soft spring and low force values occur for $\bar{e} < 0.99$, where $\bar{e} = 2 z_c/(r'-r)$; such that,

$$P = 10 \cdot r \cdot e \quad \text{for } e \leq 0.99 \qquad \text{(I 8.27)}$$

A hard spring function is assumed for $\bar{e} > 0.99$, such that

$$\bar{e}_1 = 0.99 + 0.01\ (\bar{e} - 0.99)/\bar{e}$$

$$\bar{e}_p = \bar{e}_1 + 1.01$$

$$P = 0.0506 r \left\{ \bar{e}_1 / [1 - \bar{e}^{(1/\bar{e}_p)}] \right\} (\bar{e}_p/2)^3 \cdot \bar{e}_1 \qquad \text{(I 8.28)}$$

I 8.6 CAGE POCKET/ROLLING ELEMENT FRICTION FORCES

Friction forces which arise in the rolling element/cage pocket contacts are calculated according to Appendix I 6 for wet friction. Dry friction forces are calculated with a Coulomb model.

I 8.7 CALCULATION OF CAGE LAND NORMAL FORCES AND FRICTION MOMENT

The lubricant forces which develop between a cage rail and its supporting ring surface are obtained using the hydrodynamic solution for self-acting short-journal bearings. According to [32] the resultant of the pressure distribution on the cage has orthogonal force components, one of which lies along the cage lin of centers (the line which passes through the cage center and its point of closest approach to the ring). Both components pass through the cage center.

Figure 2.5 depicts the geometric and operating parameters for the inner land riding situation, and Figure 2.6 the outer land riding situation. u_i, u_o, u_c are the surface speeds of the inner ring, outer ring, and cage land, respectively. The cage undergoes a displacement in the bearing XYZ frame of a magnitude e and direction θ'_c. An xyz frame is attached to the cage, such that the y axis passes through the point of minimum film thickness. The y axis is rotated θ_c from the ring Y axis. The short bearing solution for an isoviscous, Newtonian fluid gives the magnitude of the normal first terms in Eq. (I 8.29) through Eq. (I 8.31). The second terms account for cage elastic flexure.

$$W_y = \frac{\eta_o U L^3}{C^2} \cdot \frac{\epsilon^2}{(1-\epsilon^2)^2} + 13500\, R\, \delta_{el} = \pm F_y \qquad \text{(I 8.29)}$$

$$W_z = \frac{\eta_o U L^3}{C^2} \cdot \frac{\epsilon}{4(1-\epsilon^2)^{3/2}} - 475\, R\, \delta_{el} \frac{V}{|V|} = \mp F_z \qquad \text{(I 8.30)}$$

and of the friction torque as,

$$M_c = \eta_o \frac{V R^2 L}{C} \cdot \frac{2\pi}{(1-\epsilon^2)^{1/2}} + 475\, R^2 \delta_{el} \frac{V}{|V|} \qquad \text{(I 8.31)}$$

where $\delta_{el} = \epsilon - 0.999\, C$

C = radial clearance, (in.)

η_o = viscosity, (lb-sec/in.^{2})

L = cage ring width, (in.)

R = cage ring radius, (in.)

U = entrainment velocity,)(in/sec)

V = $(u_i + u_c)$ for inner land riding cage

V = $(u_o + u_c)$ for outer land riding cage

V = $(u_{i,o} - u_c)$ sliding velocity

ϵ = eccentricty ratio, e/C

W_y = cage land normal force component along line of centers, (lb)

W_z = cage land normal force component normal to line centers,(lb)

M_c = cage land friction torque, (in-lb)

In using Eqs.(I 8.29) and (I 8.30),the upper sign applies to an inner ring riding cage and the lower to an outer.

Subroutine CGWET makes the calculations.

For dry contact a load displacement relationship is assumed which has the following form.

$$W_y = XK \cdot \epsilon = \pm F_y \qquad \text{(I 8.32)}$$

$$XK = L^3/C^2 \text{ for } \epsilon \leq 0.9 \qquad \text{(I 8.33)}$$

$$XK = 0.2111 \cdot L^3/C^2 \, \epsilon / (1-\epsilon^2) \qquad \epsilon > 0.9$$

$$WZ = \bar{f} \, W_y \cdot \frac{U}{|U|} = +F_Z \qquad \text{(I 8.34)}$$

$$M_C = WZ \cdot R \qquad \text{(I 8.35)}$$

Subroutine CGDRY makes the calculations.

In order to insert the values for W_y, W_z and M_c into the cage equilibrium equations, the following transformations are made for inner and outer rings:

$$\begin{Bmatrix} M_{cX} \\ F_{cY} \\ F_{cZ} \end{Bmatrix} = \begin{bmatrix} 1 & 0 & 0 \\ 0 & \cos\theta_c & -\sin\theta_c \\ 0 & \sin\theta_c & \cos\theta_c \end{bmatrix} \begin{Bmatrix} M_c \\ F_y \\ F_z \end{Bmatrix} \qquad \text{(I 8.36)}$$

where $\tan\theta_c = (-\Delta Z/-\Delta Y)$ for an inner ring riding cage and $\tan\theta_c = \Delta Z/\Delta Y$ for an outer ring riding cage.

I 8.7 FRICTION HEAT GENERATION RATES

The heat generated by fluid shearing between the cage and land is calculated as the product of the cage friction moment and rotational speed, i.e.,

$$q_c = M_c \cdot |\omega - \omega_c| \qquad \text{(I 8.37)}$$

where M_c is calculated according to Equation I8.31 and $|\omega - \omega_c|$ is the absolute value of the difference between the cage speed and the speed of the ring that guides the cage.

APPENDIX I 9

'ING FATIGUE LIFE CALCULATIONS

APPENDIX I 9

BEARING FATIGUE LIFE CALCULATIONS

I 9.1 INTRODUCTION

Within SHABERTH, ball and roller bearing raceway fatigue life is calculated with the methods of Lundberg Palmgren {33} and {34}. The life thus calculated is modified by multiplicative factors which account for material and lubrication effects.

I 9.2 BALL BEARING RACEWAY LIFE

Bearing raceway L_{10} fatigue life in millions of revolutions as determined by Lundberg-Palmgren, {33} is expressed by

$$L_{10m} = \left(\frac{Q_{cm}}{Q_{em}}\right)^3 \qquad \text{(I 9.1)}$$

Q_{cm} is the raceway dynamic capacity, the load for which the bearing raceway will have 90 percent assurance of surviving 1 million revolutions. From ref. {33}.

$$Q_{cm} \quad 7140 \left\{\left(\frac{2\ fm}{2\ fm-1}\right)\frac{0.41\ (1+\gamma_m)^{1.39}}{\left[Z\ (1+\gamma_m)\right]^{0.33}}\left(\frac{\gamma_m}{\cos\alpha_m}\right)^{0.3}\right\}^{1.8} \qquad \text{(I 9.2)}$$

where:

- f = groove curvature, raceway radius/ball diameter (r_m/D)
- γ = $D \cos\alpha_m/d_m$
- D = Ball diameter
- α = Raceway contact angle
- d_m = Bearing pitch diameter
- Z = Number of rolling elements
- m = is a subscript, it is 1 for the outer raceway and 2 for the inner raceway.

The upper sign is used for the outer race, the lower for the inner race.

Q_{em} is the raceway equivalent load,

$$Q_{em} = \left\{ \frac{1}{Z} \left(\sum_{j=1}^{Z} Q_{mj}^{\epsilon} \right) \right\}^{1/\epsilon} \qquad m = 1, 2 \qquad \text{(I 9.3)}$$

where Q_{mj} is the individual ball contact load, and $\epsilon = 3$ or $\epsilon = 3.3$ depending respectively upon whether the applied load rotates or is stationary with respect to the raceway in question.

I 9.3 ROLLER BEARING RACEWAY LIFE

To account for non symmetrical load distributions across a line contact, the roller and raceways are thought of as being comprised of a number of sliced discs. Raceway L_{10} fatigue life, *in millions of revolutions at a given slice as determined by* Lundberg-Palmgren, {34} is expressed by

$$L_{10mk} = \left(\frac{Q_{cmk}}{Q_{emk}} \right)^2 \qquad \text{(I 9.4)}$$

Q_{cmk} *is the dynamic capacity of a raceway slice*, defined as the load for which the slice will have a 90 percent assurance of surviving 1 million revolutions. m refers to raceway, k refers to slice, n is the index of the last slice, from {34}

$$Q_{cmk} = \frac{49500\lambda \{D(1 \pm \gamma)\}^{1.074} \Delta l_{re}^{0.778} (\gamma_m)^{0.222}}{\{Z(1 \pm \gamma_n\}^{0.26}} \qquad \text{(I 9.5)}$$

$\lambda = 0.61$ $\quad k = 1$ or $k = n$

$\lambda = 1.0$ $\quad k = 2 \rightarrow n - 1$ $\quad \Delta l_{re}$ = slice width.

The upper sign is used for the outer race, the lower sign refers to the inner race.

Q_{mek} is the equivalent load for the slice.

$$Q_{mek} = \frac{1}{Z} \left(\sum_{j=1}^{Z} Q_{mkj}^{\epsilon} \right)^{1/\epsilon} \qquad \text{(I 9.6)}$$

Q_{mkj} is the individual roller contact load on the k-th slice and $\epsilon = 4.0$ or $\epsilon = 4.5$ depending respectively upon whether the applied load rotates or is stationary with respect to the raceway in question.

The L_{10} life of a raceway is given by

$$L_{10m} = a_2 a_3 a_3^* \left\{ \sum_{k=1}^{n} L_{10mk}^{-e} \right\}^{-1/e} \qquad \text{(I 9.7)}$$

where e is the Weibull slope exponent, here taken to be 9/8 for roller bearings and 10/9 for ball bearings

a_2 is a life improvement factor to account for improved materials.

a_3 is a life improvement factor to account for full film lubrication which

a^*_3 is less than 1 when full film lubrication is not obtained. See I 9.5.

I 9.4 BEARING LIFE

The L_{10} life of the bearing considering both raceways is:

$$L_{10} = \left\{ \sum_{m=1}^{2} (L_{10m})^{-e} \right\}^{-1/e} \qquad \text{(I 9.8)}$$

I 9.5 BEARING LIFE REDUCTION DUE TO ASPERITY INTERACTION

In {23} and {27} the form of a reduction factor accounting for the effect of surface asperity interaction was deduced and its parameters were set to best fit to a large body of rolling contact life test data.

As employed in Program SHABERTH, the reduced tenth percentile life L_{10} is calculated as follows,

$$a_3^* = \left[1 + \frac{\psi^2 (h/\sigma)}{\psi (1.5)} \right]^{-1/\beta} \qquad \text{(I 9.9)}$$

where

$$\psi(h/\sigma) = \frac{\phi^2(h/\sigma)}{1-\Phi(h/\sigma)} \qquad \text{(I 9.10)}$$

$\phi(\cdot)$ = density function of standard normal distribution

$\Phi(\cdot)$ = cumulative distribution function of standard normal distribution

h/σ = ratio of plateau film thickness to surface roughness for most heavily loaded ball

$(L_{10})_\infty$ = the full film life

$$L_{10} = a_3{}^* \, (L_{10})_\infty \qquad \text{(I 9.11)}$$

The term $(L_{10})_\infty$ is calculated using the principles of Lundberg-Palmgren and multiplying by the user supplied product of two factors which represent by Industry practice the life improvement due to the type of material from which the bearings is fabricated and the life improvement due to full EHD film conditions. $(L_{10})_\infty$ is then down-rated to actual film conditions by Eq. (I 9.11).

APPENDIX - II 1

S K F COMPUTER PROGRAM AT75Y004 "SHABERTH/SKF"

HIERARCHIAL FLOW CHART

APPENDIX II 1

S K F COMPUTER PROGRAM AT75Y004 FLOW CHART

Flow Chart

The hierarchical flow chart presents the program structure, listing the program elements in the order in which they would be called to solve the shaft-bearing dynamic, as well as steady state and transient temperature distribution problems. The various solution loops are indicated, as well as notes which indicate the functions of various subroutine groupings.

Each line in the flow chart represents a program element, subroutine, function or the main program ALWAYS. The call of one subroutine by another is denoted by indenting the called subroutine relative to the routine doing the calling. As an example, subroutine SKF calls subroutines FLAGS, TYPE, PROPST, LUBPROP, LUBCON, DATOT, CNVRT, CONS and SPRING.
Subroutine CONS calls CONST, CONST calls BCON and CRCON and BCON calls ABDEL.

The first mention of a subroutine within the flow chart includes the entire list of subordinate program elements. At subsequent calls to that subroutine the list of subordinate elements is omitted. As an example the first call to subroutine AXLBOJ is followed by the subordinate elements JMVIKT, SNITMT, NUMLOS, DUBSIM, MEIE, MEIL and SIMQ. After the call of AXLBOJ from INDEL, the subordinate elements are not listed but are, nevertheless, employed. The list of subordinate program elements are omitted in repeated calls of subordinate GUESS, BEAR, SOLV13 and DELIV3 as well as AXLBOJ.

As noted earlier, rolling equilibrium is calculated, first without, then if required, with friction forces included. Whether or not friction is considered is highlighted with the words Frictionless or Friction beside subroutine BEAREQ.

If the Program is too large to fit in its entirety on the user's computer, segments of the program may be "overlaid". For this purpose the Program is subdivided into ten (10) modules which can be sequentially "overlaid". The contents of the ten modules are listed below.

The Program segments SKF, TEMPIN, SHAFT and GUESS all perform initiation functions and with the exception of GUESS, are called only once per program execution.

The real problem solving portion of the program is embodied in segment ALLT. Within this segment the shaft bearing solution is obtained through the call to SHABE, then the steady state or transient temperature distributions are obtained.

This scheme is repeated until the end objective, steady state thermal equilibrium or time up for the transient scheme, is realized.

The nonlinear equation solver SOLV13 is central to the program and deserves special discussion as related to the flow chart. The first call to SOLV13 is from BEAR. Only for this first call are all of the SOLV13 subordinate subroutines listed as noted earlier. These include INSOLV, EQS, PARDER, SIMQ, EQCHEK, ERWRIT and ERCHEK. In the subsequent call to SOLV13 in which the steady state temperatures are being calculated, the above listed subroutines are again called but these calls with the exception of EQS are not listed on the flow chart.

EQS is the name given by SOLV13 to a subroutine which sets up the system of equations to be solved. EQS is brought into SOLV13 through the argument list. When the bearing equations are being solved, subroutine BRGGEQ is brought into SOLV13 and within SOLV13 is referenced by the name EQS. When the heat transfer equations are being solved as a consequence of the call of SOLV13 from ALLT, NET is brought into SOLV13 and is referenced as EQS.

```
ALWAYS
SKF                                   Read and set bearing and bearing solution
  FLAGS                               control data
  TYPE
  PROPST                              Set lubricant properties and calculate
  LUPROP                              constants for temperature dependency calculations
  LUBCON
  DATOT                               Write bearing input and hardcoded, preset data
    TITLE
    FITRAT
    ROLDAT
  CNVRT                               Calculate bearing related constants
  CONS
    CONST
      BCON
        ABDEL
      CRCON
  SPRING
TEMPIN                                Read and write thermla and thermal solution
  INDUM                               control data and calculate heat transfer
  RWHTC                               coefficients
  RWG
  RWHC
  TMAP
SHAFT                                 Read and write shaft geometry, loading
  ARRANG                              and bearing position data
    ORDERR
  OUTINP
  AXLBOJ                              Calculate shaft deflection constants
    JMVIKT
    SNITMT                            Make initial guesses of bearing reaction loads
    NUMLOS                            and displacements
      DUBSIM
        MEIE
        MEIL
    SIMQ
  REACT
  INDEL
    AXLBOJ
  PART                                Calculate shaft influence coefficients
    PAR
      AXLBOJ
GUESS                                 Guess values of bearing variables
  GBRG
    GROLL
  GBRG
    GBALL
  VARRDC
  GUESCG
ALLT                                  Begin the solution of the steady state or transient
  SHABE                               thermal and temperature dependent shaft-bearing
1 FIT                                 anslyses
2   INTFIT                            Calculate bearing diametral clearance
      SIMEQ
    SONRI                             Establish iteration scheme to satisfy
    3 BEARC                           inner ring equilibrium
      BEAR
        4 PREPAR
          INITX
            UNLOAD
          MAXMIN
          SOLVIB
            INSOLV
            EQS = BRGGEQ
              BEAREQ (FRICTIONLESS)
                BGCTRL
                BALLIN
                BALLEQ
                ROLLIN
                ROLLEQ
                  TNORM.
            PARDER                    Calculate rolling element raceway normal
              EQS = BRGGEQ            forces
            SIMEQ
            EQCHEK
              EQS = BRGGEQ
              ERWRIT
              DAMPCO.
              ERCHEK
          SUMF                        Sum the rolling element forces and moments
            SUMK                      acting on the inner ring
          LIFE                        Calculate bearing fatigue life
      BFILL                           Add bearing inner ring forces and moments to the
      SHAPA                           shaft equilibrium equations and predict new shaft
        FILL8                         displacements
      SIMEQ
    BEAR                              Calculate rolling element raceway normal loads
    GUESS                             with the new shaft displacements and guess
    VISCO2                            bearing component speeds
      ALPHAO                          Calculate temperature dependent lubricant
    DRAGNO                            properties
    STCON
    EVALUT (IF NPASS = 1)             Begin the calculation of bearing friction with
      PREPAR                          the guessed component speeds
      BRGGEQ
        BEAREQ (WITH FRICTION)
          BGCTRL
          BALLIN
          BALLEQ
            FMIX                      Calculate ball-race film thickness plus the
              TINT                    hydrodynamic and concentrated contact
              THERFC                  friction forces
              STARFC
```

2

2

```
SHAPA
  FILL8
SIMEQ                                  shaft equilibrium equations and predict new shaft
                                       displacements
BEAR
GUESS                                  Calculate rolling element raceway normal loads
                                       with the new shaft displacements and guess
                                       bearing component speeds
VISCO2
  ALPHAO
DRAGNO                                 Calculate temperature dependent lubricant
STCON                                  properties
EVALUT (IF NPASS = 1)
 PREPAR                                Begin the calculation of bearing friction with
 BRGGEQ                                the guessed component speeds
  BEAREQ (WITH FRICTION)
   BGCTRL
   BALLIN
   BALLEQ
    FMIX
     TINT
     THERFC                            Calculate ball-race film thickness plus the
     STARFC                            hydrodynamic and concentrated contact
       HOHI                            friction forces
     HDFRIC
     ASLOAD
     FRINT
       EHDSKF
         FRICTN
    DRAG
   ROLLIN
   ROLLEQ
    TNORM
    FMIXR
     HDFRIC
     THERFC                            Calculate the raceway normal and all friction
     STARFC                            forces acting on each roller
       HOHI
     ASLOAD
     EHDSKF
       FRICTN
   CAGESP                              Calculate the bearing cage speed
   CAGGEQ                              Calculate the forces acting on the cage
    CGLAND
     CGDRY                             Calculate the cage-ring land forces and moments
     CGWET
    CGRE
     CGBAL1
      CGNRMW
       CGEHDP                          Calculate the ball/cage normal and friction
       CGHDP                           forces for the ball in question
      CGFRN
       CGHDF
       CGEHI
         EHDSKF
           FRICTN
      CGNRMD
      CGFRD
    SUMCGL                             Calculate the cage equilibrium equations
    SUMRE
   BRGAX                               Calculate the rolling element inertia terms
     BRAX
   LIFE                                Calculate bearing fatigue life and bearing
     LRHS                              heat transfer coefficients
   HUT
BEAR IF (NPASS = 2)
4 PREPAR                               Calculate component equilibrium using the inner
  SOLVXX                               ring positions determined with elastic rolling
   EQS = BRGGEQ                        element-raceway forces
    BEAREQ (WITH FRICTION)
SONRI IF (NPASS = 3)
3 BEARC                                Calculate inner ring and component equilibrium
   BEAR                                using friction as well as elastic component
    4 PREPAR                           forces
    4 SOLVXX
       EQS = BRGGEQ
         BEAREQ (WITH FRICTION)
      SUMF
      SUMK
DELIV3
  TITLE
  RITE                                 Write bearing output
  REOUT3
    RITE2
FILLGT
SOLVXX
5 EQS = NET                            Calculate the steady state temperature distribu-
    NETEET                             tion and write results
DELIV3
TMAP
STEPMA
  NET
    NETEET
DELIV3
NET                                    Calculate transient temperature distribution
  NETEET                               and write results
TMAP
DELIV3
TMAP
```

Solution Loops

1. Steady State and Transient Thermal
2. Change in Clearance
3. Shaft-Inner Ring Equilibrium
4. Rolling Element and Cage Equilibrium
5. Temperature Equilibrium

APPENDIX - II 2

S K F COMPUTER PROGRAM "SHABERTH/SKF"

INPUT FORMAT FORMS

HOW TO READ AND USE THE FOLLOWING FORMS

Program Names of input Items, for example: W1 D1A BD(5) 1Z A(6) R(2,3)

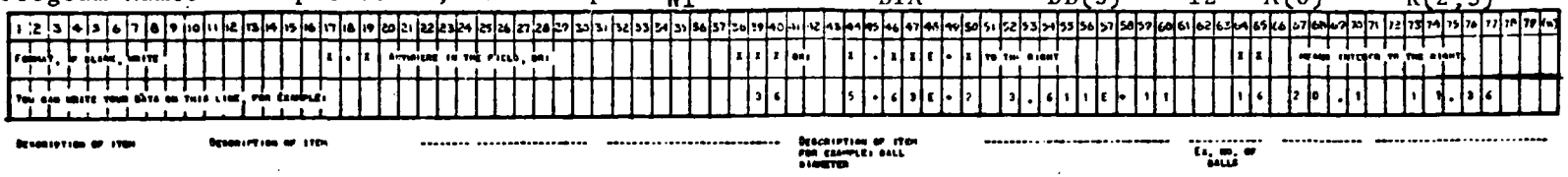

ALL VALUES ARE TO BE GIVEN IN THE UNITS OF THE SI-SYSTEM, THE INTERNATIONAL SYSTEM. EXCEPTIONS ARE LENGTHS WHICH ARE EXPRESSED IN MILLIMETERS INSTEAD OF METERS, AND PRESSURES WHICH ARE GIVEN IN NEWTONS/MM^2 INSTEAD OF NEWTONS/M^2. VOLUMES IN MM^3.

Unless noted, all numerical input data is in F format, F10.0 or F5.0

TITLE CARD

Card Type TT1

| Title(28) | | |

TITLE CARD

Card 2, One Card

GOV(1)	IFLAG (1) NBRC	IFLAG (2) NPRINT	IFLAG(3) IFIT	IFLAG(4) ITMAIN	GOV(2) EPSFIT	GOV(3) EPS1	GOV(4) EPS2	NPASS IMT
Shaft speed revolutions per minute	Number of Bearings	Print flag if not blank debug output will be obtained. If = 1 main loop debug only. If = 2 full debug output.	Fit calc. flag. Blank means no fit calculation and no iteration. Positive no. means fit iteration with max = 5 negative no. means fit iteration max = given no.	Main loop iteration flag. Positive no. means pre-set max is used = 10 negative no. means iteration limit = given no. blank = one iteration	Fit loop accuracy if is defined as change of diametral clearance divided by roller element diameter. If left blank, pre-set accuracy of 0.0001 is used.	Main loop accuracy for frictionless solution. When the latest change of bearing deflection is less than EPS1 or EPS2 * bearing deflection, or the bearing angular deflection is less than 2×10^{-5} and linear deflection is less than 5×10^{-5}, then iteration is stopped. If left blank, pre-set accuracy of 0.001 is used.	Main loop accuracy for EHD or coulomb solution. If left blank, pre-set accuracy of 0.0001.	Bearing Solution Level Flag* MATERIAL PROPERTY FLAG

*NPASS, IFLAG(5), Bearing Solution Level Flag

0 Elastic Contact Forces are calculated, no lubrication or friction effects are considered

1 Elastic Contact Forces are calculated. Lubrication and friction effects are considered using raceway control (ball bearing) or epicyclic (roller bearing) assumptions to estimate rolling element and cage speeds

2 Inner Equilibrium is satisfied considering only the Elastic Contact Forces. Using the inner ring positions thus obtained, rolling element and cage equilibrium are determined considering friction

3 Complete Solution. The inner ring, rolling element and cage equilibrium is determined considering all elastic and friction forces

BEARING DATA, One set per bearing cards B1-B16 for bearing 1, followed by cards B1-B16 for bearing 2, etc.

Card Type B1, one card

BD(1)	Steel Designations		BD(43) Steel Life Factors	BD(44)	BD(2)	NC
A1	5A4	5A4			F8 0	
Bearing Type Ball or Cylindrical Must Begin in Column 1	Inner Ring	Outer Ring	Outer	Inner	Orientation Angle in Degrees of Rolling Elements. 0.0 means first rolling element is on the Z-axis. $0 \le \phi_1 \le \frac{2\pi}{N}$	Crown Drop Flag

NC Normally zero or blank, if set to 1, nonuniform roller-raceway profile geometry is input on card types B5 and B6.

BEARING DATA

Card Type B2, one card

BD(5)	BD(6)	BD(7)	BD(8)		BD(3)		
Pitch Diameter (mm)	No. of Rolling Elements	Diametral Clearance (mm)	Contact Angle (Deg.)		Outer Ring Speed (RPM)		

BEARING DATA

Card Type B3, one card

BD(4)

| 1 | 2 | 3 | 4 | 5 | 6 | 7 | 8 | 9 | 10 | 11 | 12 | 13 | 14 | 15 | 16 | 17 | 18 | 19 | 20 | 21 | 22 | 23 | 24 | 25 | 26 | 27 | 28 | 29 | 30 | 31 | 32 | 33 | 34 | 35 | 36 | 37 | 38 | 39 | 40 | 41 | 42 | 43 | 44 | 45 | 46 | 47 | 48 | 49 | 50 | 51 | 52 | 53 | 54 | 55 | 56 | 57 | 58 | 59 | 60 | 61 | 62 | 63 | 64 | 65 | 66 | 67 | 68 | 69 | 70 | 71 | 72 | 73 | 74 | 75 | 76 | 77 | 78 | 79 | 80 |
|---|---|---

BEARING DATA

Card Type B4, one card

BD(21) BD(22)

| 1 | 2 | 3 | 4 | 5 | 6 | 7 | 8 | 9 | 10 | 11 | 12 | 13 | 14 | 15 | 16 | 17 | 18 | 19 | 20 | 21 | 22 | 23 | 24 | 25 | 26 | 27 | 28 | 29 | 30 | 31 | 32 | 33 | 34 | 35 | 36 | 37 | 38 | 39 | 40 | 41 | 42 | 43 | 44 | 45 | 46 | 47 | 48 | 49 | 50 | 51 | 52 | 53 | 54 | 55 | 56 | 57 | 58 | 59 | 60 | 61 | 62 | 63 | 64 | 65 | 66 | 67 | 68 | 69 | 70 | 71 | 72 | 73 | 74 | 75 | 76 | 77 | 78 | 79 | 80 |
|---|---|---

BEARING DATA

Omit Cards B5 and B6 if crown drop flag is 0

Card Type B5, as amny as needed, maximum of 3, for the inner race.

BLAN(1,5) (2,5) (3,5) (4,5) (5,5) (6,5) (7,5)

Crown Drop at Laminum 1 (mm)	Crown Drop at Laminum 2	... and so on, use more than one card if No. of laminae is greater than 7					

Card Type B6, as many as needed, maximum of 3, for the outer race.

BLAN(1,4) (2,4) (3,4) (4,4) (5,4) (6,4) (7,4)

Crown Drop at Laminum 1 (mm)	Crown Drop at Laminum 2	...and so on					

BEARING DATA

Card Type B7, one card, omit if NPASS, Title Card 2 is zero or blank

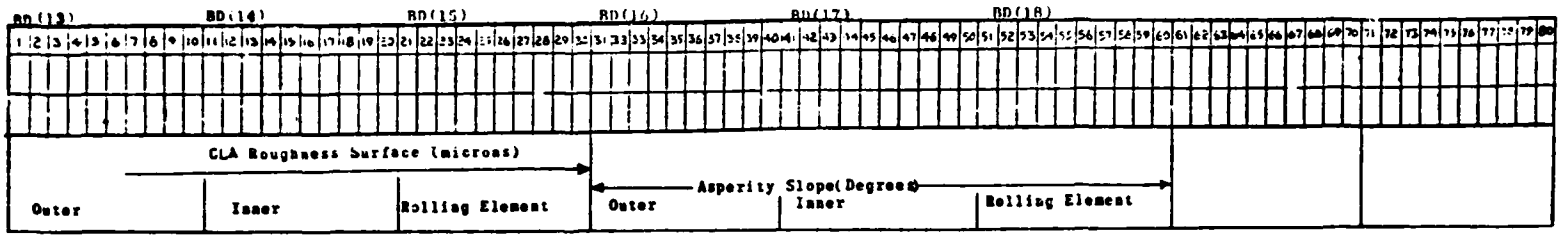

BEARING DATA

Card Type B8, one card, Omit if NPASS, Title Card 2, is zero or blank

BD(36)	BD(37)	BD(38)	BD(39)	BD(40)	BD(41)		
Cage Type -1. for outer-ring lead riding +1. for inner-ring lead riding 0. for rolling element riding	Rail-Lead Diameter (mm)	Single Rail Width (mm)	Rail-Lead Diametral Clearance (mm)	Rolling Element-Cage Pocket Diametral Clearance (mm)	Cage Weight Kg.		

BEARING DATA

Omit Cards B9 and B10 if operating clearances are not to be calculated

Card Type B9, one card

BD(51)	BD(52)	BD(53)	BD(54)	BD(55)	BD(56)		
Shaft Fit Positive if interference (mm)	Housing Fit, Positive if Interference (mm)	Shaft Effective Length (mm)	Bearing Inner Ring Width (mm)	Bearing Outer Ring Width (mm)	Housing Effective Width (mm)		

Card Type B10, one card

BD(57)	BD(58)	BD(60)	BD(61)	BD(62)	BD(64)		
Shaft Inner Diameter (mm)	Bearing Bore Diameter (mm)	Bearing Inner Ring Mean Outer Diameter (mm)	Bearing Outer Ring Mean Inner Diameter (mm)	Bearing Outer Diameter (mm)	Housing Outer Diameter (mm)		

BEARING DATA

Omit Card Types B11 through B14 if operating clearances are not to be calculated.

Card Type B11, one card

BD(66)	BD(67)	BD(68)	BD(69)	BD(70)
Modulus of Elasticity N/mm^2				
Shaft	Inner Ring	Rolling Element	Outer Ring	Housing

Card Type B12, one card

BD(71)	BD(72)	BD(73)	BD(74)	BD(75)
Poisson's Ratio				
Shaft	Inner Ring	Rolling Element	Outer Ring	Housing

Card Type B13, one card

BD(76)	BD(77)	BD(78)	BD(79)	BD(80)
Density gm/cm^3				
Shaft	Inner Ring	Rolling Element	Outer Ring	Housing

Card Type B14, one card

BD(81)	BD(82)	BD(83)	BD(84)	BD(85)
Coefficient Thermal Expansion 1/°C				
Shaft	Inner Ring	Rolling Element	Outer Ring	Housing

BEARING DATA

Card Type B15, one card, Omit if NPASS, Title Card 2, is zero or blank.

BD(102)		BD(103)	BD(104)	BD(106)			
Lubricant Replenishment Layer Thickness (mm)			Percent Lubricant in Bearing Cavity	Raceway-Rolling Element Asperity Friction Coefficient			
Outer Raceway	Inner Raceway						

BEARING DATA
Card Type B16, one card, Omit if NPASS, Title Card 2, is zero or blank
Lubricant Properties

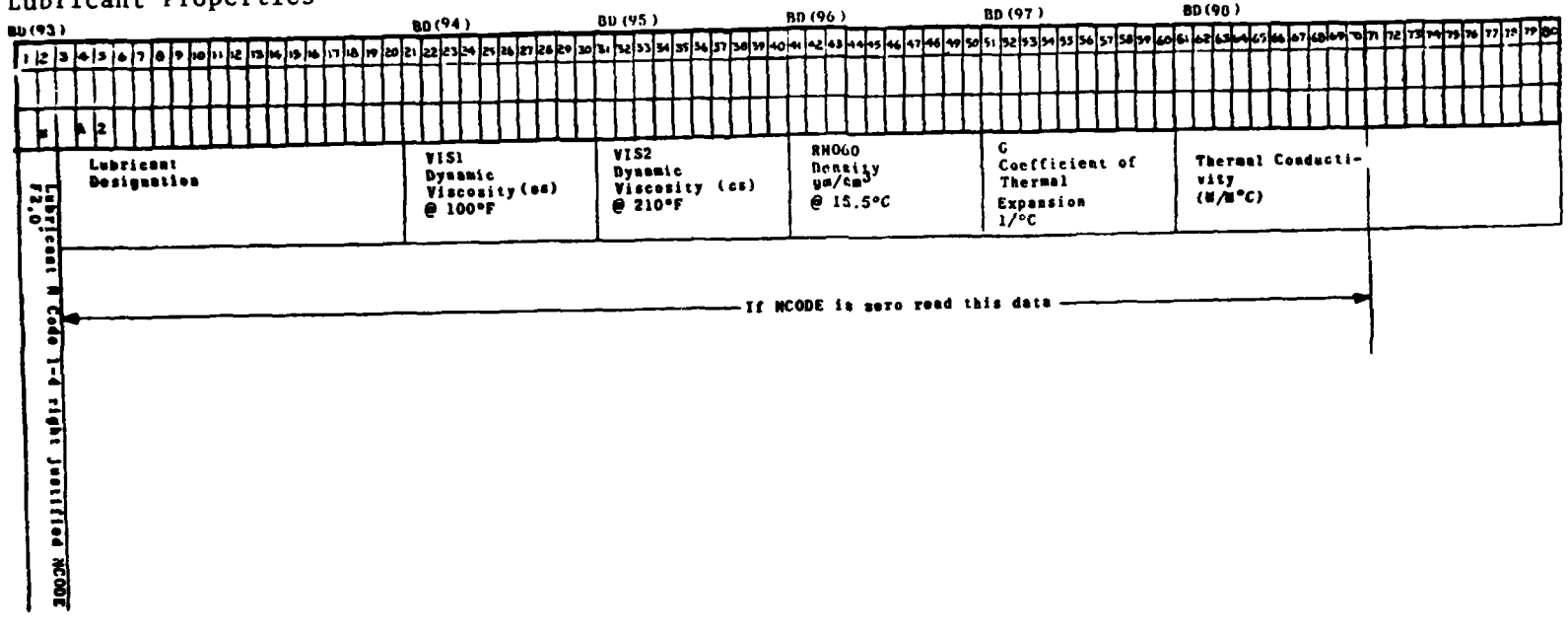

THERMAL DATA
Card Type T1

Once controlling card. If no temp. calculation is desired, then leave the card blank.

N	B	TEMP	IPUNCH	HB	IT1	EP1	IT2	EP2	START	STOP	STEP IN	TIME	BTIME
x	x		x	x		x		x					

GENERAL						STEADY STATE ONLY			TRANSIENT ONLY					
Highest Node Number	Highest Unknown Node Number. Same as number of unknown nodes	Common Initial Temperature Selected temperatures can be given different initial values using card T3.	Punch Flag, usually zero. If ≠ 0 final temperatures will be punched according to the format of Card T3. Then, they can be read in as initial temperatures in a later run.	Output Flag, usually zero. If ≠ 0 bearing output and a temperature map will be printed every time the shaft-bearing program has been called.	Maximum no. of calls of the shaft-bearing program.	Absolute Accuracy of temperatures	Iteration Limit, usually left blank If ≠ 0 the intermediate iteration limit. If blank pre-set limit is used	Accuracy usually left blank. If ≠ 0 it is the intermediate rel. accuracy	Starting Time	Stopping Time	Calculation Time Step. If left blank, the program will calculate a suitable step.	Time interval between printed temp. maps. The interval will always be at least equal to the calc. time step.	Time interval between calls of shaft-bearing program. Always at least equal to the calc. time step.	

THERMAL DATA - BEARING TEMPERATURES

T2, One card/brg. Use only if no temperature calc. is desired, and then give no more thermal data.

| 1 | 2 | 3 | 4 | 5 | 6 | 7 | 8 | 9 | 10 | 11 | 12 | 13 | 14 | 15 | 16 | 17 | 18 | 19 | 20 | 21 | 22 | 23 | 24 | 25 | 26 | 27 | 28 | 29 | 30 | 31 | 32 | 33 | 34 | 35 | 36 | 37 | 38 | 39 | 40 | 41 | 42 | 43 | 44 | 45 | 46 | 47 | 48 | 49 | 50 | 51 | 52 | 53 | 54 | 55 | 56 | 57 | 58 | 59 | 60 | 61 | 62 | 63 | 64 | 65 | 66 | 67 | 68 | 69 | 70 | 71 | 72 | 73 | 74 | 75 | 76 | 77 | 78 | 79 | 80 |
|---|---|---

THERMAL DATA - INDIVIDUAL INITIAL TEMPERATURES

T3, As many cards as needed, followed by a blank card

Node Number	Initial Temperature	Etc.	Node Number	Initial Temperature

THERMAL DATA - BEARING NODE NUMBERS

T4, One card/brg.

| 1 | 2 | 3 | 4 | 5 | 6 | 7 | 8 | 9 | 10 | 11 | 12 | 13 | 14 | 15 | 16 | 17 | 18 | 19 | 20 | 21 | 22 | 23 | 24 | 25 | 26 | 27 | 28 | 29 | 30 | 31 | 32 | 33 | 34 | 35 | 36 | 37 | 38 | 39 | 40 | 41 | 42 | 43 | 44 | 45 | 46 | 47 | 48 | 49 | 50 | 51 | 52 | 53 | 54 | 55 | 56 | 57 | 58 | 59 | 60 | 61 | 62 | 63 | 64 | 65 | 66 | 67 | 68 | 69 | 70 | 71 | 72 | 73 | 74 | 75 | 76 | 77 | 78 | 79 | 80 |
|---|---|---

THERMAL DATA-NODES WHERE BEARING FRICTIONAL HEAT IS GENERATED

T5, One card/brg.

1	2	3	4	5	6	7	8	9	10	11	12	13	14	15	16	17	18	19	20	21	22	23	24	25	26	27	28	29	30	31	32	33	34	35	36	37	38	39	40	41	42	43	44	45	46	47	48	49	50	51	52	53	54	55	56	57	58	59	60	61	62	63	64	65	66	67	68	69	70	71	72	73	74	75	76	77	78	79	80
				x					x					x					x					x					x					x					x					x					x																															

THERMAL DATA - NODES WITH A CONSTANT POWER SOURCE

T6, as many cards as needed, followed by a blank card

| 1 | 2 | 3 | 4 | 5 | 6 | 7 | 8 | 9 | 10 | 11 | 12 | 13 | 14 | 15 | 16 | 17 | 18 | 19 | 20 | 21 | 22 | 23 | 24 | 25 | 26 | 27 | 28 | 29 | 30 | 31 | 32 | 33 | 34 | 35 | 36 | 37 | 38 | 39 | 40 | 41 | 42 | 43 | 44 | 45 | 46 | 47 | 48 | 49 | 50 | 51 | 52 | 53 | 54 | 55 | 56 | 57 | 58 | 59 | 60 | 61 | 62 | 63 | 64 | 65 | 66 | 67 | 68 | 69 | 70 | 71 | 72 | 73 | 74 | 75 | 76 | 77 | 78 | 79 | 80 |
|---|---|---

THERMAL DATA - HEAT TRANSFER COEFFICIENTS

T7, one or two cards/coefficient, as many as needed, followed by a blank card

1-10	11-20	21-30	31-40	41-50
INDEX FOR LATER IDENTIFICATION OF THE HEAT TR. COEFFICIENT				
$\dot{q} = \lambda A/\hat{x}\Delta\tau$	(CONDUCTIVITY W/m°C)			
$\dot{q} = \alpha A \Delta\tau^{n}$	(FREE CONV. NO.) n	(1 F BLANK = 1.25)		
$\dot{q} = \alpha A \Delta\tau$	(FORCED CONV. NO.)			
$\dot{q} = \epsilon \hat{A} (T_1^4 - T_2^4)$	(EMISSIVITY, 0≤ε≤1) ϵ			
$\rho \cdot C_p \cdot \dot{V}$ (W/°C)		(ρ IS DENSITY, KG/M^3, CP SPECIFIC HEAT, WSEC/KG°C, V VOLUME FLOW M^3/SEC, V IS VELOCITY (M/SEC)		

THE FORCED CONVECTION NO. α CAN BE CALCULATED BY THE PROGRAM FROM THE FORMULA $\alpha = \lambda_m/L \cdot Nu$, WHERE $Nu = Re^{A} \cdot Pr^{B}$, $Re = (U \cdot L \cdot \rho)/\eta$, $Pr = (\eta \cdot cp)/\lambda_m$, η = CONSTANT, OR $\eta = \eta$ (TEMP), η = DYNAMIC VISCOSITY. THEN THE FOLLOWING DATA MUST BE GIVEN AND A SECOND CARD MUST IMMEDIATELY FOLLOW. USE ONE OF THE 3 OPTIONS.

21-30	31-40	41-50	51-60	61-70	71-80
m = CONST.)	E	A	B	L METER	U	OR 1	(OPTION 1)
$m = C \cdot \eta^{A} \cdot q \cdot \eta(t)$	O	B	BLANK	BLANK	BLANK	BLANK	(OPTION 2)
$m = m(\eta(t))$	E	A	B	L METER	U	OIL	(OPTION 3)

21-30	31-40	41-50	51-60	61-70	71-80
DYNAMIC VISCOSITY (N/m^{2}S) BLANK BLANK	DENSITY (KG/M^3) BLANK DENSITY	SPECIFIC HEAT (WS/KG°C) BLANK SPECIFIC HEAT	BLANK LOW TEMP. T_L °C	BLANK DYNAMIC VISCOSITY AT T_L DYNAMIC VISCOSITY AT T_L	BLANK HIGH TEMP. T_H (°C)	BLANK DYNAMIC VISCOSITY AT T_H DYNAMIC VISCOSITY AT T_H	(OPTION 1) (OPTION 2) (OPTION 3)

THERMAL DATA - HEAT FLOW PATHS
T8, as many cards as needed, max. 500, followed by a blank card
Index

| 1 | 2 | 3 | 4 | 5 | 6 | 7 | 8 | 9 | 10 | 11 | 12 | 13 | 14 | 15 | 16 | 17 | 18 | 19 | 20 | 21 | 22 | 23 | 24 | 25 | 26 | 27 | 28 | 29 | 30 | 31 | 32 | 33 | 34 | 35 | 36 | 37 | 38 | 39 | 40 | 41 | 42 | 43 | 44 | 45 | 46 | 47 | 48 | 49 | 50 | 51 | 52 | 53 | 54 | 55 | 56 | 57 | 58 | 59 | 60 | 61 | 62 | 63 | 64 | 65 | 66 | 67 | 68 | 69 | 70 | 71 | 72 | 73 | 74 | 75 | 76 | 77 | 78 | 79 | 80 |
|---|---|---

THERMAL DATA - NODE HEAT CAPACITIES, ONLY FOR TRANSIENT CALCULATIONS

T9, One card/node

Node Number If it is given without a sign, rotational symmetry is assumed and the volume is multiplied by 2π If it is negative the volume is not changed.	Volume at Node=$L_1 \cdot L_2 \cdot L_3$			Density (KG/M^3)	Specific Heat $WS/KG°C$		
	L_1 mm	L_2 mm	L_3 mm				

SHAFT DATA - SHAFT GEOMETRY

Omit all shaft data cards if there are no bearings

S1, as many cards as needed

| 1 | 2 | 3 | 4 | 5 | 6 | 7 | 8 | 9 | 10 | 11 | 12 | 13 | 14 | 15 | 16 | 17 | 18 | 19 | 20 | 21 | 22 | 23 | 24 | 25 | 26 | 27 | 28 | 29 | 30 | 31 | 32 | 33 | 34 | 35 | 36 | 37 | 38 | 39 | 40 | 41 | 42 | 43 | 44 | 45 | 46 | 47 | 48 | 49 | 50 | 51 | 52 | 53 | 54 | 55 | 56 | 57 | 58 | 59 | 60 | 61 | 62 | 63 | 64 | 65 | 66 | 67 | 68 | 69 | 70 | 71 | 72 | 73 | 74 | 75 | 76 | 77 | 78 | 79 | 80 |
|---|---|---

SHAFT DATA - BEARING POSITION AND SUPPORT, X-Y PLANE

S2, As many cards as the number of bearings. Arranged in order of increasing X-coordinate.

| 1 | 2 | 3 | 4 | 5 | 6 | 7 | 8 | 9 | 10 | 11 | 12 | 13 | 14 | 15 | 16 | 17 | 18 | 19 | 20 | 21 | 22 | 23 | 24 | 25 | 26 | 27 | 28 | 29 | 30 | 31 | 32 | 33 | 34 | 35 | 36 | 37 | 38 | 39 | 40 | 41 | 42 | 43 | 44 | 45 | 46 | 47 | 48 | 49 | 50 | 51 | 52 | 53 | 54 | 55 | 56 | 57 | 58 | 59 | 60 | 61 | 62 | 63 | 64 | 65 | 66 | 67 | 68 | 69 | 70 | 71 | 72 | 73 | 74 | 75 | 76 | 77 | 78 | 79 | 80 |
|---|---|---

SHAFT DATA - SHAFT LOADING, X-Y PLANE FORCES, Z-MOMENTS

S3, as many cards as needed, followed by a blank card.

| 1 | 2 | 3 | 4 | 5 | 6 | 7 | 8 | 9 | 10 | 11 | 12 | 13 | 14 | 15 | 16 | 17 | 18 | 19 | 20 | 21 | 22 | 23 | 24 | 25 | 26 | 27 | 28 | 29 | 30 | 31 | 32 | 33 | 34 | 35 | 36 | 37 | 38 | 39 | 40 | 41 | 42 | 43 | 44 | 45 | 46 | 47 | 48 | 49 | 50 | 51 | 52 | 53 | 54 | 55 | 56 | 57 | 58 | 59 | 60 | 61 | 62 | 63 | 64 | 65 | 66 | 67 | 68 | 69 | 70 | 71 | 72 | 73 | 74 | 75 | 76 | 77 | 78 | 79 | 80 |
|---|---|---

SHAFT DATA - BEARING POSITION AND SUPPORT, X-Z PLANE

S2, as many cards as needed. Card needed only if any data is different from X-Y plane.

| 1 | 2 | 3 | 4 | 5 | 6 | 7 | 8 | 9 | 10 | 11 | 12 | 13 | 14 | 15 | 16 | 17 | 18 | 19 | 20 | 21 | 22 | 23 | 24 | 25 | 26 | 27 | 28 | 29 | 30 | 31 | 32 | 33 | 34 | 35 | 36 | 37 | 38 | 39 | 40 | 41 | 42 | 43 | 44 | 45 | 46 | 47 | 48 | 49 | 50 | 51 | 52 | 53 | 54 | 55 | 56 | 57 | 58 | 59 | 60 | 61 | 62 | 63 | 64 | 65 | 66 | 67 | 68 | 69 | 70 | 71 | 72 | 73 | 74 | 75 | 76 | 77 | 78 | 79 | 80 |
|---|---|---

SHAFT DATA - SHAFT LOADING, X-Z PLANE FORCES, Y-MOMENTS.

S3, as many cards as needed, followed by a blank card

| 1 | 2 | 3 | 4 | 5 | 6 | 7 | 8 | 9 | 10 | 11 | 12 | 13 | 14 | 15 | 16 | 17 | 18 | 19 | 20 | 21 | 22 | 23 | 24 | 25 | 26 | 27 | 28 | 29 | 30 | 31 | 32 | 33 | 34 | 35 | 36 | 37 | 38 | 39 | 40 | 41 | 42 | 43 | 44 | 45 | 46 | 47 | 48 | 49 | 50 | 51 | 52 | 53 | 54 | 55 | 56 | 57 | 58 | 59 | 60 | 61 | 62 | 63 | 64 | 65 | 66 | 67 | 68 | 69 | 70 | 71 | 72 | 73 | 74 | 75 | 76 | 77 | 78 | 79 | 80 |
|---|---|---

APPENDIX - II 3

COMPUTER PROGRAM SHABERTH/SKF

SAMPLE OUTPUT

*** S H A B E R T H / S K F ** TECHNOLOGY DIVISION S K F INDUSTRIES INC. ** S H A B E R T H / S K F ***

WPAFB LUBRICATION BRANCH * R.E.B. TEST MACHINE ASSEMBLY I * SOLUTION LEVEL 2

THIS DATA SET CONTAINS 2 BEARINGS

BEARING NO. (1) - CYLINDRICAL ROLLER BEARING

BEARING NO. (2) - BALL BEARING

THE MAXIMUM NUMBER OF FIT ITERATIONS ALLOWED IS 2 AND THE RELATIVE ACCURACY REQUIRED IS .00010

*** S H A B E R T H / S K F ** TECHNOLOGY DIVISION S K F INDUSTRIES INC. ** S H A B E R T H / S K F ***

WPAFB LUBRICATION BRANCH * R.E.B. TEST MACHINE ASSEMBLY I * SOLUTION LEVEL 2

UNLESS OTHERWISE STATED, LINEAR DIMENSIONS ARE SPECIFIED IN MILLIMETERS, TEMPERATURES IN DEGREES CENTIGRADE, FORCES IN NEWTONS, WEIGHTS IN KILOGRAMS, PRESSURES AND ELASTIC MODULI IN NEWTONS PER SQUARE MILLIMETER, ANGLES AND SLOPES IN DEGREES, SURFACE ROUGHNESS IN MICRONS, SPEEDS IN REVOLUTIONS PER MINUTE, DENSITY IN GRAMS PER CUBIC CENTIMETER, KINEMATIC VISCOSITY IN CENTISTOKES AND THERMAL CONDUCTIVITY IN WATTS PER METER-DEGREE CENTIGRADE.

BEARING NUMBER	NUMBER OF ROLLING ELEMENTS	AZIMUTH ANGLE ORIENTATION	PITCH DIAMETER	DIAMETRAL CLEARANCE	CONTACT ANGLE	INNER RING SPEED	OUTER RING SPEED
1	14	-0.000	65.000	.060	-0.000	15000.	-0.
2	18	-0.000	140.000	-0.000	25.000	15000.	-0.

C A G E D A T A

BEARING NUMBER	CAGE TYPE	CAGE POCKET CLEARANCE	RAIL-LAND WIDTH	RAIL-LAND DIAMETER	RAIL-LAND CLEARANCE	WEIGHT
1	INNER RING LAND RIDING	.290000	2.6800	58.8880	.240	.050000
2	INNER RING LAND RIDING	.826000	4.0030	128.4700	1.270	.300000

S T E E L D A T A

BRG.NO.	INNER RING TYPE	LIFE FACTOR	OUTER RING TYPE	LIFE FACTOR
1	AISI 52100	3.000	AISI 52100	3.000
2	M50 CVM	5.000	M50 CVM	5.000

*** S H A B E R T H / S K F ** TECHNOLOGY DIVISION S K F INDUSTRIES INC. ** S H A B E R T H / S K F ***

WPAFB LUBRICATION BRANCH * R.E.B. TEST MACHINE ASSEMBLY I * SOLUTION LEVEL 2

R O L L I N G E L E M E N T D A T A

BEARING NUMBER (1) TYPE - CYLINDRICAL ROLLER BEARING

ROLLER DIAMETER	ROLLER LENGTH	ROLLER END SPHERE RADIUS	ROLLER INCL. ANGLE	AXIAL PLAY OUTER RING	AXIAL PLAY INNER RING	FLANGE ANGLE OUTER RING	FLANGE ANGLE INNER RING
10.0000	10.0000	200.0000	0.000	0.0000	0.0000	0.000	0.000

EFF.LENGTH	OUTER RACEWAY FLAT LENGTH	OUTER RACEWAY CROWN RAD.	EFF.LENGTH	INNER RACEWAY FLAT LENGTH	INNER RACEWAY CROWN RAD.	NO. OF AXIAL LAMINAE
8.0000	3.0000	1000.000	8.0000	3.0000	1000.000	10

BEARING NUMBER (2) TYPE - BALL BEARING

BALL DIAMETER	OUTER RACEWAY CURVATURE	INNER RACEWAY CURVATURE
19.0500	.520	.540

*** S H A B E R T H / S K F ** TECHNOLOGY DIVISION S K F INDUSTRIES INC. ** S H A B E R T H / S K F ***

WPAFB LUBRICATION BRANCH * R.E.B. TEST MACHINE ASSEMBLY I * SOLUTION LEVEL 2

S U R F A C E D A T A

BEARING NUMBER	CLA ROUGHNESS OUTER	CLA ROUGHNESS INNER	CLA ROUGHNESS ROLL. ELM.	RMS ASPERITY SLOPE OUTER	RMS ASPERITY SLOPE INNER	RMS ASPERITY SLOPE ROLL. ELM.
1	.15	.15	.10	2.000	2.000	2.000
2	.08	.08	.04	2.000	2.000	2.000

L U B R I C A N T D A T A

BEARING NUMBER	DESIGNATION	KINEMATIC VISCOSITY (37.78 C)	KINEMATIC VISCOSITY (98.89 C)	DENSITY AT (15.56 C)	THERMAL EXPAN. COEFFICIENT	THERMAL CONDUCTIVITY
1	MIL-L-7808G	12.76	3.20	.9526	7.09E-04	.152
2	MIL-L-7808G	12.76	3.20	.9526	7.09E-04	.152

L U B R I C A T I O N A N D F R I C T I O N D A T A

BEARING NUMBER	PERCENT LUBE IN CAVITY	FILM REPLENISHMENT LAYER THICKNESS (ROLL.ELM. + RACEWAY) OUTER	FILM REPLENISHMENT LAYER THICKNESS (ROLL.ELM. + RACEWAY) INNER	ASPERITY FRICTION COEFFICIENT
1	1.00	.9000E-03	.3000E-03	.10
2	1.00	.6000E-03	.2000E-03	.10

*** S H A B E R T H / S K F ** TECHNOLOGY DIVISION S K F INDUSTRIES INC. ** S H A B E R T H / S K F ***

WPAFB LUBRICATION BRANCH * R.E.B. TEST MACHINE ASSEMBLY I * SOLUTION LEVEL 2

F I T D A T A A N D M A T E R I A L P R O P E R T I E S

BEARING NUMBER	COLD FITS (MM TIGHT) SHAFT	HOUSING	EFFECTIVE WIDTHS SHAFT	INNER RING	OUTER RING	HOUSING
1	.0380	-.0250	24.0000	19.0000	19.0000	22.0000
2	.0050	-.0380	22.0000	17.0000	34.0000	67.0000

BEARING NUMBER	EFFECTIVE DIAMETERS SHAFT I.D.	BEARING BORE	INNER RING AVE. O.D.	OUTER RING AVE. I.D.	BEARING O.D.	HOUSING O.D.
1	1.000	45.000	54.000	73.000	85.000	120.000
2	20.000	100.000	127.000	155.000	180.000	205.000

BEARING NUMBER (1)	SHAFT	INNER RING	ROLL. ELEM.	OUTER RING	HOUSING
MODULUS OF ELASTICITY	204083.0	204083.0	204083.0	204083.0	204083.0
POISSONS RATIO	.3000	.3000	.3000	.3000	.3000
WEIGHT DENSITY	7.806	7.806	7.806	7.806	7.806
COEFF. OF THERMAL EXP.	.00001224	.00001224	.00001224	.00001224	.00001224

BEARING NUMBER (2)	SHAFT	INNER RING	ROLL. ELEM.	OUTER RING	HOUSING
MODULUS OF ELASTICITY	204083.0	204083.0	204083.0	204083.0	204083.0
POISSONS RATIO	.3000	.3000	.3000	.3000	.3000
WEIGHT DENSITY	7.806	7.806	7.806	7.806	7.806
COEFF. OF THERMAL EXP.	.00001224	.00001224	.00001224	.00001224	.00001224

UNLESS OTHERWISE STATED, INTERNATIONAL UNITS ARE USED

GIVEN TEMPERATURES

BRG	SHAFT	I. RING	I. RACE	ROLL EL.	O. RACE	O. RING	HOUSING	BULK	FLANGE
1	66.00	71.00	74.00	77.00	74.00	71.00	66.00	57.00	-0.00
2	177.00	182.00	185.00	189.00	188.00	185.00	177.00	141.00	-0.00

*** S H A B E R T H / S K F ** TECHNOLOGY DIVISION S K F INDUSTRIES INC. ** S H A B E R T H / S K F ***

WPAFB LUBRICATION BRANCH * R.E.B. TEST MACHINE ASSEMBLY I * SOLUTION LEVEL 2

SHAFT GEOMETRY, BEARING LOCATIONS AND SHAFT LOAD, PLANE X - Y.

20 GEOMETRIC SECTIONS 1 LOAD SECTION(S), 2 BEARINGS. MODULUS OF ELASTICITY = 2.041E+05

	POSI-TION	INNER DIAM. LEFT	INNER DIAM. RIGHT	OUTER DIAM. LEFT	OUTER DIAM. RIGHT	POINT FORCE	POINT MOMENT	LOAD INTENSITY LEFT	LOAD INTENSITY RIGHT		BEARING SEAT POS.ERR	BEARING SEAT DEFL/FOR	BEARING SEAT ANG.ERR	BEARING SEAT DEFL/MOM
1	0.0	0.0	0.0	0.0	29.0					1				
2	45.0	0.0	0.0	29.0	45.0					2				
3	54.0	0.0	0.0	45.0	45.0					3	-0.000	-0.	-0.0000	-0.
4	63.5	0.0	0.0	45.0	52.0					4				
5	69.0	0.0	0.0	52.0	52.0					5				
6	71.0	0.0	0.0	44.0	44.0					6				
7	73.0	0.0	0.0	42.0	42.0					7				
8	322.0	0.0	0.0	42.0	42.0					8				
9	324.0	0.0	0.0	44.0	44.0					9				
10	326.0	0.0	0.0	58.0	56.0					10				
11	340.0	0.0	0.0	58.0	85.0					11				
12	355.0	0.0	0.0	85.0	85.0	2224.1	-4000.0			12				
13	368.0	0.0	0.0	85.0	100.0					13				
14	378.0	0.0	0.0	100.0	41.5					14				
15	439.0	0.0	24.0	41.5	39.0					15				
16	441.0	28.0	28.0	38.0	38.0					16				
17	459.0	30.0	30.0	38.0	38.0					17				
18	461.0	30.0	30.0	41.5	41.5					18				
19	470.0	20.0	20.0	41.5	41.5					19				
20	480.0	20.0	20.0	41.5	116.0					20				
21	487.0	20.0	20.0	116.0	100.0					21				
22	504.0	20.0	20.0	100.0	100.0					22	-0.000	-0.	-0.0000	-0.
23	524.0	20.0	20.0	100.0	100.0					23				

*** S H A B E R T H / S K F ** TECHNOLOGY DIVISION S K F INDUSTRIES INC. ** S H A B E R T H / S K F ***

WPAFB LUBRICATION BRANCH * R.E.B. TEST MACHINE ASSEMBLY I * SOLUTION LEVEL 2

SHAFT GEOMETRY, BEARING LOCATIONS AND SHAFT LOAD, PLANE X - Z.

20 GEOMETRIC SECTIONS 1 LOAD SECTION(S), 2 BEARINGS. MODULUS OF ELASTICITY = 2.041E+05

THRUST LOAD = 8.896E+03

	POSI-TION	INNER DIAM. LEFT	INNER DIAM. RIGHT	OUTER DIAM. LEFT	OUTER DIAM. RIGHT	POINT FORCE	POINT MOMENT	LOAD INTENSITY LEFT	LOAD INTENSITY RIGHT		BEARING SEAT POS.ERR	DEFL/FOR	ANG.ERR	DEFL/MOM
1	0.0	0.0	0.0	0.0	29.0					1				
2	45.0	0.0	0.0	29.0	45.0					2				
3	54.0	0.0	0.0	45.0	45.0					3	-0.000	-0.	0.0000	-0.
4	63.5	0.0	0.0	45.0	52.0					4				
5	69.0	0.0	0.0	52.0	52.0					5				
6	71.0	0.0	0.0	44.0	44.0					6				
7	73.0	0.0	0.0	42.0	42.0					7				
8	322.0	0.0	0.0	42.0	42.0					8				
9	324.0	0.0	0.0	44.0	44.0					9				
10	326.0	0.0	0.0	58.0	58.0					10				
11	340.0	0.0	0.0	58.0	85.0					11				
12	368.0	0.0	0.0	85.0	100.0					12				
13	378.0	0.0	0.0	100.0	41.5					13				
14	439.0	0.0	24.0	41.5	39.0					14				
15	441.0	28.0	28.0	38.0	38.0					15				
16	459.0	30.0	30.0	38.0	38.0					16				
17	461.0	30.0	30.0	41.5	41.5					17				
18	470.0	20.0	20.0	41.5	41.5					18				
19	480.0	20.0	20.0	41.5	116.0					19				
20	487.0	20.0	20.0	116.0	100.0					20				
21	504.0	20.0	20.0	100.0	100.0					21	-0.000	-0.	0.0000	-0.
22	524.0	20.0	20.0	100.0	100.0					22				

*** S H A B E R T H / S K F ** TECHNOLOGY DIVISION S K F INDUSTRIES INC. ** S H A B E R T H / S K F ***

WPAFB LUBRICATION BRANCH * R.E.B. TEST MACHINE ASSEMBLY I * SOLUTION LEVEL 2

B E A R I N G S Y S T E M O U T P U T METRIC UNITS

	LINEAR (MM) AND ANGULAR (RADIANS) DEFLECTIONS					REACTION FORCES (N) AND MOMENTS (MM-N)				
BRG.	DX	DY	DZ	GY	GZ	FX	FY	FZ	MY	MZ
1	5.565E-03	2.016E-02	-1.874E-09	8.940E-13	8.166E-05	0.	741.	.574	2.070E-03	48.8
2	5.565E-03	-7.335E-03	-9.457E-10	-7.850E-12	-3.414E-04	9.074E+03	1.477E+03	14.2	657.	-7.323E+04

	FATIGUE LIFE (HOURS)			H/SIGMA		LUBE-LIFE FACTOR		MATERIAL FACTOR	
BRG.	O. RACE	I. RACE	BEARING	O. RACE	I. RACE	O. RACE	I. RACE	O. RACE	I. RACE
1	2.637E+06	1.286E+06	9.268E+05	1.86	1.66	.645	.582	3.00	3.00
2	2.519E+03	2.223E+03	1.265E+03	1.52	1.37	.542	.505	5.00	5.00

TEMPERATURES RELEVANT TO BEARING PERFORMANCE (DEGREES CENTIGRADE)

BRG.	SHAFT	I. RING	I. RACE	I. FLNG.	ROLL. EL.	O. FLNG.	O. RACE	O. RING	HSG.	BULK LUBE
1	66.0	71.0	74.0	74.0	77.0	74.0	74.0	71.0	66.0	57.0
2	177.	182.	185.	185.	189.	188.	188.	185.	177.	141.

*** S H A B E R T H / S K F ** TECHNOLOGY DIVISION S K F INDUSTRIES INC. ** S H A B E R T H / S K F ***

WPAFB LUBRICATION BRANCH * R.E.B. TEST MACHINE ASSEMBLY I * SOLUTION LEVEL 2

B E A R I N G S Y S T E M O U T P U T METRIC UNITS

FRICTIONAL HEAT GENERATION RATE (WATTS) AND FRICTION TORQUE (N-MM)

BRG.	O. RACE	O. FLNGS.	I. RACE	I. FLNGS.	R.E.DRAG	R.E.-CAGE	CAGE-LAND	TOTAL	TORQUE
1	224.	0.	44.8	0.	64.9	19.7	40.1	394.	251.
2	601.	0.	607.	0.	782.	22.8	23.8	2.037E+03	1.297E+03

EHD FILM THICKNESS, FILM REDUCTION FACTORS AND HEAT CONDUCTIVITY DATA FOR THE OUTER AND INNER RACEWAYS RESPECTIVELY

BRG.	FILM (MICRONS)		STARVATION FACTOR		THERMAL FACTOR		MENISCUS DIST. (MM)		CONDUCTIVITY (W/DEG.C)	
1	.302	.269	1.00	.998	.925	.925	1.17	.509	2.36	.760
2	.117	.105	.998	.986	.947	.960	.647	.250	31.3	16.7

BRG.	FIT PRESSURES (N/MM2) SHAFT-COLD.	OPER.	HSG.-COLD.	OPER.	BEARING CLEARANCES (MM) ORIGINAL	CHANGE	SPEED GIVING ZERO FIT PRESSURE OPERATING SHAFT-INNER RING (RPM)
1	26.9	23.2	0.	0.	6.000E-02	-3.165E-02	2.835E-02 5.575E+04
2	1.97	0.	0.	0.	0.	-2.281E-02	-2.281E-02 3.957E+03

*** S H A B E R T H / S K F ** TECHNOLOGY DIVISION S K F INDUSTRIES INC. ** S H A B E R T H / S K F ***

WPAFB LUBRICATION BRANCH * R.E.B. TEST MACHINE ASSEMBLY I * SOLUTION LEVEL 2

B E A R I N G S Y S T E M O U T P U T METRIC UNITS

LUBRICANT TEMPERATURES AND PHYSICAL PROPERTIES

	LOCATION	TEMPERATURES (DEGREES C.)	DENSITY (GM/CM3)	VISCOSITY KINEMATIC (CS)	VISCOSITY DYNAMIC (CP)	PRESSURE VISCOSITY COEFFICIENT (MM2/N)
BRG. 1	OUTER	74.000	.9112	5.010	4.565	.1189E-01
	INNER	74.000	.9112	5.010	4.565	.1189E-01
	BULK	57.000	.9232	7.377	6.810	.1322E-01
BRG. 2	OUTER	188.000	.8303	1.228	1.020	.5941E-02
	INNER	185.000	.8324	1.255	1.045	.6060E-02
	BULK	141.000	.8636	1.855	1.602	.8100E-02

C A G E D A T A METRIC UNITS

	CAGE RAIL - RING LAND DATA				CAGE SPEED DATA					
BRG.	TORQUE (MM-N)	HEAT RATE (WATTS)	SEP.FORCE (NEWTONS)	ECCENTRICITY RATIO	EPICYCLIC SPEED (RAD/SEC)	EPICYCLIC SPEED (RPM)	CALCULATED SPEED (RAD/SEC)	CALCULATED SPEED (RPM)	CALC/EPIC RATIO	CAGE/SHAFT RATIO
1	44.2	40.1	0.	0.	665.	6.346E+03	664.	6.342E+03	.999	.423
2	28.3	23.8	0.	0.	731.	6.981E+03	729.	6.962E+03	.997	.464

*** S H A B E R T H / S K F ** TECHNOLOGY DIVISION S K F INDUSTRIES INC. ** S H A B E R T H / S K F ***

WPAFB LUBRICATION BRANCH * R.E.B. TEST MACHINE ASSEMBLY I * SOLUTION LEVEL 2

R O L L I N G E L E M E N T O U T P U T FOR BEARING NUMBER 1 METRIC UNITS

AZIMUTH	ANGULAR SPEEDS (RADIANS/SECOND)				SPEED VECTOR ANGLES (DEGREES)		
ANGLE (DEG.)	WX	WY	WZ	TOTAL	ORBITAL	TAN-1(WY/WX)	TAN-1(WZ/WX)
0.00	-4985.252	-.159	0.000	4985.252	664.239	-180.00	180.00
25.71	-4985.375	-.098	0.000	4985.375	664.077	-180.00	180.00
51.43	-4988.160	0.000	0.000	4988.160	663.630	180.00	180.00
77.14	-4978.986	0.000	0.000	4978.986	662.592	180.00	180.00
102.86	-4988.216	0.000	0.000	4988.216	664.124	180.00	180.00
128.57	-4990.272	0.000	0.000	4990.272	664.435	180.00	180.00
154.29	-5000.465	0.000	0.000	5000.465	665.500	180.00	180.00
180.00	-4992.588	0.000	0.000	4992.588	664.135	180.00	180.00
205.71	-4991.293	0.000	0.000	4991.293	663.892	180.00	180.00
231.43	-4980.645	0.000	0.000	4980.645	662.727	180.00	180.00
257.14	-4988.110	0.000	0.000	4988.110	664.002	180.00	180.00
282.86	-4988.086	0.000	0.000	4988.086	664.150	180.00	180.00
308.57	-5000.599	0.000	0.000	5000.599	665.408	180.00	180.00
334.29	-4986.118	-.098	0.000	4986.118	664.351	-180.00	180.00

*** S H A B E R T H / S K F ** TECHNOLOGY DIVISION S K F INDUSTRIES INC. ** S H A B E R T H / S K F ***

WPAFB LUBRICATION BRANCH * R.E.B. TEST MACHINE ASSEMBLY I * SOLUTION LEVEL 2

R O L L I N G E L E M E N T O U T P U T FOR BEARING NUMBER 1 METRIC UNITS

AZIMUTH	NORMAL FORCES (NEWTONS)			HZ STRESS (N/MM**2)		LOAD RATIO QASP/QTOT		CONTACT ANGLES (DEG.)	
ANGLE (DEG.)	CAGE	OUTER	INNER	OUTER	INNER	OUTER	INNER	OUTER	INNER
0.00	-.081	463.758	375.831	864.714	871.402	.0520	.0768	0.00	0.00
25.71	-.102	290.537	202.677	663.352	673.547	.0512	.0761	0.00	0.00
51.43	-.029	87.948	0.000	406.601	0.000	.0440	0.0000	0.00	0.00
77.14	.277	87.493	0.000	405.573	0.000	.0442	0.0000	0.00	0.00
102.86	.520	87.903	0.000	406.281	0.000	.0439	0.0000	0.00	0.00
128.57	.456	87.984	0.000	406.421	0.000	.0438	0.0000	0.00	0.00
154.29	.172	88.260	0.000	406.898	0.000	.0435	0.0000	0.00	0.00
180.00	-.055	87.895	0.000	406.267	0.000	.0438	0.0000	0.00	0.00
205.71	-.031	87.830	0.000	406.155	0.000	.0439	0.0000	0.00	0.00
231.43	.212	87.527	0.000	405.630	0.000	.0442	0.0000	0.00	0.00
257.14	.448	87.869	0.000	406.22[illegible]	0.000	.0439	0.0000	0.00	0.00
282.86	.453	87.908	0.000	406.291	0.000	.0439	0.0000	0.00	0.00
308.57	.229	88.425	0.000	407.422	0.000	.0436	0.0000	0.00	0.00
334.29	-.018	290.575	202.641	663.390	673.499	.0511	.0762	0.00	0.00

*** S H A B E R T H / S K F ** TECHNOLOGY DIVISION S K F INDUSTRIES INC. ** S H A B E R T H / S K F ***

WPAFB LUBRICATION BRANCH * R.E.B. TEST MACHINE ASSEMBLY I * SOLUTION LEVEL 2

R O L L I N G E L E M E N T O U T P U T FOR BEARING NUMBER 2 METRIC UNITS

AZIMUTH	ANGULAR SPEEDS (RADIANS/SECOND)				SPEED VECTOR ANGLES (DEGREES)		
ANGLE (DEG.)	WX	WY	WZ	TOTAL	ORBITAL	TAN-1(WY/WX)	TAN-1(WZ/WX)
0.00	-6279.481	182.321	-38.747	6282.247	728.668	178.34	-179.65
20.00	-6281.129	186.768	-40.295	6284.034	728.800	178.30	-179.63
40.00	-6277.956	188.121	-41.730	6280.912	728.984	178.28	-179.62
60.00	-6270.635	186.271	-42.886	6273.548	729.199	178.30	-179.61
80.00	-6260.268	181.644	-43.620	6263.054	729.413	178.34	-179.60
100.00	-6248.235	174.871	-43.780	6250.835	729.588	178.40	-179.60
120.00	-6236.013	166.911	-43.300	6238.397	729.686	178.47	-179.60
140.00	-6224.970	158.674	-42.192	6227.134	729.695	178.54	-179.61
160.00	-6216.102	151.073	-40.599	6218.070	729.613	178.61	-179.63
180.00	-6210.338	144.860	-38.766	6212.148	729.466	178.66	-179.64
200.00	-6208.115	140.661	-36.956	6209.818	729.282	178.70	-179.66
220.00	-6209.970	138.969	-35.452	6211.625	729.101	178.72	-179.67
240.00	-6215.752	139.997	-34.430	6217.424	728.933	178.71	-179.68
260.00	-6225.147	143.754	-33.974	6226.899	728.794	178.68	-179.69
280.00	-6237.220	150.027	-34.123	6239.118	728.691	178.62	-179.69
300.00	-6250.454	158.061	-34.789	6252.549	728.630	178.55	-179.68
320.00	-6263.035	166.916	-35.867	6265.362	728.595	178.47	-179.67
340.00	-6273.241	175.406	-37.235	6275.803	728.612	178.40	-179.66

*** S H A B E R T H / S K F ** TECHNOLOGY DIVISION S K F INDUSTRIES INC. ** S H A B E R T H / S K F ***

WPAFB LUBRICATION BRANCH * R.E.B. TEST MACHINE ASSEMBLY I * SOLUTION LEVEL 2

R O L L I N G E L E M E N T O U T P U T FOR BEARING NUMBER 2 METRIC UNITS

AZIMUTH	NORMAL FORCES (NEWTONS)			HZ STRESS (N/MM**2)		LOAD RATIO QASP/QTOT		CONTACT ANGLES (DEG.)	
ANGLE (DEG.)	CAGE	OUTER	INNER	OUTER	INNER	OUTER	INNER	OUTER	INNER
0.00	.151	2154.726	1189.237	1564.349	1652.950	.0675	.0886	16.64	31.49
20.00	.169	2141.116	1174.570	1561.049	1646.126	.0674	.0887	16.51	31.45
40.00	.179	2102.111	1132.959	1551.511	1626.453	.0674	.0891	16.14	31.31
60.00	.179	2045.274	1072.319	1537.400	1596.901	.0674	.0897	15.58	31.10
80.00	.168	1980.338	1002.905	1520.954	1561.673	.0674	.0906	14.90	30.34
100.00	.148	1916.554	934.578	1504.447	1525.370	.0675	.0915	14.20	30.54
120.00	.123	1861.069	875.085	1489.786	1492.291	.0675	.0923	13.55	30.26
140.00	.095	1818.611	829.610	1478.370	1465.980	.0676	.0930	13.04	30.02
160.00	.071	1791.876	801.163	1471.389	1449.029	.0677	.0935	12.71	29.86
180.00	.052	1782.256	791.244	1468.452	1443.024	.0679	.0937	12.59	29.81
200.00	.040	1790.240	800.334	1470.641	1448.529	.0679	.0937	12.71	29.86
220.00	.037	1815.656	828.094	1477.568	1465.087	.0680	.0933	13.05	30.02
240.00	.040	1857.296	873.118	1488.779	1491.172	.0680	.0928	13.57	30.25
260.00	.050	1912.540	932.441	1503.396	1524.207	.0680	.0920	14.22	30.54
280.00	.065	1976.640	1000.881	1520.007	1560.621	.0679	.0911	14.92	30.83
300.00	.084	2042.307	1070.641	1536.656	1596.068	.0678	.0902	15.59	31.09
320.00	.106	2100.058	1131.771	1551.006	1625.884	.0677	.0895	16.15	31.31
340.00	.129	2140.107	1173.970	1560.804	1645.846	.0676	.0889	16.52	31.45

```
  CSA    NOS/BE L414C        6600 CMR1 07/31/76
03.12.16.BC1AERA  FROM
03.12.16.IP  00002960 WORDS - FILE INPUT  , DC 00
03.12.16.BC1AE,T1500,IO900,CM200000,STCSA. P74058
03.12.16.0 CRECELIUS
03.12.17.ATTACH,FILEMAN,ID=P720611.
03.12.17.PFN IS
03.12.17.FILEMAN
03.12.17.PF CYCLE NO. = 001
03.12.17.FILEMAN.
03.12.18.
03.12.18.*************************************
03.12.18.AFAPL PERM FILE SUPPORT PACKAGE  V2.1
03.12.18.
03.12.18. PURGE,YY,BILL,CY=2.
03.12.19.FILE NOT CATALOGED ON THIS SN. **
03.12.19. PURGE,YY,BILL,CY=3.
03.12.19.FILE NOT CATALOGED ON THIS SN. **
03.12.19. RETURN,XX.
03.12.19.FUNCTION SUCCESSFUL.
03.12.19. RETURN,YY.
03.12.19.FUNCTION SUCCESSFUL.
03.12.19.
03.12.19.CONTROL RETURNED TO NOS
03.12.19.*************************************
03.12.19.
03.12.19.    STOP
03.12.19.      .027 CP SECONDS EXECUTION TIME
03.12.19.ATTACH,OLDPL,BILL,CY=1.
03.12.19.UPDATE,P,F.
03.12.49. UPDATE COMPLETE.
03.12.49.FTN,I=COMPILE,L=0,PL=15000.
03.19.49.    53.023 CP SECONDS COMPILATION TIME
03.19.50.MAP,ON.
03.19.50.SEGLOAD.
03.19.50.LOAD,LGO.
03.19.50.EXECUTE.
03.24.50.     END  SHABTH
03.24.50.OP  00027264 WORDS - FILE OUTPUT , DC 40
03.24.50.MS  275968  WORDS  (  275968 MAX USED)
03.24.50.SCM 164000  WORDS MAXIMUM
03.24.50.CPA     111.881 SEC.       40.254 ADJ.
03.24.50.IO      105.327 SEC.       57.066 ADJ.
03.24.50.CM     6456.629 KWS.       77.556 ADJ.
03.24.50.CRUS                      174.878
03.24.50.COST                $      10.49
03.24.50.PP      237.362 SEC.     DATE 07/22/76
03.24.50.EJ  END OF JOB, **  P740580.

***********          BC1AERA  //// END OF LIST ////
***********          BC1AERA  //// END OF LIST ////
```


*U.S. Government Printing Office: 1977 — 757-001/10